NASA CONTRACTOR REPORT 166572

NASA-CR-166572
19840017574

A Numerical Study of the Controlled Flow Tunnel for a High Lift Model

Pareshkumar C. Parikh

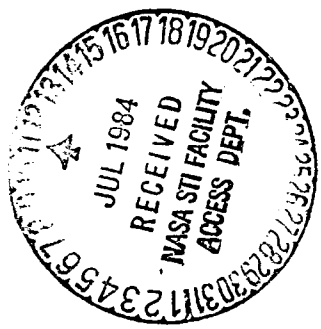

Grant NSG 2260
1984

NASA

NASA CONTRACTOR REPORT 166572

A Numerical Study of the Controlled Flow Tunnel for a High Lift Model

Pareshkumar C. Parikh

University of Washington
Seattle, Washington

Prepared for
Ames Research Center
under Grant NSG 2260

National Aeronautics and
Space Administration

Ames Research Center
Moffett Field, California 94035

TABLE OF CONTENTS

LIST OF FIGURES

LIST OF SYMBOLS

AR	aspect ratio
$\{A\}$	N x N matrix of model influence coefficients
b	model span
$\{B\}$	M x M matrix of tunnel influence coefficients
c	model chord
C	tunnel cross section area
C_J	jet momentum coefficient
C_L	lift coefficient
D_p	pressure drag
H	wind tunnel height
J	jet momentum flux per unit span
L	wind tunnel length
L_p	pressure lift
M	number of vortex rings describing the tunnel geometry
$\vec{n}$	unit normal
N	number of vortex elements describing the model
R	radius of curvature of the jet
S_w	model wing area
U_∞	free stream velocity
U_t	tangential velocity at bound vortices in the jet
$\vec{V}$	velocity vector
$[V_n]$	N dimensional column matrix of free stream velocity components at model control points

$[V_{FA}]$	M dimensional column matrix of desired net normal velocity through tunnel control points
$[V_{MT}]$	M dimensional column matrix representing the effect of the model at tunnel control points
$[V_{TM}]$	N dimensional column matrix representing the effect of the tunnel at model control points
w	vertical component of tunnel induced velocity
W	wind tunnel width
X	streamwise coordinate with origin at model quarter chord; positive downstream
Y	vertical coordinate; positive upwards
Z	lateral coordinate, positive to the right looking downstream
α	model angle of attack
δ	jet thickness, also interference factor
γ	model bound vorticity per unit length
$[\Gamma_m]$	N dimensional column matrix of model vortex strength
$[\Gamma_T]$	M dimensional column matrix of tunnel vortex lattice strength
ε	downwash angle at tail
ρ_0	density of the free stream fluid
Θ	exit angle of the jet measured with respect to the chord

University of Washington

Abstract

A NUMERICAL STUDY OF THE CONTROLLED FLOW TUNNEL FOR A HIGH LIFT MODEL

by Pareshkumar C. Parikh

Chairperson of the Supervisory Committee: Professor R. G. Joppa
Department of
Aeronautics and Astronautics

A controlled flow tunnel employs active control of flow through the walls of the wind tunnel so that the model is in approximately free air conditions during the test. This improves the wind tunnel test environment, enhancing the validity of the experimentally obtained test data.

In the present study this concept is applied to a three dimensional jet flapped wing with full span jet flap. It is shown that a special treatment is required for the high energy wake associated with this and other V/STOL models. An iterative numerical scheme is developed to describe working of an actual controlled flow tunnel and comparisons are shown with other available results. It is shown that control need be exerted over only part of the tunnel walls to closely approximate free air flow conditions. It is concluded that such a tunnel is able to produce a nearly interference free test environment even with a high lift model in the tunnel.

CHAPTER 1

INTRODUCTION

The possibility of integrating aircraft propulsive and lift systems to achieve performance gains has renewed interest in high lift systems in recent years. This has led to a variety of configurations for the so called V/STOL (Vertical/Short Takeoff and Landing) aircraft. The high lift required for a V/STOL operation at low forward speeds is produced either by deflecting the incoming air to high angles or by increasing its velocity. In either case the change in angle or the increase in velocity is not small. As a result the associated aerodynamics is nonlinear. Classical aerodynamic theories, being linear in nature, are obviously incapable of predicting performance for these new machines and several attempts have been made to develop new methods which include nonlinear effects. Unfortunately, over the last two decades combinations of wings, rotors, flow deflecting devices and fans have resulted in so many different configurations that theoretical development has not kept pace and the designer has turned to the wind tunnel for performance predictions on these new configurations.

The wind tunnel introduces a different set of problems of its own. Besides the one of matching of the similarity parameters, a wind tunnel is known to alter flow field around the model. This latter problem is referred to as wind tunnel interference and is the direct effect of the presence of the test section boundaries. Unfortunately, both these problems are particularly severe for a V/STOL model;

firstly, because of the difficulty in reproducing the intricate details of the model, thereby compromising on similarity parameters, and secondly, because of the nonlinear nature of the downwash field around such a model. Also the characteristic high energy wake of a V/STOL model may impinge on the tunnel floor resulting in the development of flow directed upstream along the floor. Lateral recirculation may develop on the walls possibly resulting in erroneous data. Of course the presence of interference due to wind tunnel walls has been known from the earliest use of the wind tunnels and classical theories exist for the correction of the test data [Ref. 1 & 2]. Unfortunately, these theories are based on the linearizing assumptions of small angles and small downwash velocities and hence are inapplicable to a V/STOL model.

Attempts have been made in the past to cope with this lack of an adequate interference prediction method. Notable advances were made by Heyson [3] who gave a theory which partially accounted for the nonlinearities encountered. Others have tried to design so called smart wind tunnels which duplicate the free air flow field inside the tunnel test section thereby eliminating the need for interference corrections. Despite these numerous attempts a complete solution is still not available. This has forced the wind tunnel engineer to build larger tunnels effectively placing the tunnel walls farther away from the model, thereby reducing interference.

An alternate technique to the construction of large wind tunnels was proposed by Bernstein [4]. His proposal calls for construction of

a tunnel in which flow through the walls is actively controlled to match free air flow field. The model in such a tunnel is in approximate free flight conditions during the test, thus reducing need for interference corrections. Bernstein studied the concept experimentally on a two dimensional wing. Later Atkinson [5] extended this concept of a minimum interference wind tunnel to a three dimensional plane wing. He showed that, in principle, control need be exerted over only part of the tunnel walls to closely approximate free air conditions.

In this dissertation the above concept of a controlled flow tunnel is extended to include a more complex three dimensional powered lift V/STOL system. A numerical study is made of the problem of wind tunnel interference on a high lift system. It is shown that a special treatment is required for the high energy, vortical wake associated with such a powered lift system. The success of a partially controlled test section in producing nearly interference free test environment is numerically examined. Finally, some practical aspects to the construction of such a tunnel are briefly discussed. Extension of an already proven concept to a high lift system is the unique feature of this study.

CHAPTER 2

WALL INTERFERENCE ON HIGH LIFT SYSTEMS

The solution to the wind tunnel interference problem can be described using two approaches. The classical approach is to compute the effect of wall interference and then to apply appropriate corrections to measured data. Alternately, by appropriate designs wind tunnels may be constructed so that interference is minimized or in extreme cases eliminated. In the past, both these approaches have been applied, with appropriate modifications, to V/STOL systems. In this chapter some of this work is described, the main objectives of the present study are stated and the make-up of the rest of the report is outlined.

2.1 The Classical Approach and its Variations:

In the classical wind tunnel interference theories, like those due to Prandtl [1] and Glauert [2], the model lifting system is represented by a lifting line and its wake by a pair of vortex filaments which are assumed to trail downstream in a straight, level line. A pattern of image filaments is chosen outside the tunnel walls in such a way that the tunnel walls become streamlines of the flow. The effect of these image vortices at the model is then taken as the interference effect of the tunnel.

A V/STOL model is characterized by one or more highly deflected wakes making the associated aerodynamics nonlinear. Also the wake may strike the tunnel floor inducing lateral recirculation on the tunnel

walls producing a flow phenomenon known as 'flow breakdown' as studied by Rae [6] and Shindo [7]. This violates the basic assumptions of the classical interference theory and hence it cannot be used in its original form to correct data on a high lift model.

Attempts have been made in the past to modify this classical approach so as to make the theory applicable to a V/STOL system. Notable advances were made in this field by Heyson of NASA Langley Research Center who gave, in the early 1960's, a then very popular interference theory for general three dimensional V/STOL systems [3]. As in the classical theory, he represented the model by a horseshoe vortex system but represented the trailing vortex pair by straight but inclined vortex filaments. The angle of inclination of this trailing pair was found using momentum considerations. He then used the method of images by making the wind tunnel walls reflection planes and followed the classical approach to calculate interference factors as the combined effect of all the images. At the point where the trailing wake strikes the floor a special treatment is required. In Heyson's formulation it is met by the first image wake and they are assumed to move aft together in the plane of the floor. Using this approach Heyson was able to correct lift and drag on the wing but was not uniformly successful in correcting pitching moment [8-9].

Two reasons are attributed to this deficiency in correcting pitching moment data. The obvious one is the incorrect shape assumed for the highly curved wake. The other, and not so obvious, is the failure to account for the relocation of the wake in the tunnel i.e.

the fact that the wake trails along a different trajectory in the tunnel than in free air. The effect arises from the presence of tunnel boundaries which cause upwash velocities. This results in relocation of the vortex wake in the tunnel. This new position in the tunnel is different with respect to the tail and hence affects pitching moment data.

Joppa [10] put forward a novel scheme for interference calculations wherein the interference is computed for the correct wake shape and the direct effect of the relocated wake is included. His method predicts the flow field of the lifting system both in the free air and in the tunnel, and the difference in flow velocities between these two representations is charged to the wall interference. In this method, potential flow modelling is used to represent the model and its associated wake. The tunnel walls are represented using a network of vortex lattices and the model-in-the-tunnel solution is obtained using an iterative process. The vortex lattice representation has an advantage that it replaces the image network and is applicable to any tunnel cross section, to the extent that the cross section can be approximated by a polygon of equal length elements. Using this approach, Joppa reproduced very good agreement with classical results as well as showed that the effect of the relocated wake may equal or exceed the wall induced upwash, and hence dominate the pitching moment intereference. However, the solutions that he presented were limited to non-powered lift cases.

2.2 The Minimum Interference Wind Tunnel Approach:

The second approach of getting interference-free results mentioned above is referred to in the literature by various names but differ only in the means to achieve the duplication of the free air flow field in the tunnel. For the purpose of the present study the phrase 'Controlled Flow Tunnel' is used to describe a tunnel, flow through which is controlled. This is achieved by injecting into or extracting from the test section walls the required quantity of air to match free air conditions.

The basic assumption in the working of a controlled flow wind tunnel is that potential flow analysis provides an adequate description of the flow far away from the model. In accordance with this assumption, at some distance from the model a fictitious control surface may be constructed. On this control surface potential theory is applicable. Therefore, if at every point on the control surface the flow is identical to that of free air, the model inside the control volume will experience free flight flow.

For V/STOL systems, several attempts have been made in the past to design such minimum interference wind tunnels. The technique of contouring the wind tunnel walls to make them streamlines of the flow was evaluated for a V/STOL fan-in-wing model by Kroeger et al [11]. They employed potential flow representation of the model to numerically find the wall shape required. Adjustable wall louvers were used to adjust the wall. Only partial success was reported because of mechanical problems of getting the necessary wall shapes.

Some work on minimum correction wind tunnel was published by Calspan Corporation [12,13]. This proposal uses two flow components at a fictitious control surface near the tunnel walls. The method is based on the fact that in a plane potential flow the two flow components (such as two velocities) are not independent. Therefore, one of the two can be used, alongwith the potential flow simulation satisfying far field conditions, to calculate the other component. The difference between this computed and measured value of the second component is then used to adjust the porosity of the walls to give interference-free results. Though a very ingenious method, only limited experimental data was obtained to evaluate this proposal. Recently Prof. W. R. Sears at the University of Arizona has started an ambitious experimental program for getting interference- free data on V/STOL models. His proposal calls for building an unconventional wind tunnel in which the model's orientation and the freestream vector are chosen to put the wake in the desired position and simulation of the correct freestream vector, defining the desired angle of attack, is achieved by means of the adaptive-wall iterative strategy. To date the concept has only been studied numerically since the wind tunnel is under construction [14].

2.3 Working of a Controlled Flow Tunnel:

The principle of operation of a controlled flow tunnel is schematically shown in figure 1. The facility involves combining a computer selector program, a wind tunnel and auxiliary equipments to

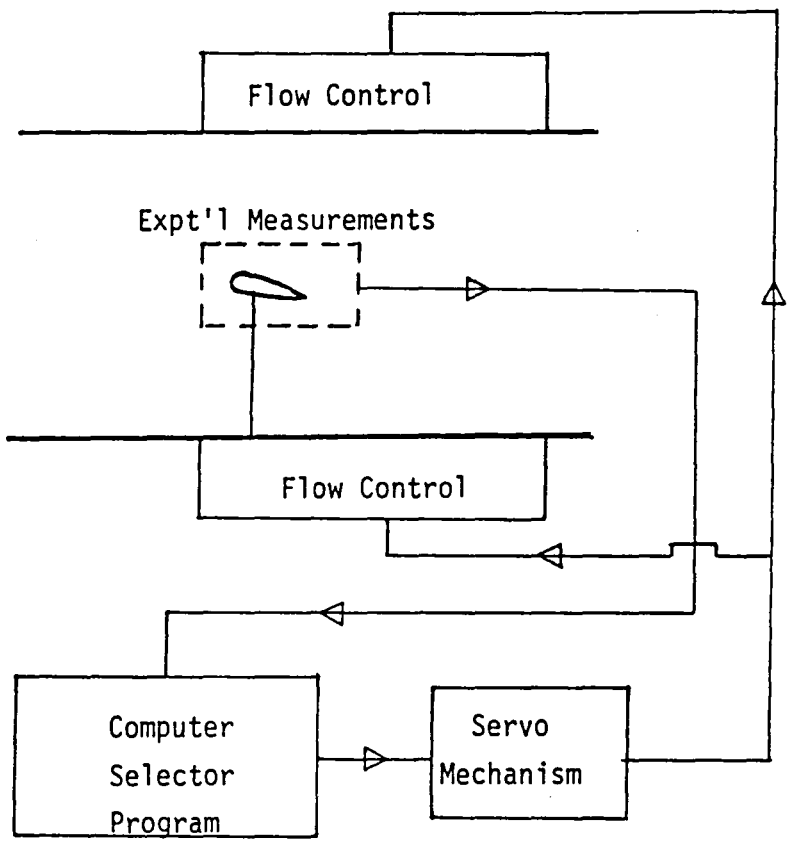

Figure 1. Feedback Model of the Controlled Flow Tunnel.

actively control flow through the tunnel walls. The tunnel employs a continuous feedback operational procedure. Operation of such a tunnel can be described as follows:

In advance of the actual wind tunnel test, a computer program is made representing the model to be tested. This program uses simple potential flow representation and is capable of calculating the lift coefficient of the model in free air and the normal velocity distribution on the surfaces where the tunnel walls would be in an actual test. This information enables one to calculate the wall flow as a function of the lift coefficient.

During an actual test, the lift coefficient on the model is measured for a set of model and tunnel parameters. Based on this value of $C_{L,}$ the required flow through the tunnel walls is computed using the computer selector program. This computed flow is then provided in the tunnel using a servo mechanism. This changes the flow environment around the model and hence the lift coefficient. With this new lift, a different setting for the wall flow is required. This process is repeated a few times until the wall flow closely matches the one that would exist in the free air, thus nearly duplicating the free air flow field inside the tunnel. This feedback process can be made continuous by the use of automatic controllers.

It can be seen that a key point in the operation of a controlled flow tunnel is that the required flow through the walls is precalculated as a function of the measured lift on the model. To do this requires that one be able to predict at least the lift on the

model and induced velocities at the far field points such as the tunnel wall to a reasonable accuracy. Thus, all that is required of the above mentioned computer model is the ability to predict far field effects. It is known that the magnitude of interference velocities due to lift at a far field point is a function only of the magnitude of the circulation and does not depend on how that circulation is produced. Potential flow representations have worked for this kind of problem. Since a potential function is uniquely defined by its normal derivative on the control surface, it is necessary to control only the normal component of flow on the boundary.

The concept of the controlled flow tunnel has been under study for some years at the University of Washington. Bernstein [4], in his doctoral dissertation, showed analytically that the above mentioned feedback system converges to the free air solution. He also proved experimentally the feasibility of a controlled flow tunnel. His experiments were done on a two dimensional model. Atkinson [5] later developed a computer model to simulate a three dimensional low speed minimum interference wind tunnel. He did this for a simple three dimensional wing in a closed tunnel using potential flow representation for the model and vortex lattice representation for the tunnel. Distribution of interference was calculated based on the difference between the flow fields in free air and in the tunnel. He also showed that it was not necessary to control all the tunnel walls and suggested some portions of the ceiling and floor which could be controlled to get nearly interference-free results.

In 1977 an experimental program was designed for the University of Washington Aeronautical Laboratory (UWAL) wind tunnel with the objective, among other things, to provide a preliminary vertification of the concept of the controlled flow tunnel for the case of a powered lift system [15]. During these tests the characteristics of a 3-D jet flapped wing were measured under three conditions: in a test section large enough to give interference-free data, in a smaller test section to present large interference, and in a test section having actively controlled areas to minimize this interference. For the last case, it was realized that the necessary flow control arrangements would be expensive. Further since the computer program required to calculate the flow through the actively controlled walls was not available, an alternate approach was used. Based on Atkinson's suggestions [5], a portion of the ceiling and the floor of the small insert test section (the portion aft of the model quarter chord and between the trailing vortices) was removed. This small test section was inturn enclosed by the large tunnel test section. Thus the free air boundary conditions were allowed to be met there naturally. This was a very crude simulation for a controlled test section, it nonetheless provided a technique for immediate verification.

Typical results from the small closed test section showed the classical increase in the lift curve slope. The data from the controlled (in this case, small open) test section followed closely that of the larger test section showing the success of the controlled flow tunnel concept even with such a crude simulation.

2.4 Objectives of the Present Study:

Both the preliminary work of Bernstein [4] and that of Atkinson [5] on the minimum interference wind tunnel were limited to two or three dimensional plane wings. Further although the UWAL experiments used a jet flapped wing, the simulation of the controlled flow tunnel used was very crude and carried no direct application over to an actual tunnel using this concept. Thus the concept was yet to be proved a success on a high lift system. The present study was, therefore, begun with the objective of extending this concept to a three dimensional powered lift system. Once proved that a nearly interference-free test environment can be produced, the validity of the experimentally obtained data on a high lift system can be enhanced.

It became clear from the beginning that a powered lift system cannot be represented by a simple horseshoe kind of representation previously used and special treatment for its characteristic highly deflected wake had to be introduced. Also the limitations imposed by the phenomenon of 'flow breakdown' resulting from the wake impingement on the tunnel floor had to be studied. Finally, the extent of the partial control needed, similar to the one reported in ref. 5, in order to get nearly interference-free results had to be investigated.

With these objectives in mind, the discussion in this dissertation is addressed to the following:

1) Show in principle that a powered lift system can be represented using potential flow and appropriate treatment of its highly curved wake

insofar as the calculation of lift and its far field effects are concerned.

2) Develop correlation with the existing experimental data for a powered lift model in both closed and controlled test sections thereby proving that controlled flow tunnel can indeed be used for reduced interference results.

3) Study the extent and distribution of controlled areas required to get reasonably interference-free data.

4) Assess practical considerations to be used in the construction of a controlled flow wind tunnel.

2.5 Outline of This Dissertation:

A successful completion of this study requires that the numerical equivalent of all the steps outlined above be developed. This is accomplished in a three step process.

The first of these steps requires development of a potential flow representation of the high lift system in free air. This is done, as shown in chapter 3, for a three dimensional jet flapped wing. Chapter 3 also includes comparisons with other available results.

The next step in an actual controlled flow tunnel requires the measurement of lift on the model enclosed in a tunnel. In the present study this is done by developing a numerical solution of the model-in-the-tunnel problem. This requires that an appropriate tunnel representation be made and that the model lift be calculated in the presence of the tunnel. Chapter 4 describes such a closed tunnel solution.

The final step in the process is the numerical equivalent of the feedback process and its effect on the tunnel flow. This requires solution of the model in the controlled flow tunnel problem. This is achieved, as detailed in chapter 5, by suitably modifying the wall boundary conditions of the model-in-tunnel solution. Chapter 5 also includes a parametric study of the effectiveness of partial control.

Finally, chapter 6 concludes the work with recommendations for further work.

CHAPTER 3

FREE AIR SOLUTION

The first step in the study of a controlled flow tunnel is the development of a potential flow simulation model for the V/STOL system under consideration. This potential flow solution should be able to predict the lift of the model for a fixed set of model parameters. Also the far field effects such as the induced velocities at the tunnel wall locations and the downwash on the tail should be predicted to a reasonable accuracy if the concept of the controlled flow tunnel is to be successfully explored. This chapter deals with such a solution for a three dimensional jet flapped wing.

3.1 Selection of Jetflap:

As this was a study in the proof-of-the-concept stage, it was thought appropriate to do preliminary work on a simple high lift system with later possible extension to more complex cases. A three dimensional jet flapped wing was selected for this purpose not only because it is the simplest of the many high lift systems but also because aerodynamic problems associated with the jet flap are common to other more practical powered lift systems. The selection of the jet flap as a preliminary configuration to be studied was also made because a two dimensional potential flow representation was already available [16] which could be used as a good starting point for three dimensional solution. In addition,the experimental program briefly described in the previous chapter had produced some results on a jet

flapped wing both with and without the interference effect of the tunnel. This could provide experimental data to compare any new theoretical developments.

A jet flap is a wing augmented with a jet of high velocity air which issues from a spanwise slot near the trailing edge at an angle to the wing. The presence of the jet causes circulation, increasing the net lifting pressure force on wing's surface. The reaction to the momentum flux of the jet also contributes to the lift. Very high lift coefficients can be obtained in this manner (Fig. 2.).

One of the first analytical investigations of a jet flap was a two dimensional theory developed by Spence [17]. This was later extended to three dimensions with the limitation of elliptic loading and small angles [18]. Since then several theories providing more generality have been published - both theoretical [19, 20] and computational [21, 22]. All these methods employ the approximation inherent in linear theory, namely that of small angles, and hence are not expected to be valid for large angles of attack or large jet deflection angles. Recently, Addessio et al have developed a nonlinear theory which is applicable to large angles as well [23].

In the next two sections the two dimensional solution of ref. 16 is described first followed by its extension to the three dimensions.

3.2 Two Dimensional Solution:

Unlike the conventional plane wing, a jet flap is characterized by a considerably deflected, high energy wake. This jet sheet acts as

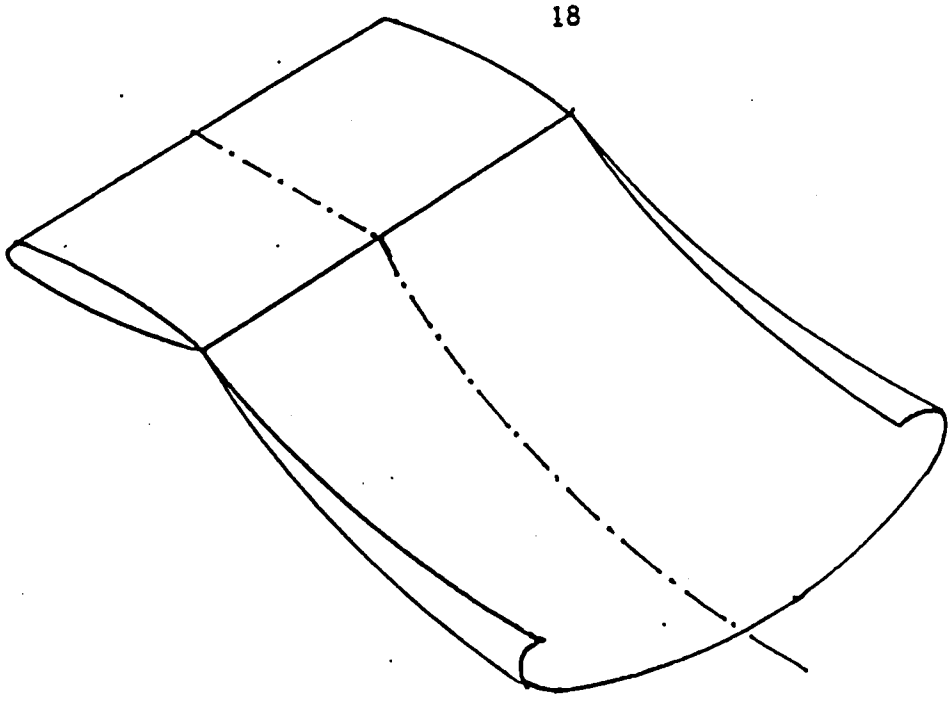

a) A Three- Dimensional Jet Flap

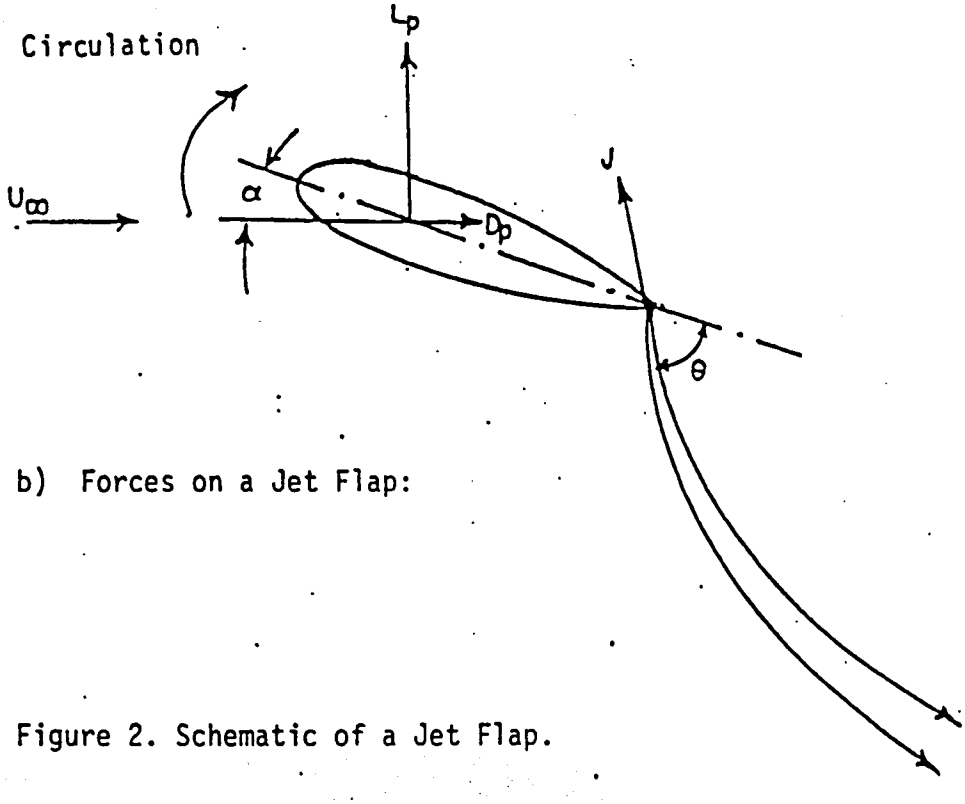

b) Forces on a Jet Flap:

Figure 2. Schematic of a Jet Flap.

a flap supporting a difference of pressure across it, but unlike a conventional flap, its shape is unknown apriori and changes as the flow field is altered. This adds an additional unknown, that of the jet shape, in any analytical formulation.

As in any preliminary study, some simplifying assumptions are made here to make the problem tractable. Most of the analytical representations mentioned above, including the present one, use assumptions made by Spence [17]. The present analysis is, however, not limited to small angles since no linearizing assumptions are made. Accordingly under the assumptions of an inviscid, incompressible external flow, an irrotational flow in the jet and neglecting the entrainment of the external flow in the jet, the wing and the jet can be represented by vortex lines. Thus on all airfoil and jet surfaces the normal component of velocity is made zero. This is referred to as the kinematic boundary condition. In addition, the jet satisfies a dynamic boundary condition relating the centrifugal and pressure forces at each point on the jet.

In the present analysis the representation of Herold [16] is used for the starting two dimensional solution. As shown in fig. 3, the vortex sheet representing the wing and the jet is replaced by equally spaced concentrated vortices and is made a streamline of the flow by satisfying kinematic boundary condition of zero through flow at as many control points as the number of vortices. This is done using the Biot-Savart law and gives the following set of simultaneous algebraic equations with strength of vortices as unknown. The initial jet

$$\{A\}[\Gamma_m] + [V_n] = 0 \qquad (3.1)$$

where $\{A\}$ is the matrix of influence coefficients having (N x N) dimensions representing the effect of model vortices at model control points. $[\Gamma_m]$ is the solution vector of dimension (N x 1) representing the strength of concentrated vortices, and $[V_n]$ is the (N x 1) vector of normal component of free stream velocity at each control point. Solution of this set gives the strengths of the vortices for an assumed location of the jet.

Next the trajectory of the jet is corrected using the dynamic boundary condition at each of the vortices representing the jet. By analyzing an arc of a jet, Spence has shown that

$$\gamma_j = \frac{U_\infty^2 C_J c}{2RU_t} \qquad (3.2)$$

where γ_j is the strength of the vortex per unit length ($\gamma_j \Delta x = \Gamma_j$), C_J is the jet momentum coefficient, R is the local radius of curvature, U_t is the tangential velocity at the vortex location under consideration and c is the wing chord. This is obtained by making the assumption that the jet thickness approaches zero in such a way that the mass flow rate is zero, but the jet momentum coefficient is finite.

This corrected jet trajectory changes the coefficient matrix $\{A\}$ hence an iterative procedure is employed until some predefined convergence criterion is satisfied. The final solution thus gives the strengths of the vortices representing the wing and the jet and also the jet trajectory for a fixed jet exit angle (Θ), angle of attack

i) Kinematic Condition: $\vec{V} \cdot \vec{n} = 0$

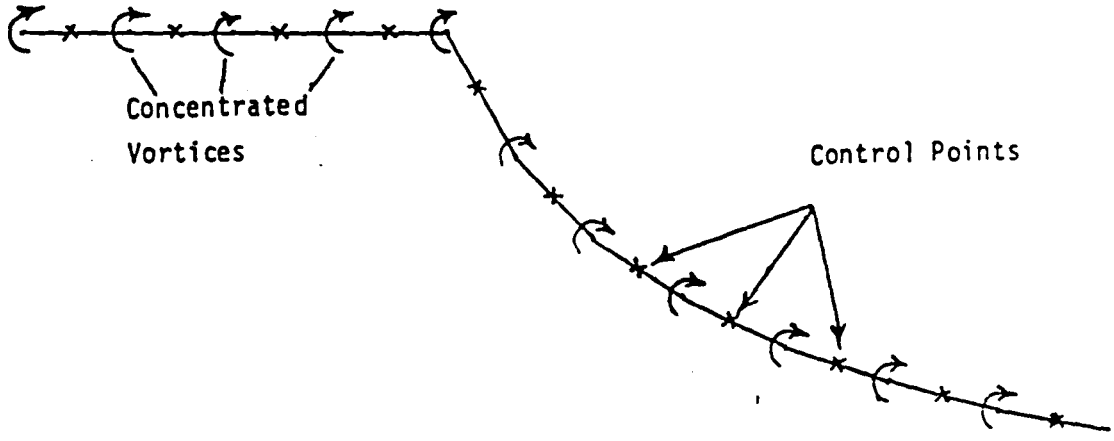

ii) Dynamic Condition:

$$\gamma_j = \frac{UJ}{R\rho_\infty U^2} = \frac{C_J U_\infty^2 c}{2RU_t}$$

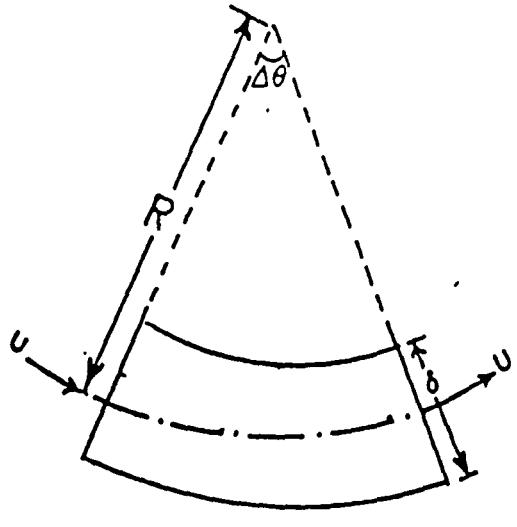

Figure 3. Two Dimensional Solution

strengths of the vortices representing the wing and the jet and also the jet trajectory for a fixed jet exit angle (Θ), angle of attack (α), free stream velocity (U_∞) and the jet momentum coefficient (C_J).

3.3 Three Dimensional Solution:

In vortex representation of any three dimensional wing there are bound vortices representing the pressure difference across the wing and trailing vortices resulting from the gradient in spanwise loading on the wing. A major aspect of any three dimensional solution is to find the strengths and the location of these trailing vortices. Also their contribution to the overall wing aerodynamics such as the induced angle of attack has to be considered. In the present analysis a three dimensional solution is developed starting from the two dimensional solution described above.

As mentioned earlier, viscous and compressibility effects are neglected. This is done in many aerodynamic theories and sacrificies the capability of accounting for boundary layer and separation phenomenon but simplifies the problem. These phenomena can be accounted for in an iterative manner, once the basic aerodynamic flow field is known. Even with these assumptions, an intractable three dimensional problem remains requiring additional assumptions. These are made in the present analysis based on the physics of the flow and computational convenience.

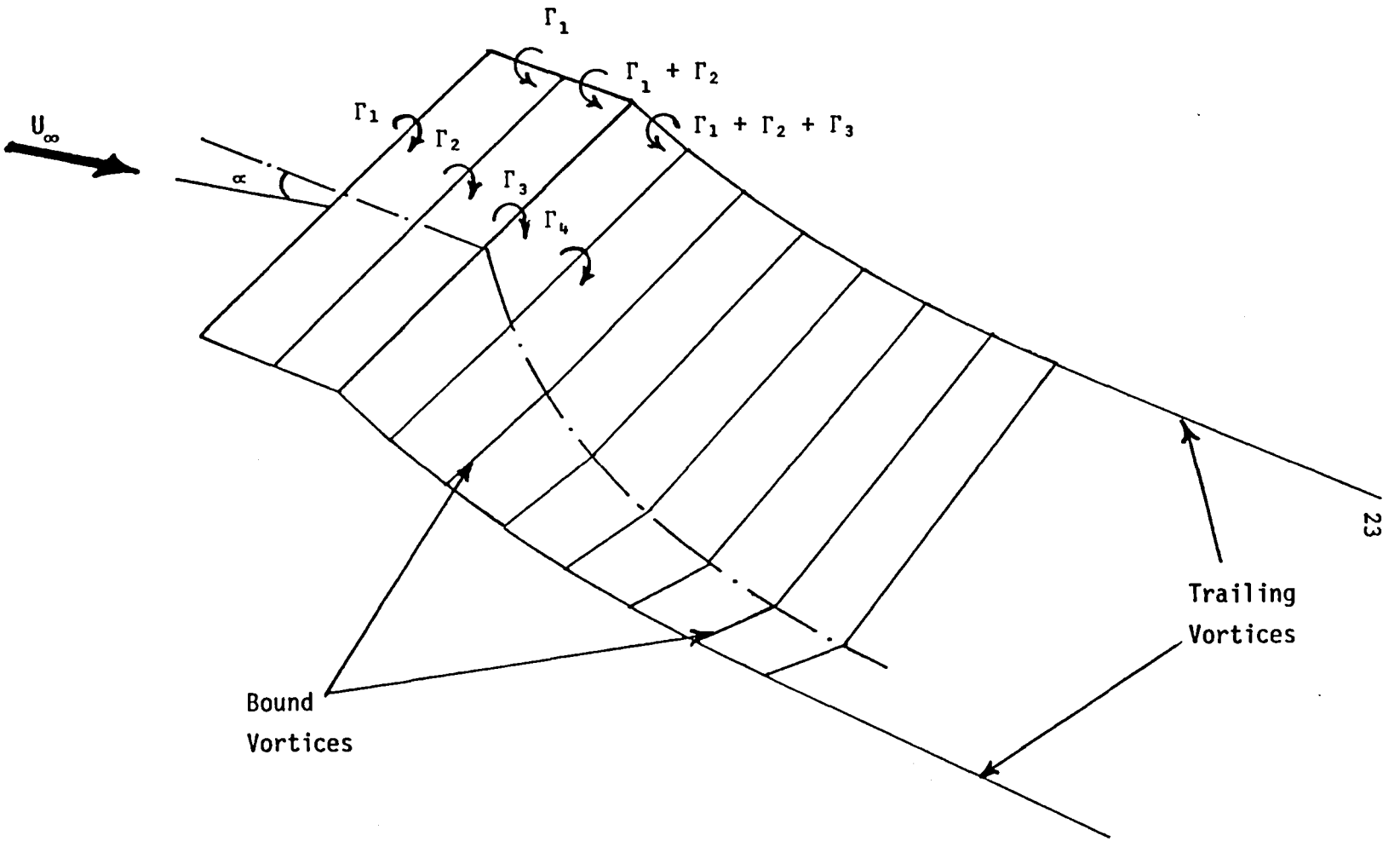

Figure 4. Three Dimensional Representation Used in the Analysis

Based on these assumptions, a flat plate wing with a thin jet exhausting from its trailing edge is schematically represented in figure 4. Both the wing and the jet are shown as single surfaces: the wing as a sheet of zero thickness in the tradition of thin wing theory and the jet as a jet sheet of infinitesimal thickness.

The geometry of the wake, which is a continuous vortex sheet, is quite complex. Its inclusion in its entirety is both unnecessary and computationally expensive. In this analysis the jet vortex sheet is represented as a ladder of concentrated bound vortex lines running spanwise and forming a ladder in the streamwise direction. The strengths of these vortex lines are obtained from the two dimensional solution. Away from the center line and downstream, the wake vortex sheet curves upwards and rolls into a core at either end. Thus the bound vortices are curved in spanwise direction. However, since the jet momentum renders the wake 'stiff' making spanwise curving almost negligible in the near field, this curvature is only approximately accounted for. Thus V-shaped bound vortices are assumed with their apex on the locus of the jet sheet in the plane of symmetry. This locus is calculated from the two dimensional solution.

The wing in this analysis is assumed to be carrying an elliptical load in the spanwise direction. This distribution falls to zero at the wing tips. Consequently a trailing vortex will be shed from every point on the span where there is a gradient in the spanwise load. Accounting for the large number of the trailing filaments may be prohibitive computationally. Thus a further simplification is made by

approximating the elliptically loaded wing by a uniformly loaded one with its effective span so adjusted as to give the same total load in both cases. This technique has been used in the past and this reduced span is referred to as vortex span [24]. This kind of load distribution results in a single pair of trailing vortices simplifying the computations.

The next step is to find the location and the strengths of these trailing vortices. Unlike the classical wake of the plane wing which is assumed to trail straight downstream, the trailing vortices lie between the jet sheet location and the plane of the wing. Rather than assume their location and introduce some uncertainty, we have used a simple approach. The trailing vortices are taken to be made of short straight vortex segments joined end-to-end to form a chain in the streamwise direction. Their initial location is calculated using the Biot-Savart law. Unlike the plane wing, the strength of these trailing segments is not constant but must increase in the streamwise direction to reflect the successive merging of the bound vortices from the jet.

It is also necessary to represent correctly the farfield downstream behavior of the trailing pair. In that region the strength of the bound vortices is negligible thus that of the trailing vortices remains almost constant. To model this correctly, the last segment of each of the trailing vortices is taken to be a long one inclined at such an angle to the freestream that the two are force free.

This procedure gives a first guess at the strengths and the location of the trailing vortices. For a steady state representation, each trailing segment has to be made force free (relaxed) under the influence of all other trailing and bound segments plus the freestream velocity. Several ways have been suggested in the literature to do this [eg 10,25]. We have followed the method suggested by Maskew which gives a faster convergence [26]. Accordingly, each segment of the trailing vortex is relocated by aligning it with the local velocity vector. The method uses the velocity at 50% of the segment length (extrapolated from the previous segment). Once a particular trailing vortex segment is relocated, the entire string of segments downstream is translated so that it stays attached, and the next segment direction is determined. Thus, the wake is relaxed by making each segment force free from the wing aft. Care is also excercised to avoid contribution of a vortex segment when it is very close to the point of velocity calculation. Also while calculating the velocity vectors for the wake relaxation the contribution of the segment being relaxed is excluded.

Next realizing that in the actual case of a three dimensional steady state all the vortex segments are in equilibrium, the effect of the trailing vortices on the bound vortices should be considered. Thus a second pass at the two dimensional solution is made this time taking the effect of the trailing pair at the location calculated by the previous iteration. In this case the solution is not strictly two dimensional but can be termed 'quasi two dimensional'. An iterative

process is carried out between this quasi two dimensional solution and the trailing pair until an equilibrium solution is found.

Once the three dimensional solution is found giving strength and location of the bound and trailing vortices representing the system, aerodynamic quantities of interest can be calculated according to the Kutta-Joukowski theorem. Also induced velocity at any location around the model, e.g. that on the tunnel walls or that needed to calcualte downwash at the tail can be calculated. It should be noted that contribution of the reaction jet momentum to lift and drag has to be added to that calculated using the pressure distribution on the wing to calculate the complete force system. This completes a three dimensional representation of a jet flapped wing.

A listing of the computer program for the solution of a three dimensional jet flap in free air is given in Appendix A. The input to the program and the calculations done are explained using comments at appropriate locations in the program.

3.4 Computational Results:

Results obtained from the numerical simulation model described in the previous section are compared with experimental and other theoretical results. However, before going to the jet flap results, it is appropriate to compare the computer program results with some three dimensional plane wing data. This was done with the objective of gaining confidence in the overall simulation process.

Accordingly, flat plate wings of various aspect ratios were simulated. To obtain plain wing results from the jet flap program, parameters pertaining to the jet in the program were given the smallest possible values whigh gave a converged solution (e.g. a jet exit angle of 2 degrees and a jet momentum coefficient of 0.05). These results are henceforth referred to as the'degenerate jet flap'. The comparison program used was a vortex lattice program developed by Rockwell International [27]. For both the programs, ten chordwise vortices and one pair of trailing vortices were used simulating uniformly loaded wings. Lift coeffieicent versus angle of attack results obtained from these two programs are compared in figure 5 for two extreme aspect ratios. As can be seen excellent agreement is obtained.

For comparison with jet flap data, the choice of parameters for the airfoil and jet geometries as well as the values for the angle of attack, the jet deflection angle and the jet momentum coefficient were chosen largely in accord with the available data. Computational efficiencies and times were of secondary importance in this study and are not given as no attempt was made to optimize them. Two sets of experimental data and one from a nonlinear theory were selected for comparison purposes. One of the experiments was the classical wind tunnel tests of Williams and Alexander [28]. These tests were done on a rectangular wing of 12.5% thick elliptic section with full span jet flap. The other set of experimental data, used for comparison here, is the UWAL test mentioned earlier [ref. 15]. For this, a

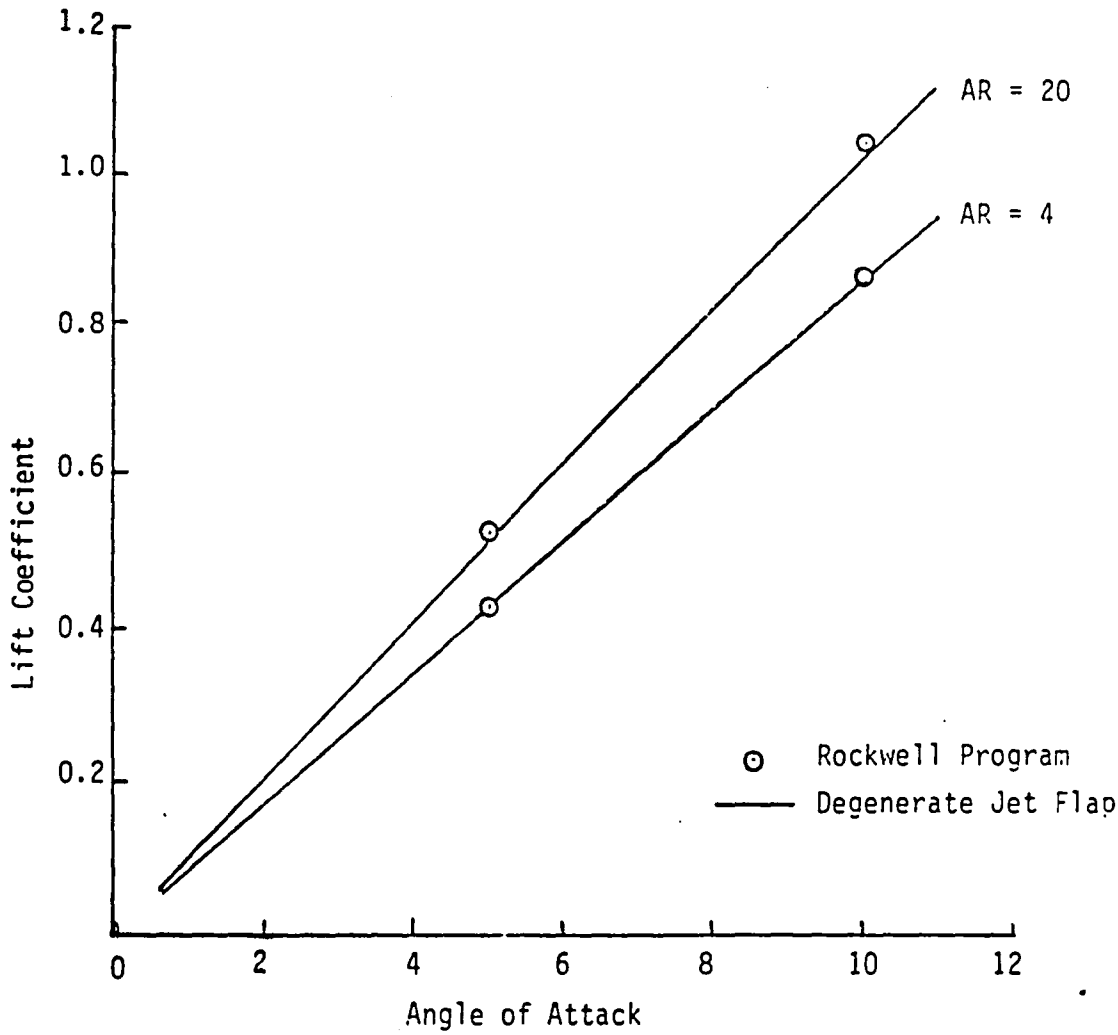

Figure 5 : Lift Coefficient of a Flat Plate Wing
(Uniform Loading)

rectangular wing with an aspect ratio of 4.05 and a jet exit angle of 80 degrees was used. These results are considered interference-free in view of the small model to tunnel ratios used in both the experiments. The former experiments are referred to as 'Williams data' while the latter as 'UWAL data' in this dissertation. The nonlinear theory used for comparison is the the one by Addessio et al [23].

It should be mentioned that the models used in these experiments were too thick for the results to be compared with those theories which assume a flat plate wing. Spence [17] derived a formula and arrived at a factor by which the analytical lift coefficient should be multiplied to account for the thickness of the experimental wing. Spence did this for the elliptic wing used in William's experiments. Lissaman [21] later generalized Spence's analysis to include wing of arbitrary planform and thickness ratio. Based on the wing parameters, this factor has an average value of 1.08 for the wing of ref. 28 and 1.11 for the UWAL wing. Thus the results obtained from the present analysis are appropriately adjusted.

Figure 6 shows the variation of lift coefficient with angle of attack for the wing of ref. 28. Results from the present analysis and from the nonlinear theory of reference 23 are also shown. The present results are quite acceptable in view of the simple representation used.

For the same wing the variation of lift coefficient at zero angle of attack with changes in the jet momentum coefficient are provided in

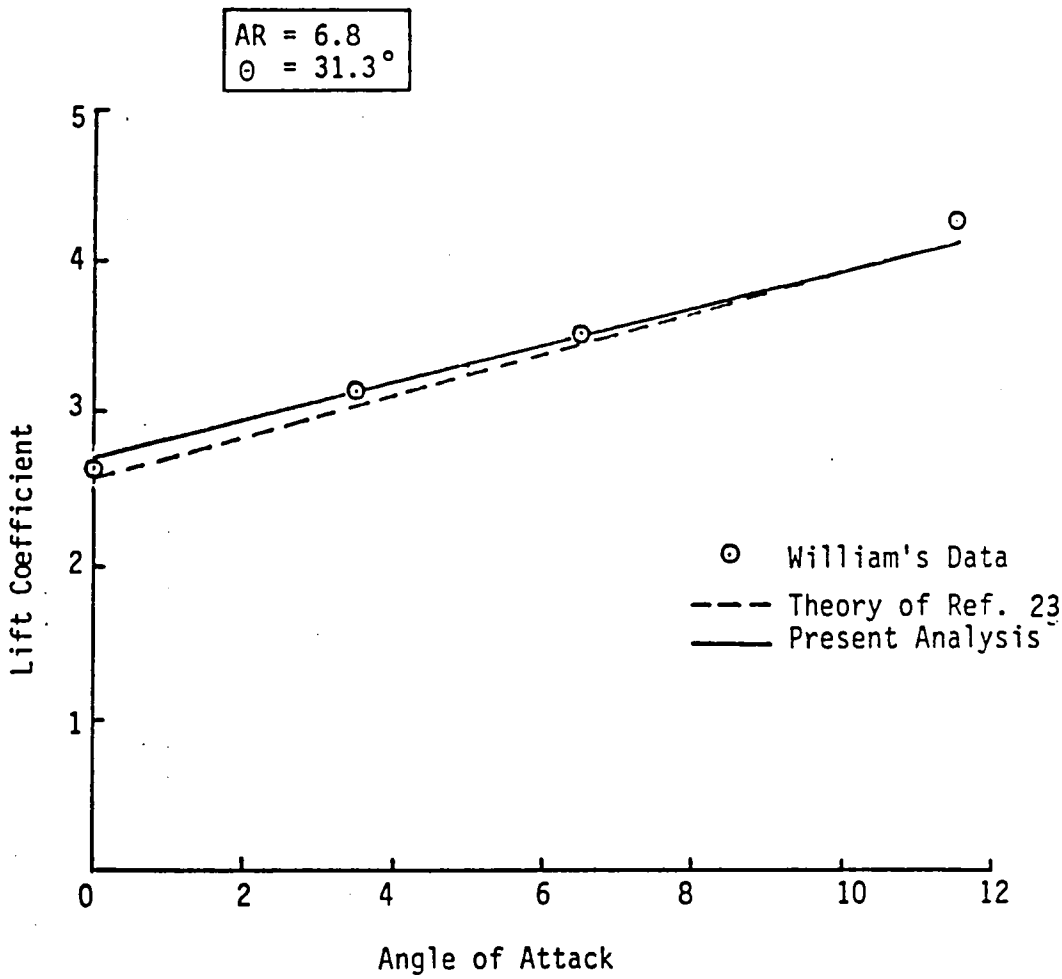

Figure 6 : Variation of Lift Coefficient with Angle of Attack.

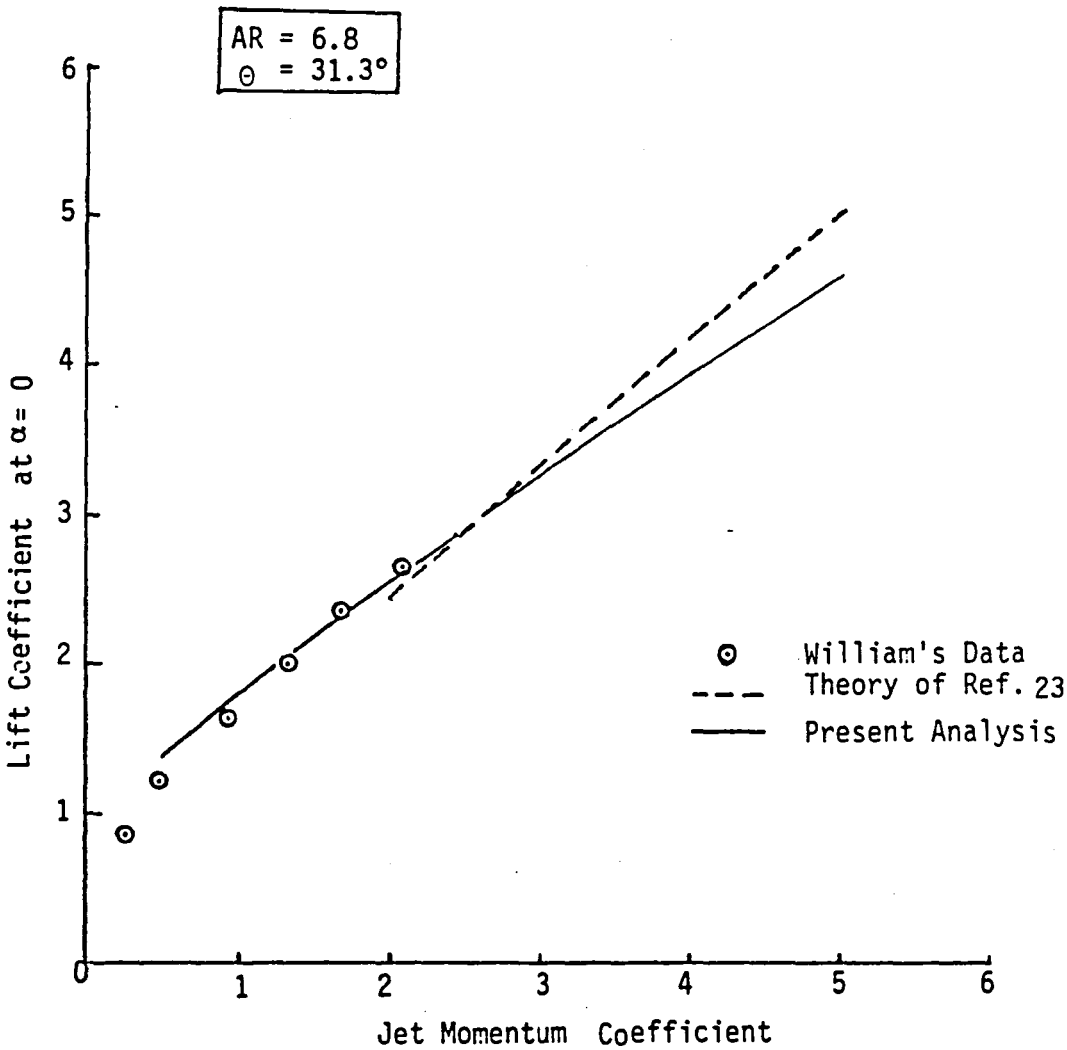

Figure 7 : Variation of the Lift Coefficient with Jet Momentum for $\alpha = 0$.

figure 7. At lower jet momentum coefficients the agreement with the experimental data is good, while at larger jet momentum coefficients (nonlinear region) the agreement with the theory of reference 23 is not so good. The discrepancies may be due to differences in formulation of the problem used in these theories. Further, reference 23 does not give any comparisons for the results at high jet momentum coefficients (non-linear region). On the other hand the present theory has been compared with highly nonlinear results from the UWAL experiments.

The present analysis was next used to compare results from the UWAL experiments. Since the jet exit angle was a high 80 degrees and since large jet momentum coefficients were used, the results of UWAL experiments can be considered nonlinear and give a correct test to the computer simulation model developed here.

Figure 8 shows the variation of lift coefficient at zero angle of attack with jet momentum coefficient. As can be seen excellent agreement is obtained. For jet momentum coefficients beyond 4.0, convergence difficulties were encountered and a converged solution could not be obtained. For this reason, results are not obtained at jet momentum coefficient larger than 4.0, instead the curve is extrapolated as shown by the broken line. It may be mentioned that contribution of the jet reaction to the total lift varies from 0.49 at jet momentum coefficient of 0.5 to 3.94 at jet momentum coefficient of 4.0.

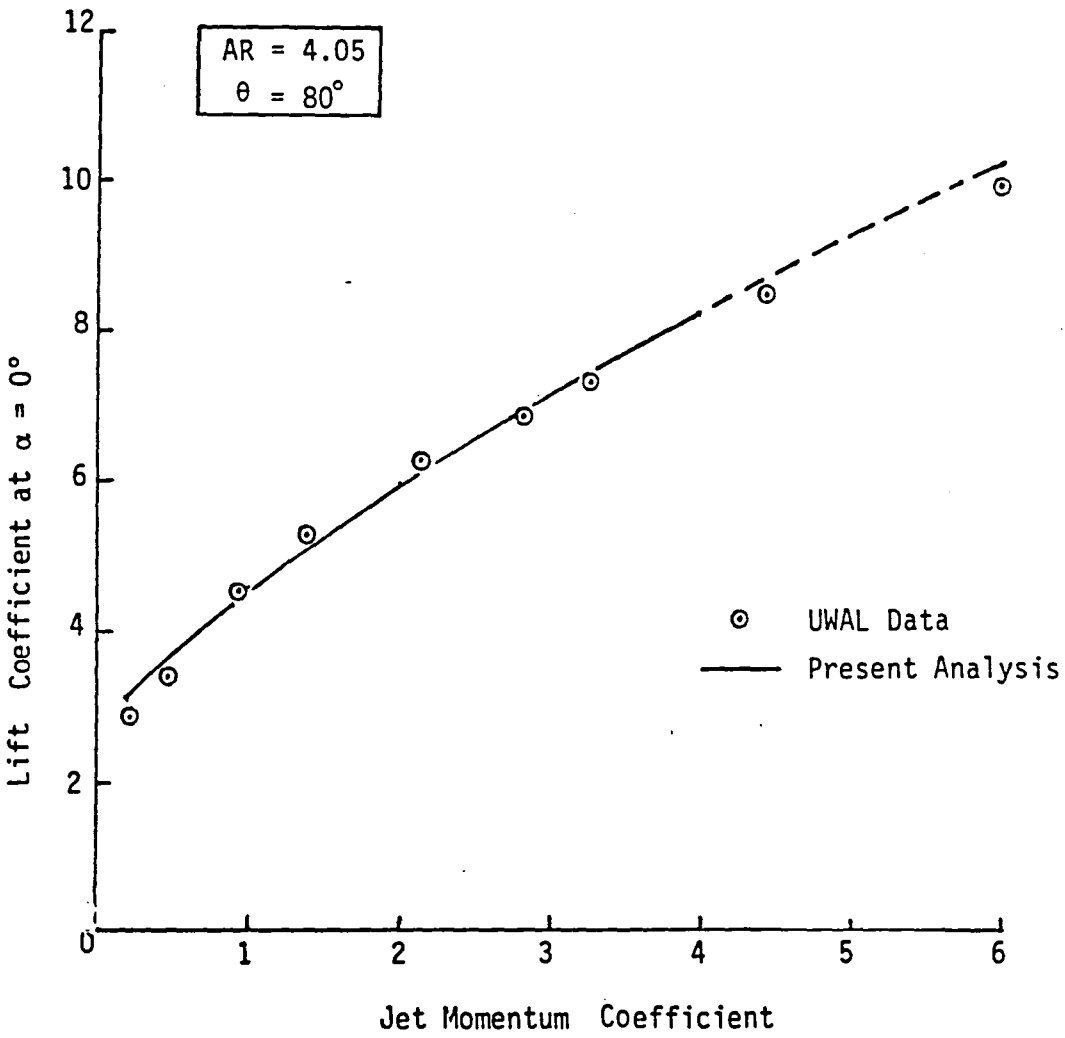

Figure 8: Variation of Lift Coefficient with Jet Momentum for $\alpha = 0$.

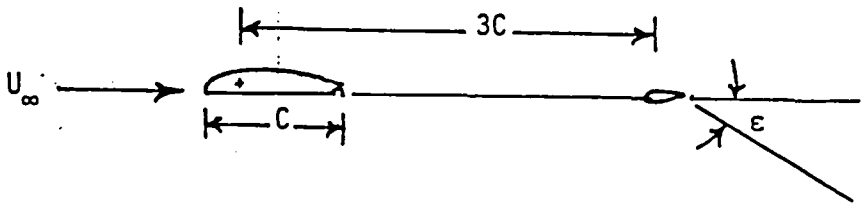

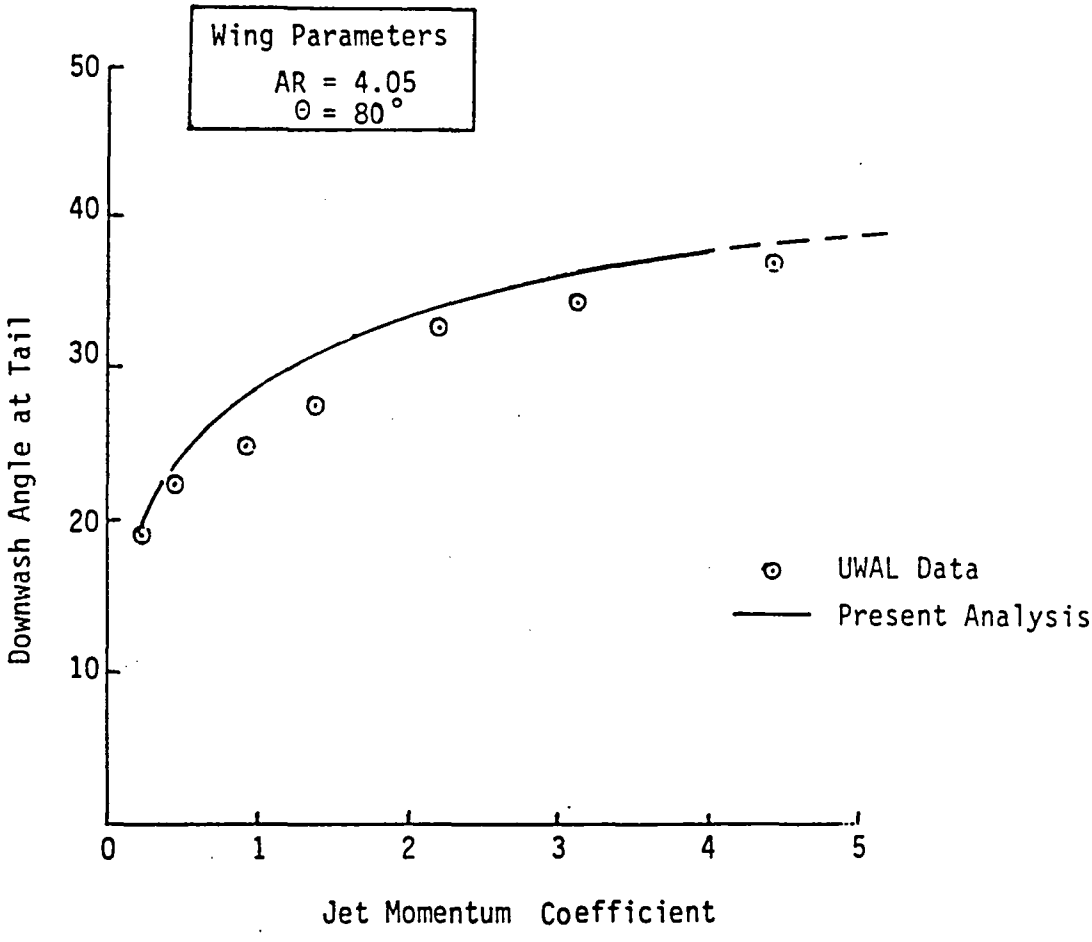

Figure 9: Variation of Downwash at Tail with Jet Momentum for Wing $\alpha = 0^\circ$

In the UWAL experiments, a tail of 1 foot span and an aspect ratio of 4.0 was mounted three chord lengths behind the wing. The tail was non-metrically mounted to the main balance fairing and a separate balance was used to measure forces on it. This data, along with the known lift characteristic of the tail section were used to calculate the downwash experienced by the tail. The angle of this downwash is compared with that obtained with the present analysis for different jet momentum coefficients and zero wing angle of attack (fig. 9). Once again a reasonable agreement is obtained. Any discrepancies may be due to the simple modelling used here and may partially be due to the fact that downwash angles in the test were derived from the force data.

The next two figures, 10 and 11, compare the variation of lift coefficient with angle of attack for jet momentum coefficients of 0.55 and 1.0 respectively. An excellent agreement is obtained. The setup of the computer program used for this analysis was such that correct converged results could not be obtained if any of the vortex segments was inclined at more than 90 degrees to the free stream direction. It was purely a matter of changing the computer program to correct the situation, but required a lot of changes and hence was not attempted. The jet exit angle being 80 degrees in UWAL test, results were thus limited to an angle of attack range of -15 degrees to 9 degrees and the curve extrapolated for angle of attack greater than 10 degrees. This is shown on figures 10 and 11 by the broken line.

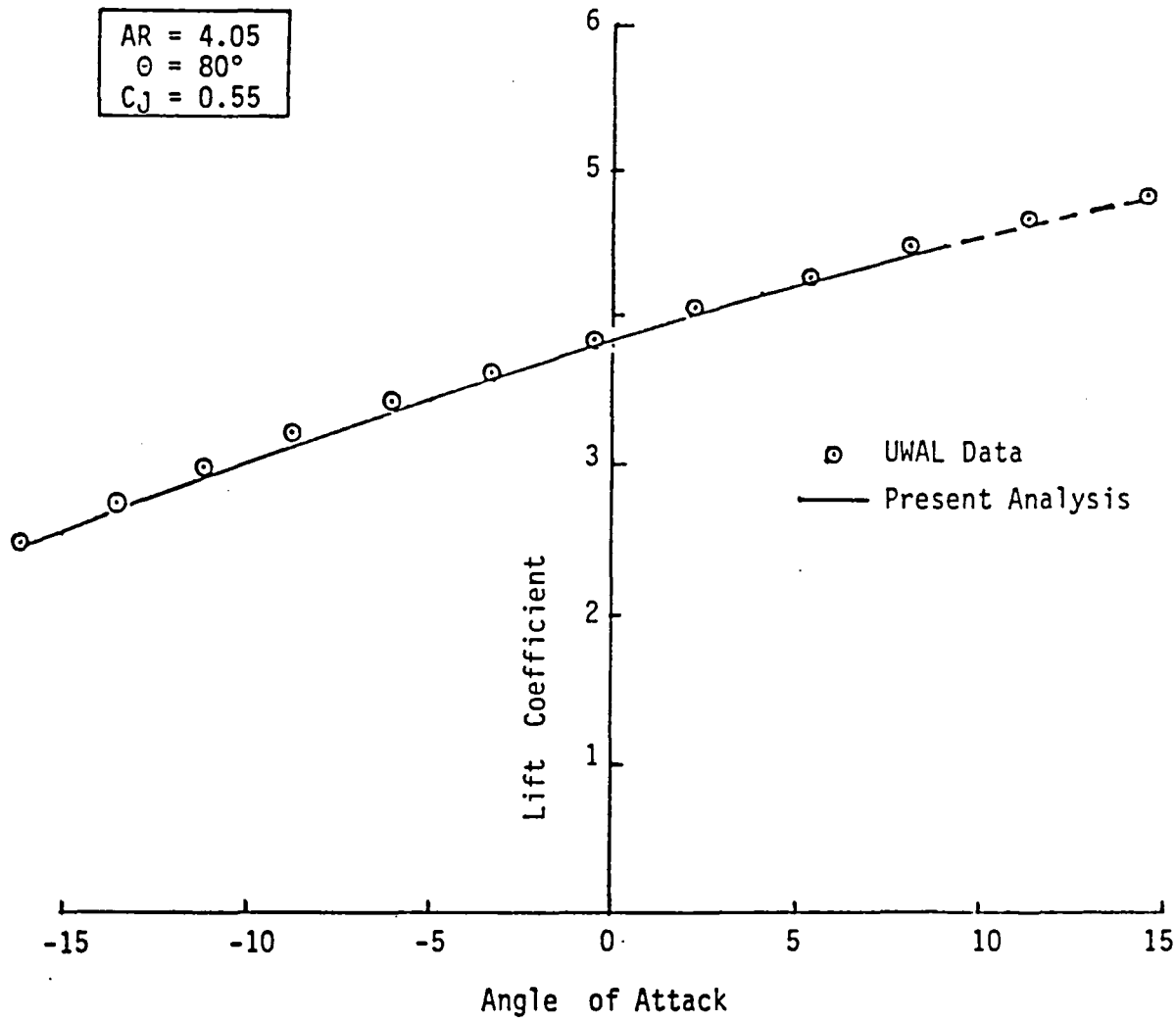

Figure 10: Comparison of Experimental and Numerical Results

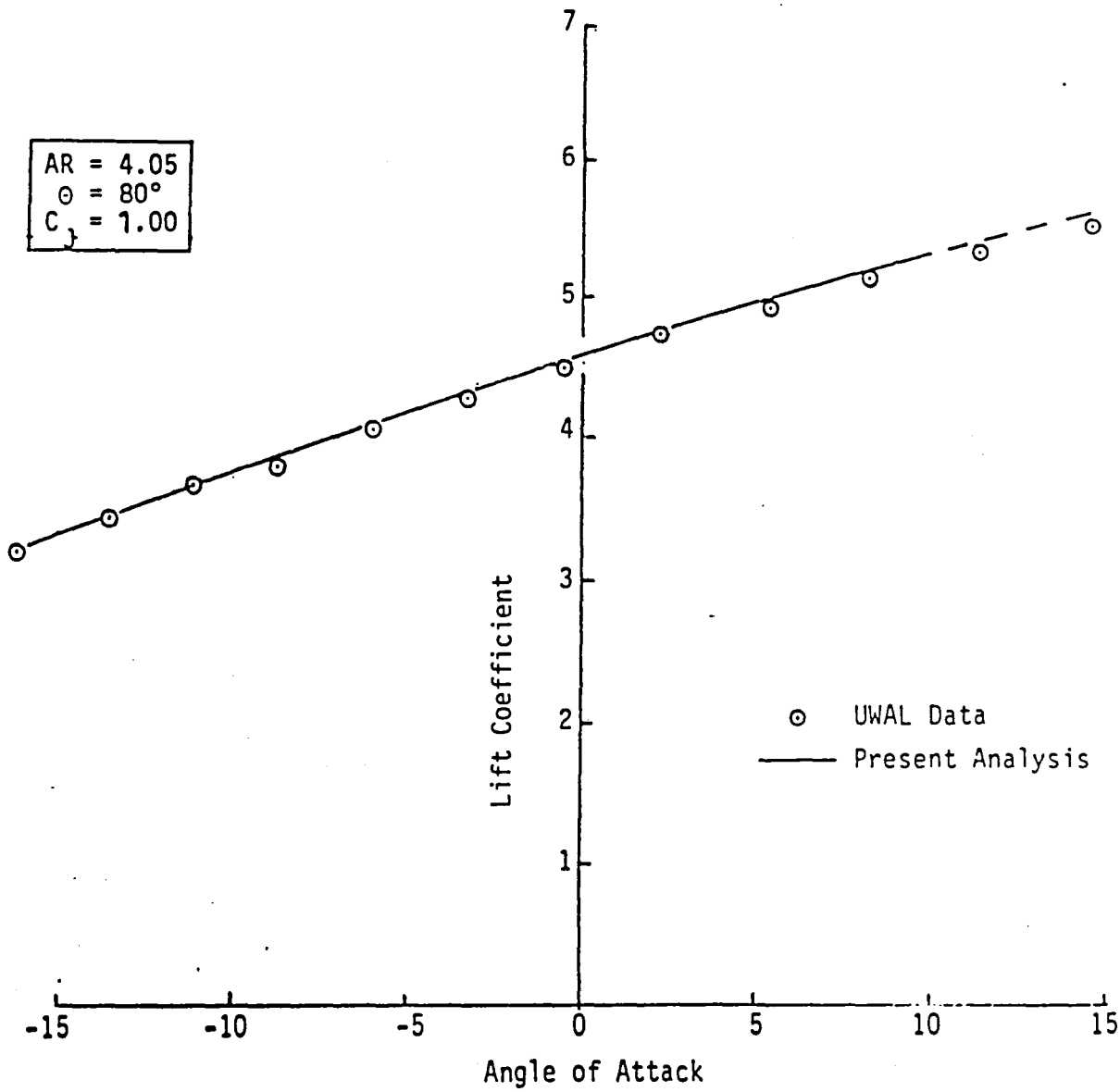

Figure 11:Further Comparison of Experimental and Numerical Results.

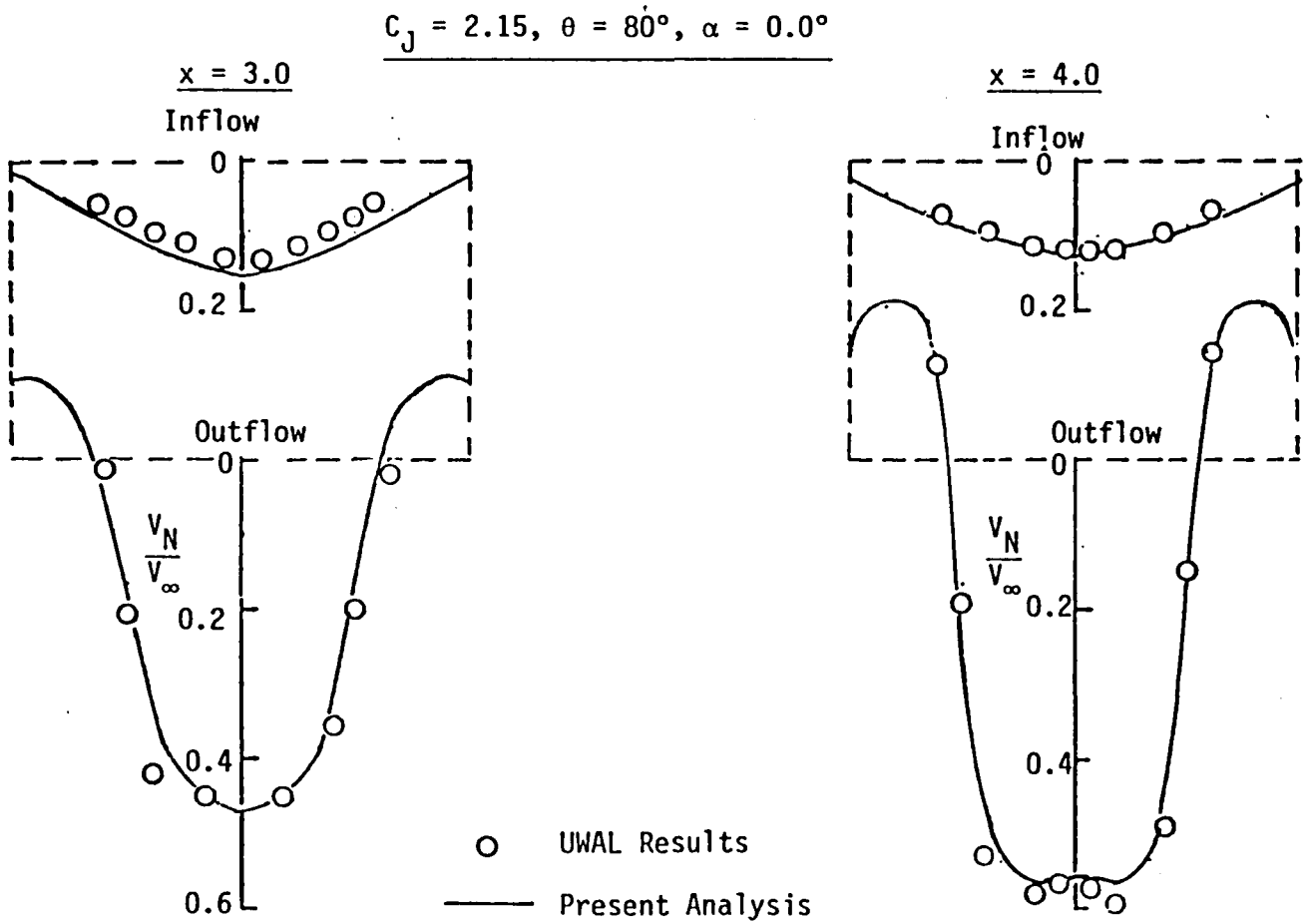

Figure 12: Distribution of Flow Normal to Control Surface

For higher jet momentum coefficients the flow may separate at the leading edge producing viscous effects and the present potential formulation will not be expected to give correct results. Thus no comparisons are made for higher jet momentum coefficients. Comparison of drag data is also not made, since experimental drag has viscous contribution.

Finally, the ability of the computer program to predict the far field effects, such as the induced velocity at tunnel wall locations, was checked. In the UWAL experiments flow field surveys were conducted, with the model in (8 x 12-ft) test section, to measure velocity component normal to some fictitious control surfaces. These results are compared with those calculated using the free air solution in figure 12, for two locations downstream of the model.

In conclusion, the present theory seems adequate for the purpose of interference study, namely estimation of total lift and far field effect such as induced velocity on the tunnel wall locations, and the results presented in this section show that potential flow analysis may be used for the purpose of studying the problem of wind tunnel wall interference.

CHAPTER 4

CLOSED TUNNEL SOLUTION

One of the steps in a practical controlled flow tunnel involves measurement of lift on a model in a closed tunnel. The numerical equivalent of this requires a suitable representation of the tunnel walls and a solution of the model-in-the-tunnel problem so that lift on the model in the presence of a tunnel can be calculated. As mentioned earlier, the effect of the tunnel on the relocation of the trailing wake needs to be calculated. Once this is done, the concept of the controlled flow tunnel can be explored numerically by employing suitable modifications to this closed tunnel program.

4.1 Vortex Lattice Representation of a Closed Tunnel:

In the classical interference theory, the effect of the tunnel on the model (the interference effect) is accounted for by using images of the lifting system outside the tunnel. In an iterative process such as the one here, the image system has some disadvantages. The curved trailing vortices have curved images. Furthermore, since the shape of these vortices change from iteration to iteration, so will that of the images. Besides proper images are only available for a rectangular tunnel. In view of these limitations, Joppa proposed an ingenious alternative for representing the tunnel walls [10]. In his method, tunnel walls are replaced by a network of vortex lattices composed of a finite number of interconnecting vortex rectangles which lie in the plane of the tunnel walls. Each vortex rectangle has a

circulation strength (Γ_T) associated with it. The closed wall boundary condition is satisfied at the center of each rectangle, referred to as the control point, by requiring that the normal component of velocity vanish. This method has the computational advantage that the geometry of this system is unchanged during each iteration and that it is applicable to any tunnel cross section insofar as the test section can be approximated by a polygon of equal length segments. The representation of a long tunnel requires a slightly different treatment. Consistent with the representation of the long last segment of the trailing vortex of a jet flapped wing, at far downstream only longitudinal vorticity should exist on the tunnel walls. This is done by elongating the last ring of vortices, while keeping the control points at the same location with respect to the last circumferential station. Figure 13 shows the vortex lattice representation for a rectangular closed wind tunnel with long length.

4.2 Solution Procedure:

The jetflap-in-the-tunnel solution requires accounting for both the effect of the tunnel on the model in terms of wake relocation and the effect of the model on the normal velocity at tunnel control points. This is accomplished in an iterative manner and is described in this section.

First the potential flow solution of the model in free air is obtained by alternately solving the kinematic and the dynamic boundary conditions (2-D solution) and by relaxing the trailing vortex wake

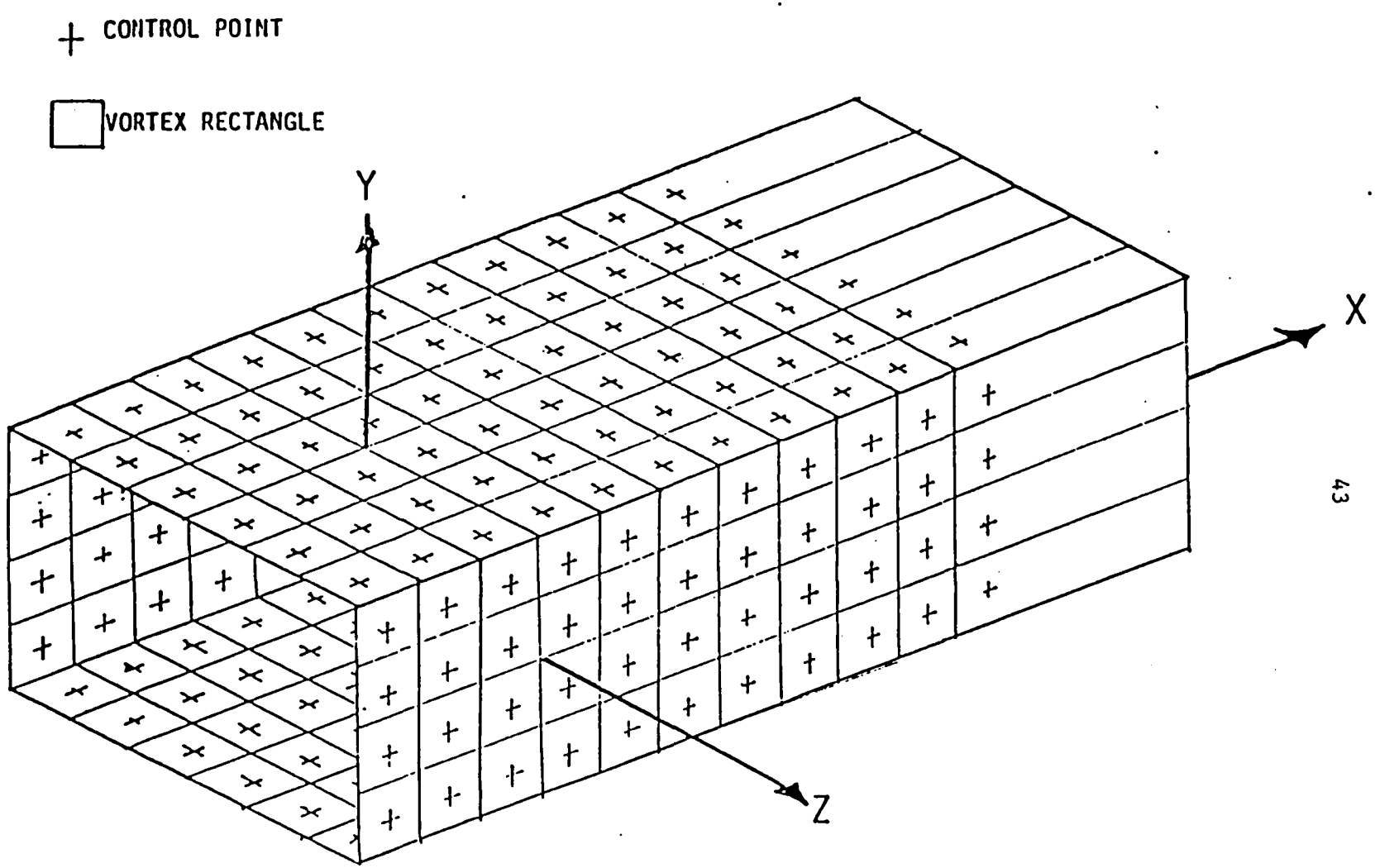

Figure 13: Representation of a Rectangular Tunnel by Vortex Lattice of Square Vortex Rings.

(3-D solution), until convergence is obtained. Next this model is enclosed in the tunnel and values of the strength of vortices representing the tunnel are found by satisfying the zero through flow boundary condition at M tunnel control points. The normal velocity at an arbitrary tunnel control point is equal to the sum of the induced velocities due to the lifting system and due to the vortex lattice network. Upon extension to include all control points, the following matrix expression results:

$$\{B\}[\Gamma_T] + [V_{MT}] = 0 \tag{4.1}$$

where the two terms represent contributions from the tunnel and the model respectively. Here $\{B\}$ is an (M x M) matrix of wind tunnel vortex lattice influence coefficients, representing the effect of the tunnel on itself and $[\Gamma_T]$ is the yet unknown column matrix of dimension M representing the strength of the wall vortex lattices. $[V_{MT}]$ is a column matrix of dimension M, each element of which represents the normal velocity induced by the model at each tunnel control point. This matrix is known from the strength of model vortices and their geometrical location in relation to control points on the tunnel. Solution of this set of equations gives strength of vortex rectangles representing the tunnel with the lifting system enclosed.

$$[\Gamma_T] = -\{B\}^{-1} [V_{MT}] \tag{4.2}$$

This accounts for the effect of the model on the tunnel. The next step is to take the presence of the tunnel, as represented by vortex lattices, on to the model. This is done by suitable modifications to the free air solution to account for the tunnel presence. The kinematic and the dynamic boundary conditions are alternately satisfied each time taking the velocity induced by the tunnel into consideration. Tunnel effect is also taken during the wake relaxation process to get the relocated wake due to the presence of the tunnel. In matrix form the equation below is solved:

$$\{A\}\ [\Gamma_m] + [V_n] + [V_{TM}] = 0 \qquad (4.3)$$

Here the first two terms are the same as in free air solution, equation (3.1), representing the effect of the model on itself and that of the freestream on the model respectively. $[V_{TM}]$ is a column matrix of dimension N representing the tunnel effect at N model control points and depends on knowing the matrix $[\Gamma_T]$ and the locations of the model control points in relation to the tunnel. Solution to this set of equations produces $[\Gamma_m]$ which represents the strength of vortex segments of the jet flap inside the tunnel. While taking the tunnel effect on the model both longitudinal as well as vertical velocity contributions are taken, accounting for interference in both these directions. With this new model solution, the column matrix $[V_{MT}]$ differs from its previous value because of the vortex wake relocation and hence equation (4.2) is solved again to get revised tunnel vortex strengths. This iterative process is repeated

until a predefined convergence criterion is satisfied. Once a converged solution is obtained, representing the strengths of model vortex segments and tunnel vortex lattices, flow field at any point in the tunnel can be found by repeated use of the Biot-Savart law.

A listing of the computer program for the solution of the jetflap in closed tunnel problem is given in Appendix B.

4.3 Computational Results:

Computational results are described in this section and comparison is made with other available information. As done for the jet flap in free air case, comparison between the degenerate jet flap and the Rockwell program [27] are shown first. For this comparison, results were obtained on an uniformly loaded (one pair of trailing vortices) flat plate wing of 4.05 aspect ratio in a closed tunnel of (3.14 x 4.71 ft) test section. The tunnel was represented using 240 square vortex rings with 20 vortices along the circumference of the cross section. Comparison of lift coefficient versus the angle of attack is shown in figure 14. Excellent agreement is obtained, giving confidence in overall set-up of the tunnel program.

A further test of the validity of the computer simulation model is made by calculating the distribution of the interference factor along the center line of a (6 x 6 ft) wind tunnel with a degenerate jet flap of aspect ratio 4.0 at its center. The interference factors for this purpose were calculated by summing the induced velocity due to all the vortex rectangles representing the tunnel walls and then

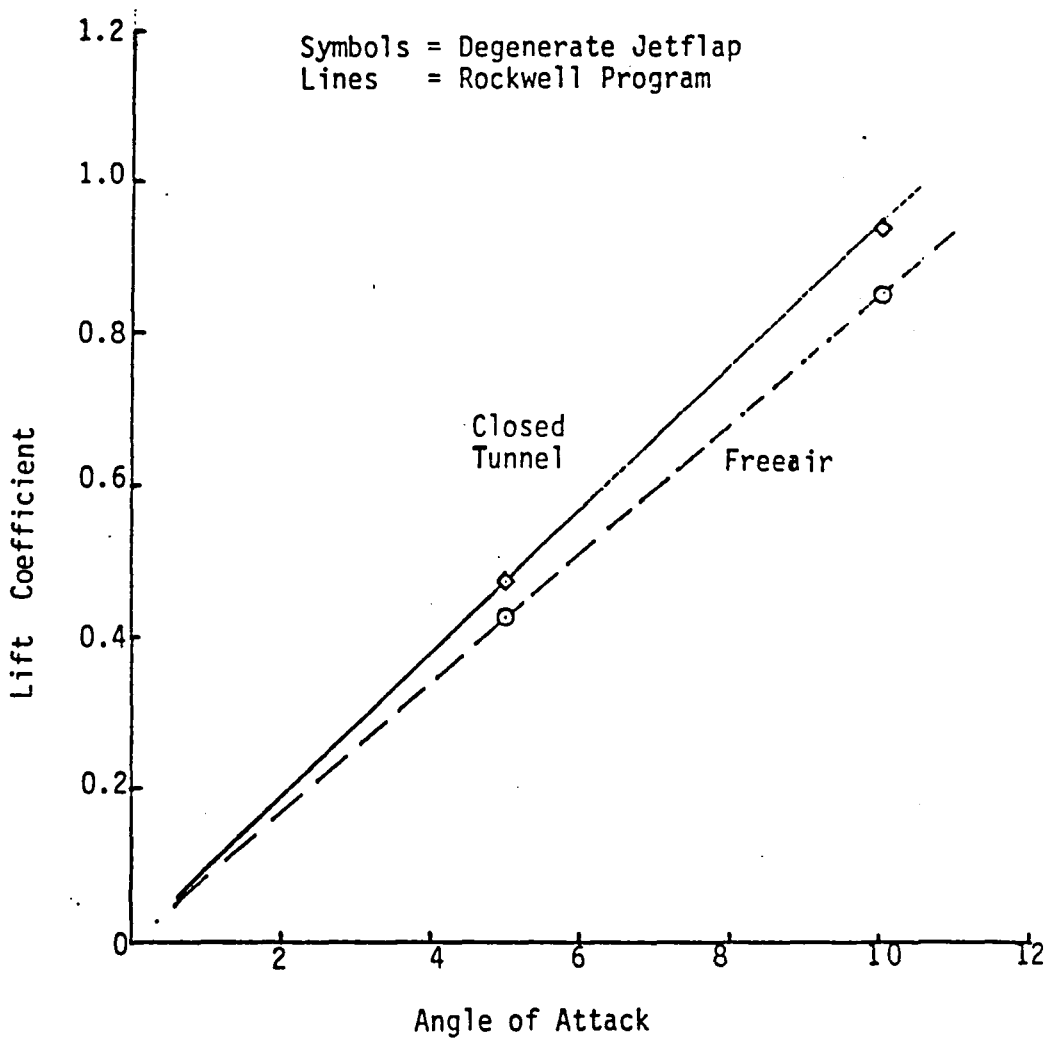

Figure 14: Flat Plate Wing of AR=4.05 in a Closed Tunnel

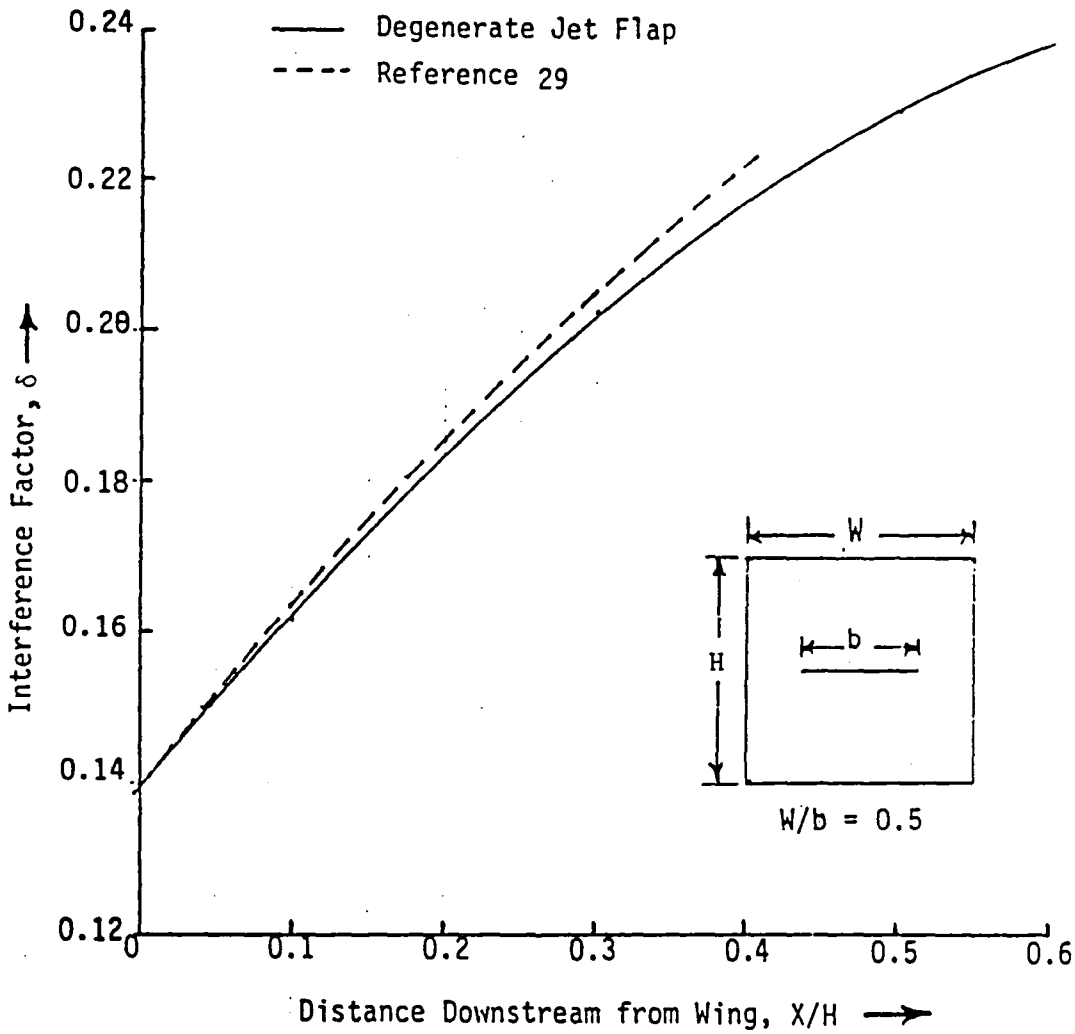

Figure 15 : Comparison of Interference Factors with Classical Values for a Square Tunnel.

using the following classical relation.

$$\delta = \frac{w\ C}{C_L U_\infty S_w} \tag{4.4}$$

Here w is the vertical component of the induced velocity, C is the tunnel cross section area, S_w is the wing area and C_L is the lift coefficient in the tunnel. The results so obtained are compared in figure 15 with those taken from reference [29] which uses Glauert's concept of images, and a very good agreement is obtained. For this comparison 20 vortex segments were used to represent tunnel cross-section. As shown by Joppa [10] a better correlation could be obtained by representing the tunnel by a larger number of vortex lattices.

Computational results were then obtained to correlate with the UWAL experimental results. In these experiments a full span jet flapped wing of aspect ratio 4.05 was first tested in the UWAL (8 x 12 ft) wind tunnel over a range of angles of attack and jet momentum coefficients. These results can be considered interference-free in view of the small model to tunnel ratio. The wing characteristics were then obtained in a smaller test section which was simulated by inserting a rectangular test section of size (3.14 x 4.71 ft) and 11.5 ft long in the bigger UWAL tunnel. The cross section of the insert was small enough to give large interference.

For comparison with the UWAL data, the small insert test section was represented in the numerical simulation by 70 vortex rectangles with 10 vortex rectangles along the circumference of the tunnel cross

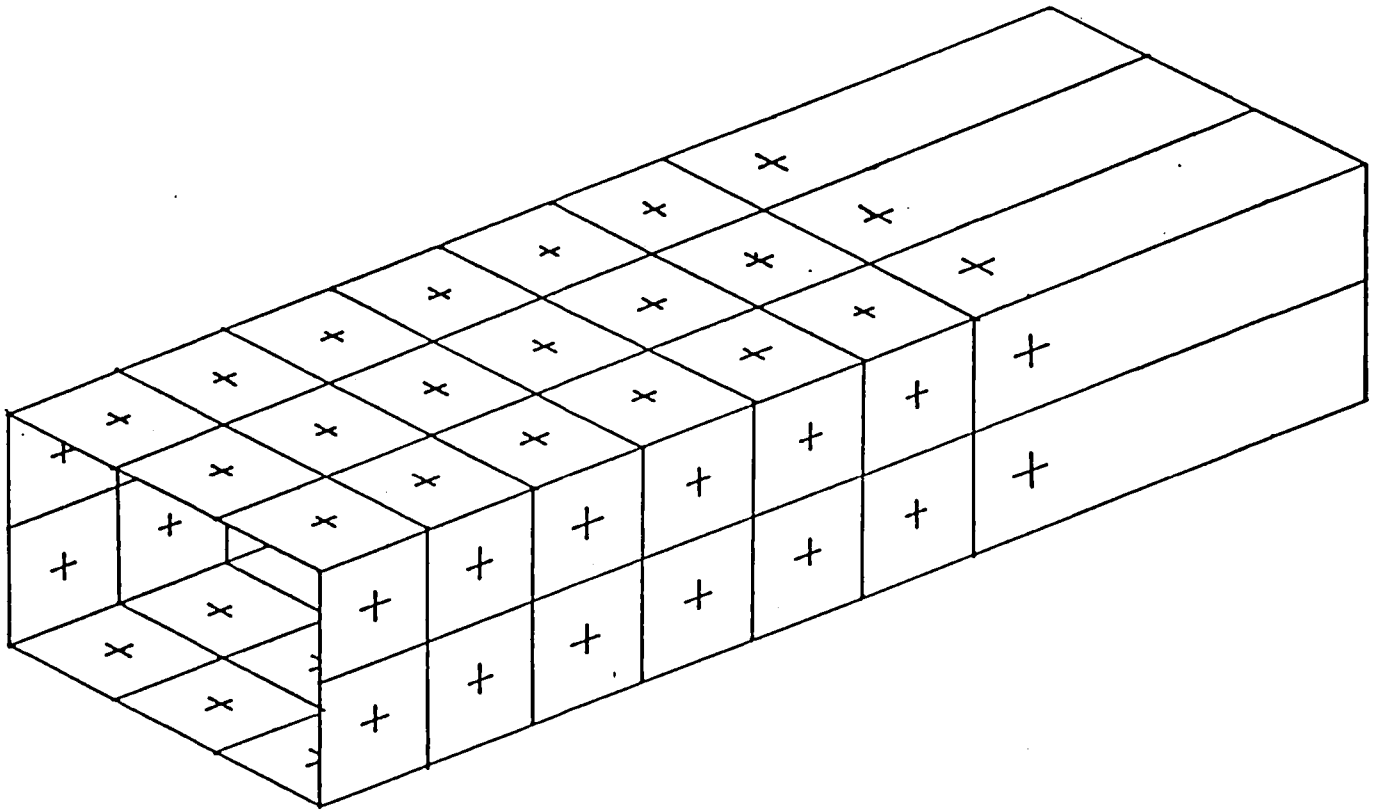

Figure 16: Vortex Lattice Representation of UWAL Closed Insert Simulated as an Infinitely Long Test Section

section. The vortices in the last ring were elongated to simulate an infinitely long test section, figure 16. It may be noted that as in any vortex lattice simulation the final results will depend, among other parameters, upon the number of vortices used to represent the tunnel(with larger number being better). A parametric study to find, among other things, the effect of number of vortices on the overall results was carried out and is reported in the next section. For the comparisons in this section, however, the above representation is used to get a look at computational trends.

The variation of lift coefficient with the angle of attack is compared with the UWAL data for two jet momentum coefficients of 0.55 and 1.00 in figure 17 and 18 respectively. For the lower jet momentum coefficient the agreement is excellent. However, for the higher C_J the lift curve slope does not agree very well. This disagreement was further explored and the results are reported in the next section. It may be noted that as for the free air case, correct results could not be obtained for the cases where the sum of the jet exit angle and the angle of attack exceeded 90 degrees. Hence the curve is extrapolated and the results are shown by broken line. Figure 19 shows the effect of the tunnel in relocating the trailing vortex wake. As expected the upwash due to the presence of the tunnel results in a lesser vertical penetration of the wake. Though not conclusive due to the unrefined nature of the tunnel representation (fewer vortex lattices to represent tunnel), the above results do show the success of the model-in-the-tunnel solution in showing the correct effect of

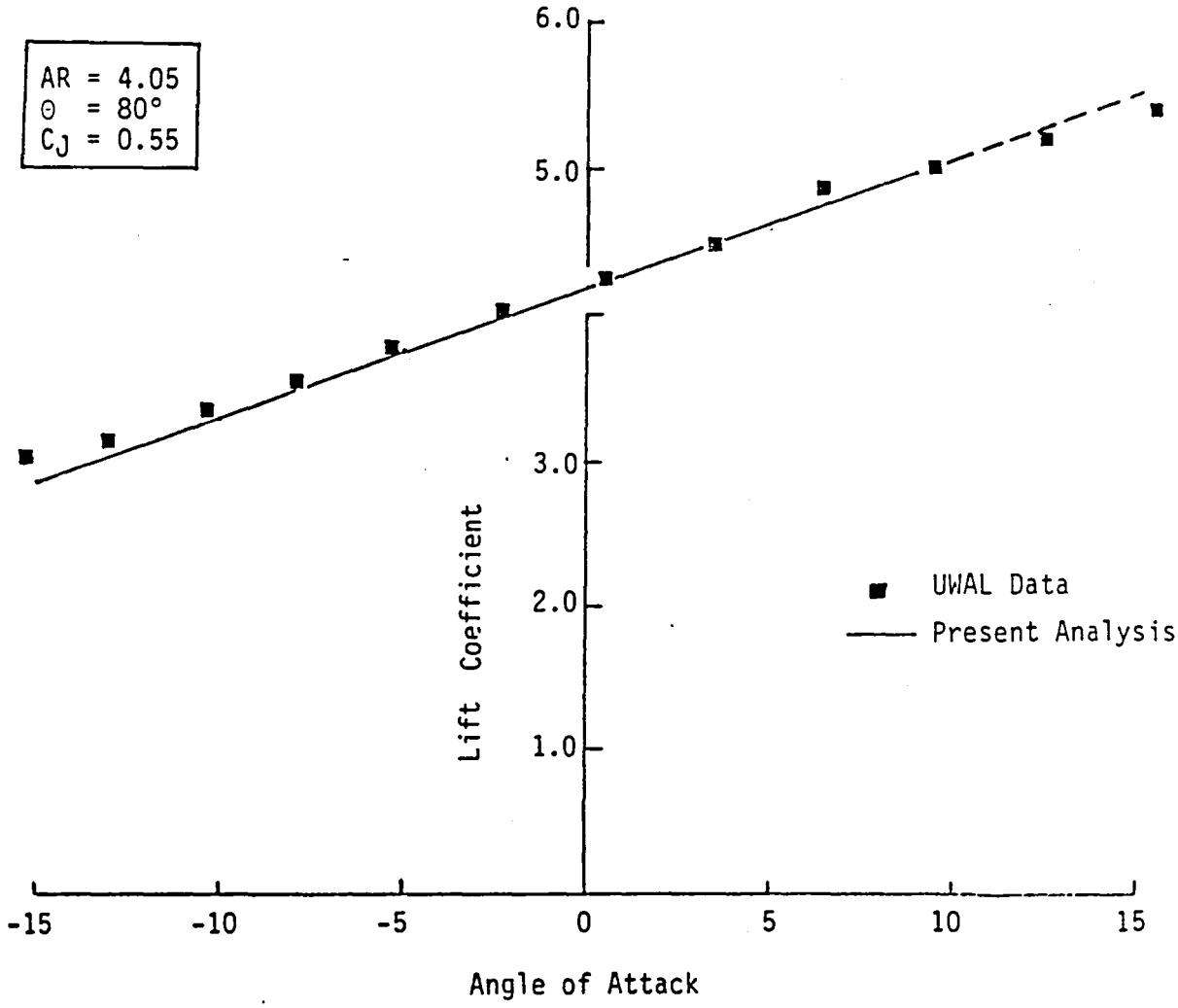

Figure 17: Comparison with Experimental Data.

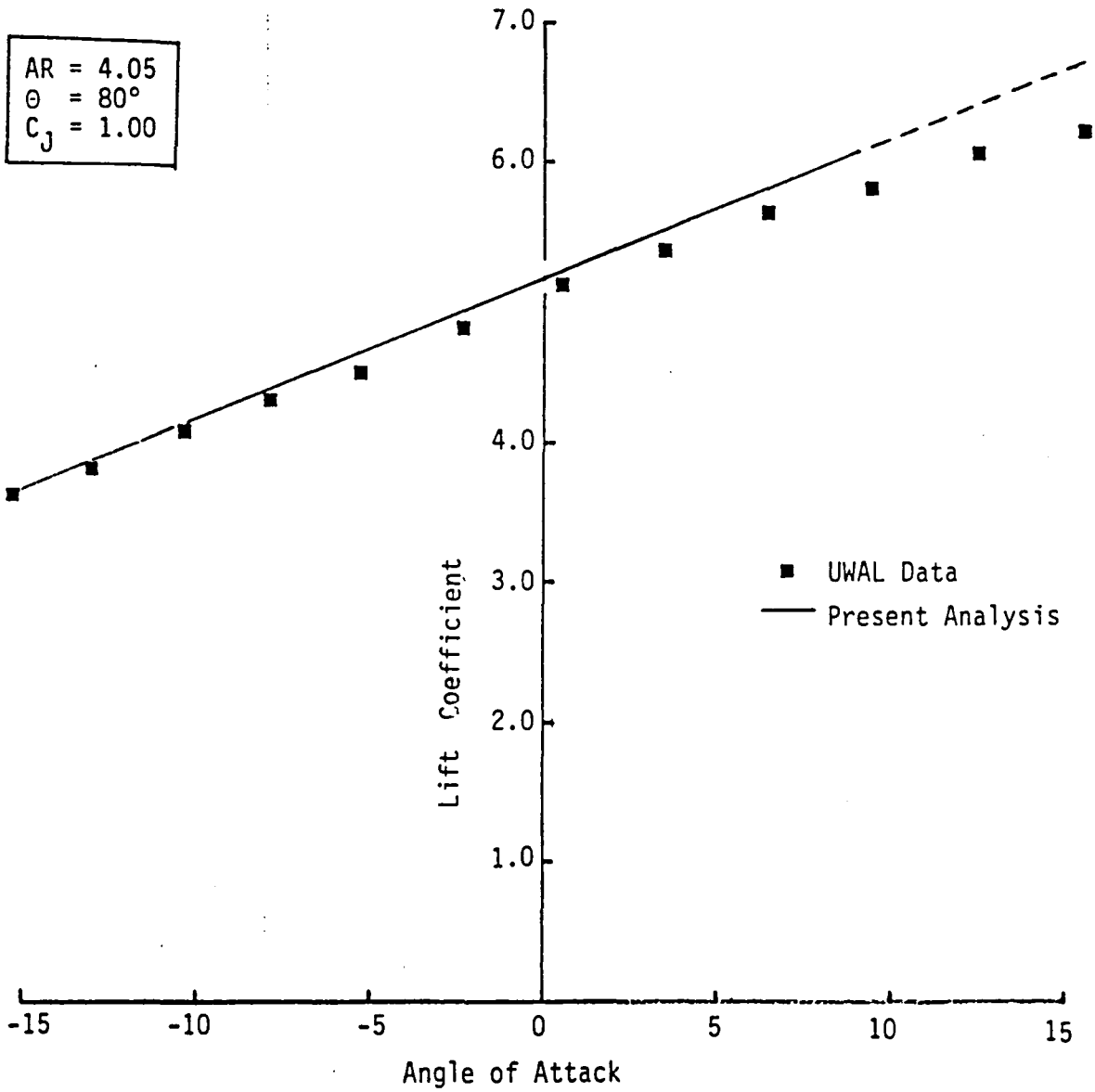

Figure 18: Further Comparison with Experimental Data

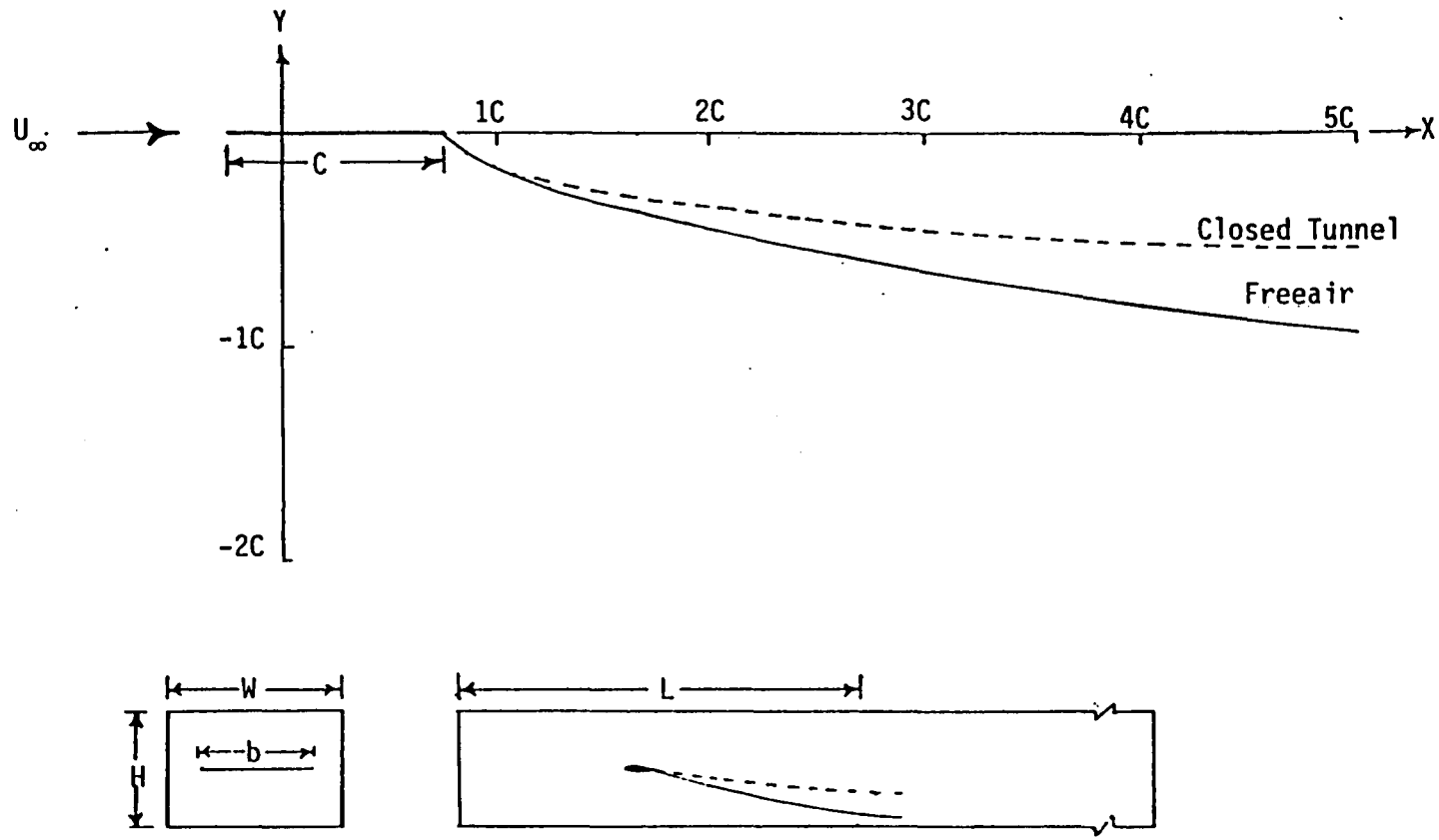

Figure 19: Vortex Wake Relocation in the Tunnel

the tunnel on lift coefficient and on the relocation of the trailing vortex wake.

4.4 Parametric Study of Input Variables:

Several input variables exist in the program which are selected by the user. In order to study the effect of the selection of these parameters on the final results, a numerical study was conducted. The study involved variation of one parameter over a reasonable range of values keeping others constant, and comparison of final results. Parameters describing both the model and the tunnel were considered.

For the model the parameters considered were the number of vortex segments representing the model chord and trailing wake, and the convergence limits. The jet flap free air program was run with a jet momentum coefficient of 1.0, a jet exit angle of 80 degrees and an angle of attack of 0.0 degree. The lift coefficient on the model and the angle of downwash at tail located 3 chord lengths behind the wing were monitored while a given parameter was changed.

With a variation of the number of vortices in the model chord from 6 to 12, a less than 2% change in C_L was observed, while the angle of downwash remained almost constant. The number of segments representing the jet was next varied such that the jet length changed from 1 to 3 chord lengths. A less than 0.5% change in the lift coefficient was observed. However, the angle of downwash changed by as much as 2 degrees. This result is not surprising because with a longer jet a better representation of the trailing wake resulted.

Finally, the sensitivity of final results to a change in the convergence limits was studied. Only the number of iterations required for convergence was affected. Based on these results, a value for each parameter was selected for all the computations.

For the tunnel the parameters studied were the length of the test section and the vortex lattice density representing the tunnel. As the closed insert used in the UWAL tests was of a fixed length, the effect of the finite test section was selected to be the first parameter to be explored. The variation of lift coefficient with the angle of attack in an infinite length tunnel has already been shown in figure 17 and 18. Next to represent a shorter tunnel, the last ring of vortex rectangles was shortened so that the total length of the tunnel roughly corresponded with the actual insert length (10.99 ft in the computer simulation against 11.5 ft in tests), figure 20. The resulting variation of lift coefficient with the angle of attack is shown in figure 21 for two jet momentum coefficients alongwith the experimental as well as the long tunnel results. As can be seen the short tunnel representation agrees better with the experimental data as it more closely represents the closed insert used in the experiments. For the negative range of the angles of attack the results are mostly unaffected by the tunnel length while those for the positive range are affected. This is hardly surprising because at a larger positive angle of attack the vortex wake penetrates more vertically and is closer to the floor compared to the negative angles and hence an obvious effect of tunnel representation in this area.

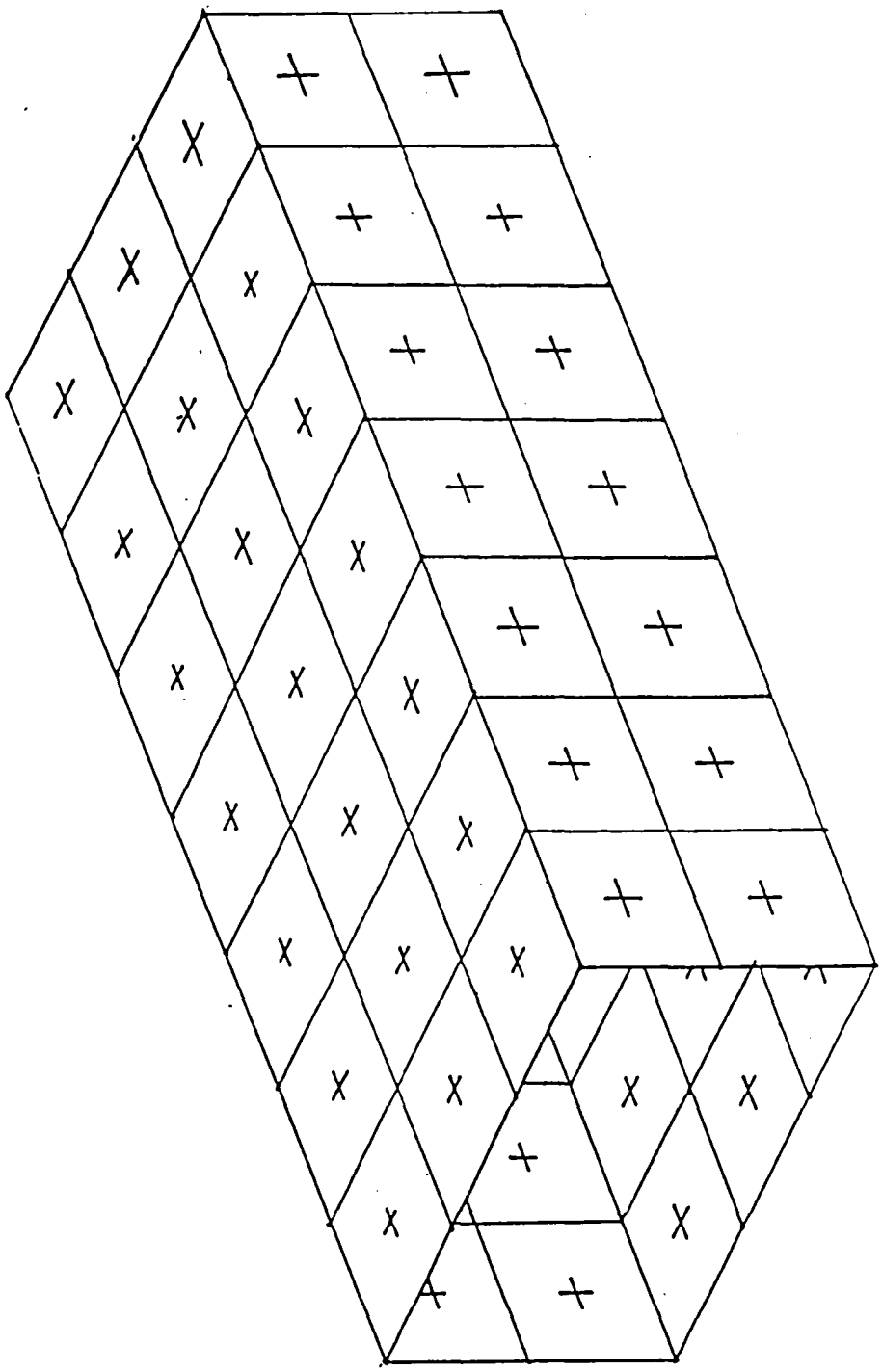

Figure 20: Vortex Lattice Representation of UWAL Closed Insert.

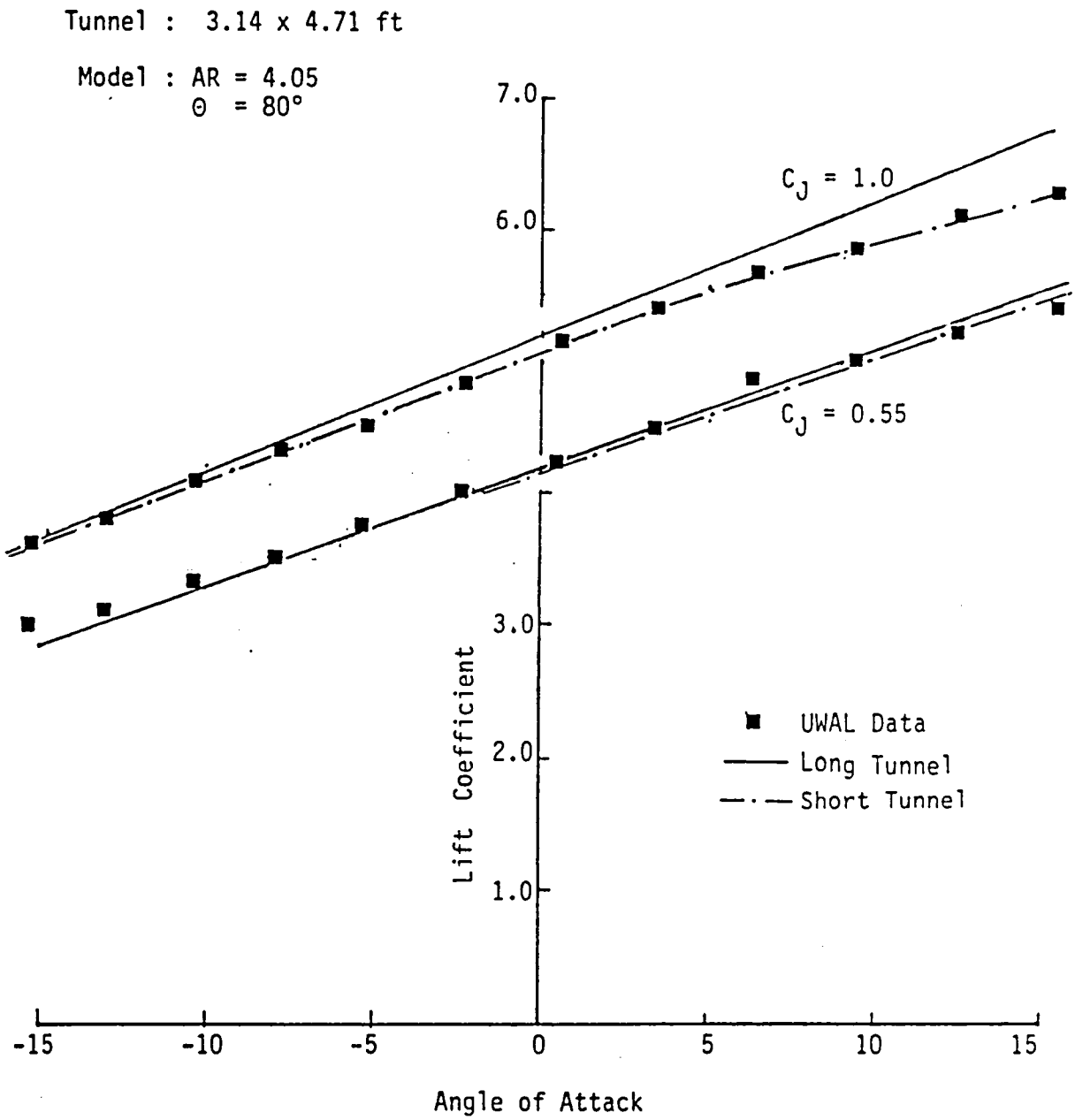

Figure 21: Comparison of Experimental Data against Long and Short Tunnel Results

The results are also substantiated by noting that for a fixed angle of attack the tunnel has larger effect for the higher jet momentum coefficient than for the lower one which has lesser vertical penetration.

Finally the effect of the vortex lattice layout on the overall results was studied. Both the shape of the vortices (rectangle versus square) and its density (number per unit area of the wall) were studied. Some effect on the relocated wake trajectory was observed while neither the lift coefficient nor the angle of downwash changed appreciably.

It can be concluded from the results presented in this chapter that the solution to the model-in-tunnel problem adequately accounts for the effect of the tunnel on the lift of the model and on the vortex wake relocation. The program developed is a numerical equivalent of an important step in the operation of a practical controlled flow tunnel- that of measurement of lift on the model in the tunnel.

CHAPTER 5

CONTROLLED FLOW TUNNEL

The final step in the numerical study of a controlled flow tunnel is to find the numerical equivalent of the feedback process and its effect on the flow around the model. In a practical controlled flow tunnel the amount and location of flow to be controlled would be decided, based on the lift measured in the tunnel, using the computer selector program such as the one developed in chapter 3. This required flow through the tunnel walls would then be achieved using some mechanical flow control device and a new measurement of lift would be made. In the present study the numerical equivalent of this flow control and its effect on the lift of the model remains to be found. This is carried out in this chapter.

5.1 Numerical Simulation of A Controlled Tunnel:

In the present numerical approach the flow through the tunnel walls is calulated using the free air representation of chapter 3 and based on this, a decision is made regarding the locations to be controlled on the tunnel. The effect of this flow control on the model is next calculated by appropriate modifications of the closed tunnel program. These modifications concern the use of correct boundary conditions on the tunnel walls to represent correct flow velocity in or out of the test section.

It may be recalled that the closed tunnel solution is obtained by alternately solving equations (4.1) and (4.3) until convergence is

obtained. The criterion for convergence used there was the difference in the calculated lift of the model between two successive iterations. For the controlled flow tunnel equation (4.1) is modified as follows

$$\{B\}\ [\Gamma_T]\ +\ [V_{MT}] = [V_{FA}] \tag{5.1}$$

Here, as before, the two terms on the left represent the normal velocity induced by the tunnel on itself and that by the model. The M components of the column matrix $[V_{FA}]$ represent the desired net normal velocity through M control points on the tunnel. Their value depends upon whether flow through a given control point is controlled or not. For an uncontrolled point this value is, of course, zero representing a solid wall segment. For a controlled wall segment on the other hand, it is equal to the value the model in the free air would induce at the same angle of attack as in the tunnel. It may be noted that the free air velocity vector being parallel to the tunnel walls has no normal component at the tunnel control points and hence does not appear in the above equation. The solution to the set of equations represented by (5.1) gives the strength of vortices representing the tunnel:

$$[\Gamma_T] = \{B\}^{-1}\ [V_{FA} - V_{MT}] \tag{5.2}$$

Next the lift coefficient of the model in the controlled flow tunnel is calculated by solving equation (4.3) which also takes the effect of the wall flow on the model via the column matrix $[V_{FA}]$. It

may be noted that the effect of the controlled flow on the model wake is taken by considering the model induced velocities during the wake relaxation process, just as in the case of the closed tunnel solution. The changed wake location (and its strength) changes the matrix $[V_{MT}]$ and hence a new solution to equation (5.2) is obtained. This process is repeated until the predefined convergence criterion is satisfied. At the end of this iterative process the value of the lift coefficient would be close to its free air value giving almost interference free results. Of course the degree to which the results from a controlled tunnel represent a free air situation would depend upon the amount and distribution of control used.

A listing of the computer program for the model in a controlled tunnel problem is given in Appendix-C. As mentioned above, this program is made by suitable modifications of the boundary conditions in the model-in-closed-tunnel program of Appendix-B. Thus only the SUBROUTINE AEROC is different between these two programs and hence this changed subroutine only is given in Appendix-C.

5.2 Normal Velocity Survey:

The "ultimate" controlled flow tunnel would duplicate the flow field experienced by a high lift vehicle in free air. For this each control point in the tunnel vortex lattice network has to be actively controlled. The result of such a process would eliminate all flow distortions caused by the tunnel wall boundaries, resulting in data requiring no corrections. A scheme to carry out such a process would

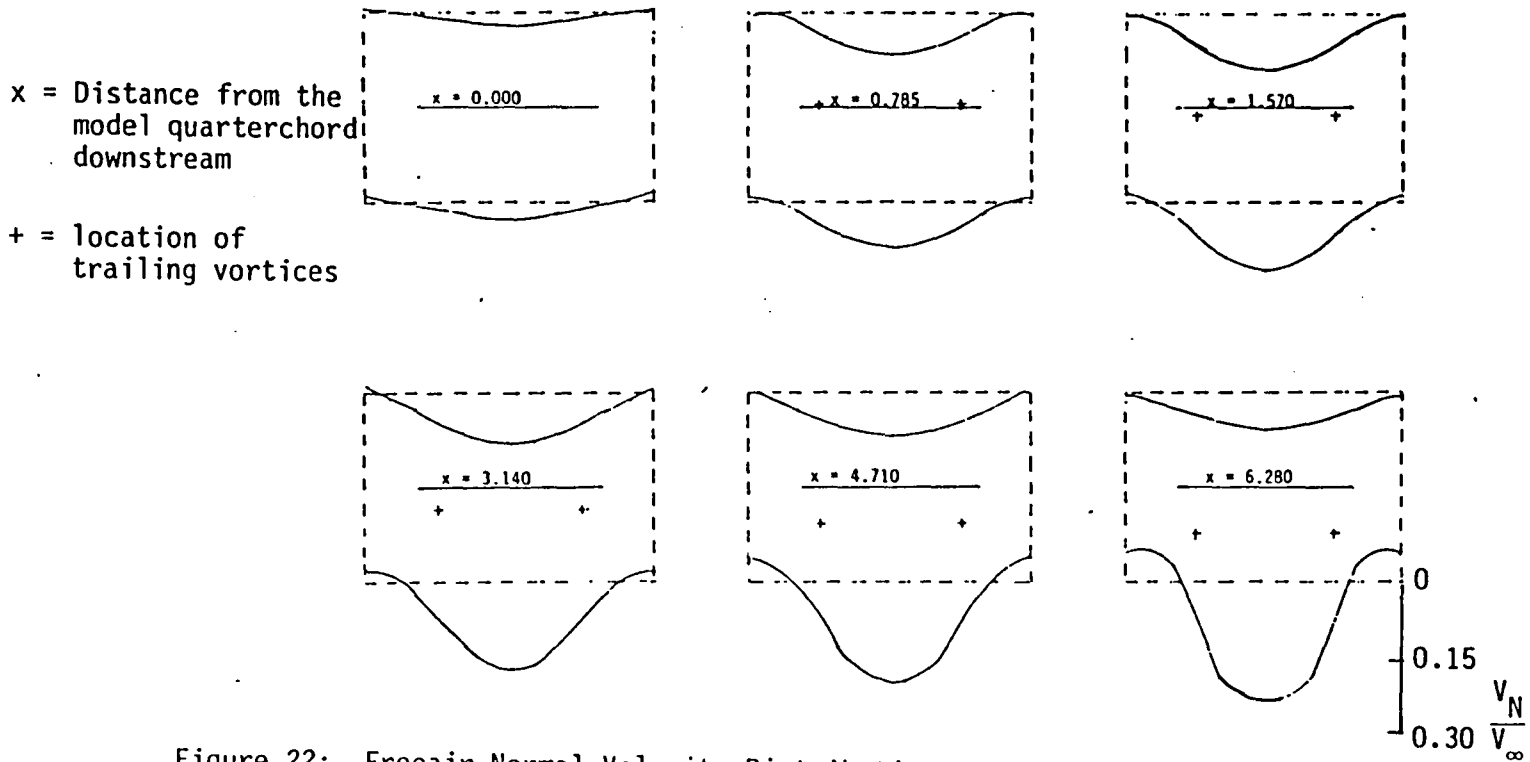

Figure 22: Freeair Normal Velocity Distribution on the Tunnel Walls.
(Model Angle of Attack = -10 degrees)

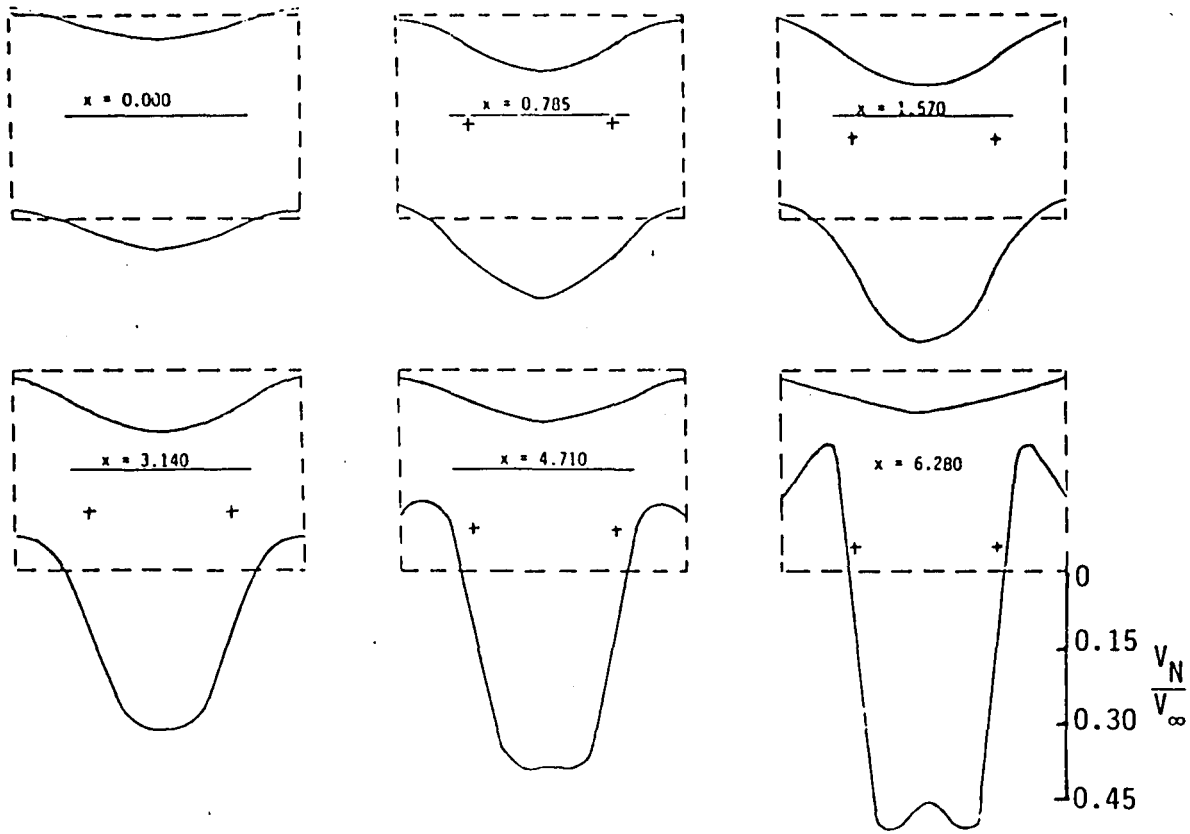

Figure 23: Freeair Normal Velocity Distribution on the Tunnel Walls.
(Model Angle of Attack = 0 Degree)

involve injection or extraction of flow through all the tunnel wall control points. The required flow control arrangement would no doubt prove to be costly. Even then the discrete nature of a real installation would be inadequate to produce completely interference-free results. These arguments prompted Atkinson [5] to study the distribution of free air normal velocity along tunnel walls. Based on this study he found that approximate free air conditions could be obtained even if flow through only part of tunnel walls is controlled. Of course there is a clear compromise between the mechanical complexity to be dealt with and the degree of interference to be tolerated.

A study similar to the one above was carried out for a jet flap model. Here the normal velocity induced by the model on the ceiling and floor of an imaginary wind tunnel test section was calculated in a free air flow environment. In figure 22 and 23 this normal velocity is plotted at six different sections normal to the free stream at and downstream of the model locations for two different angles of attack of the model. The location of the trailing wake in each cross section is also shown. As can be seen, for the most part there is a flow into the tunnel on the ceiling and out of the tunnel on the floor. On the ceiling the normal velocity increases at first with distance downstream from the model and then decreases as the trailing vortices go farther away from the ceiling. On the floor of the tunnel the magnitude becomes larger and larger as the wake comes closer and closer. Based on similar velocity surveys and those on the side walls

an effective scheme for defining a limited activity controlled flow tunnel could be developed.

5.3 Results Using Partially Controlled Flow Tunnel:

Based on the above mentioned normal velocity survey it can be seen that if a tunnel is controlled on the floor and the ceiling aft of the model quarter chord point, then reasonably interference-free results could be expected. This is a good starting point for the study of a partially controlled flow tunnel. The tunnel for this study was represent using 280 vortex rectangles, of which flow through 64 of the control points was controlled actively. This tunnel representation is shown in figure 24 and results obtained for two jet momentum coefficients are shown in figures 25 and 26.

For the lower jet momentum coefficient of 0.55, the control arrangement of figure 24 seems to have worked well in that the controlled tunnel results are close to the free air data. However, for the higher jet momentum coefficient of 1.00, the control arrangement is not uniformly successful over the entire range of the angles of attack. This discrepancy can be explained by resorting to an analysis of the relative location of the wake and the controlled portions of the tunnel. For the extreme angles of attack, e.g. -15 degree or those greater than 5 degrees, the trailing vortex wake gets quite close to either top or the bottom walls both of which are controlled. Thus for these extreme attack angles the locations with a large effect in terms of the normal velocity are controlled in this

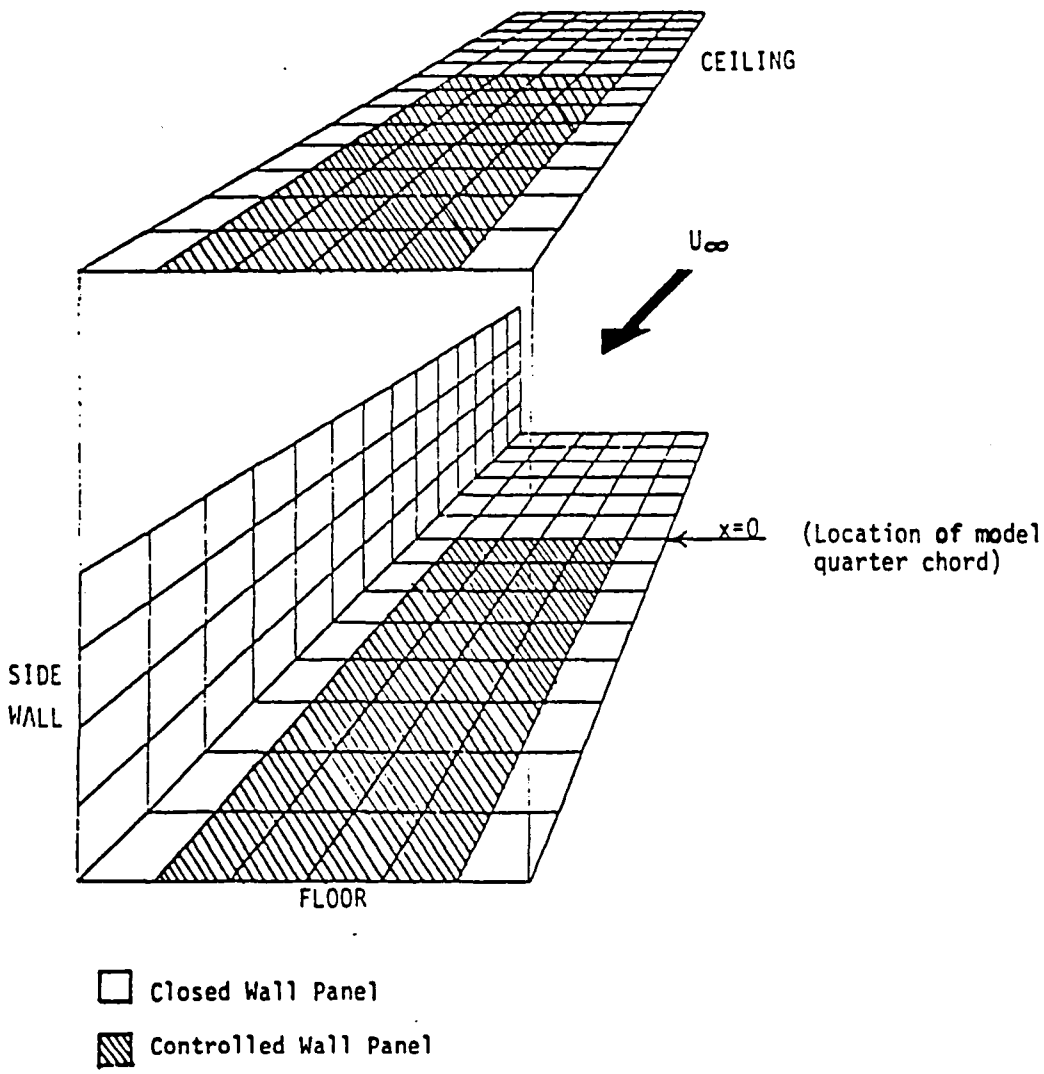

Figure 24: Control Arrangement for Partial Control

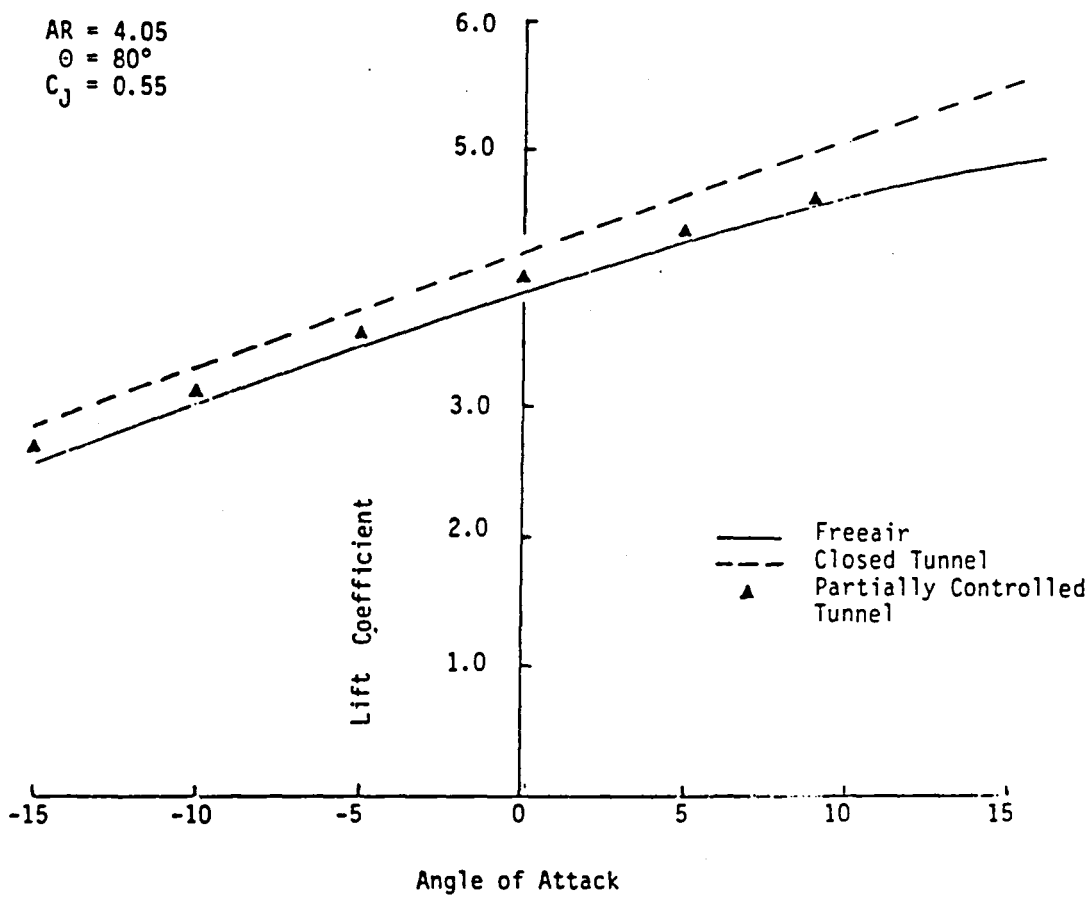

Figure 25: Comparison of Computed Results Showing Effectiveness of Partial Control.

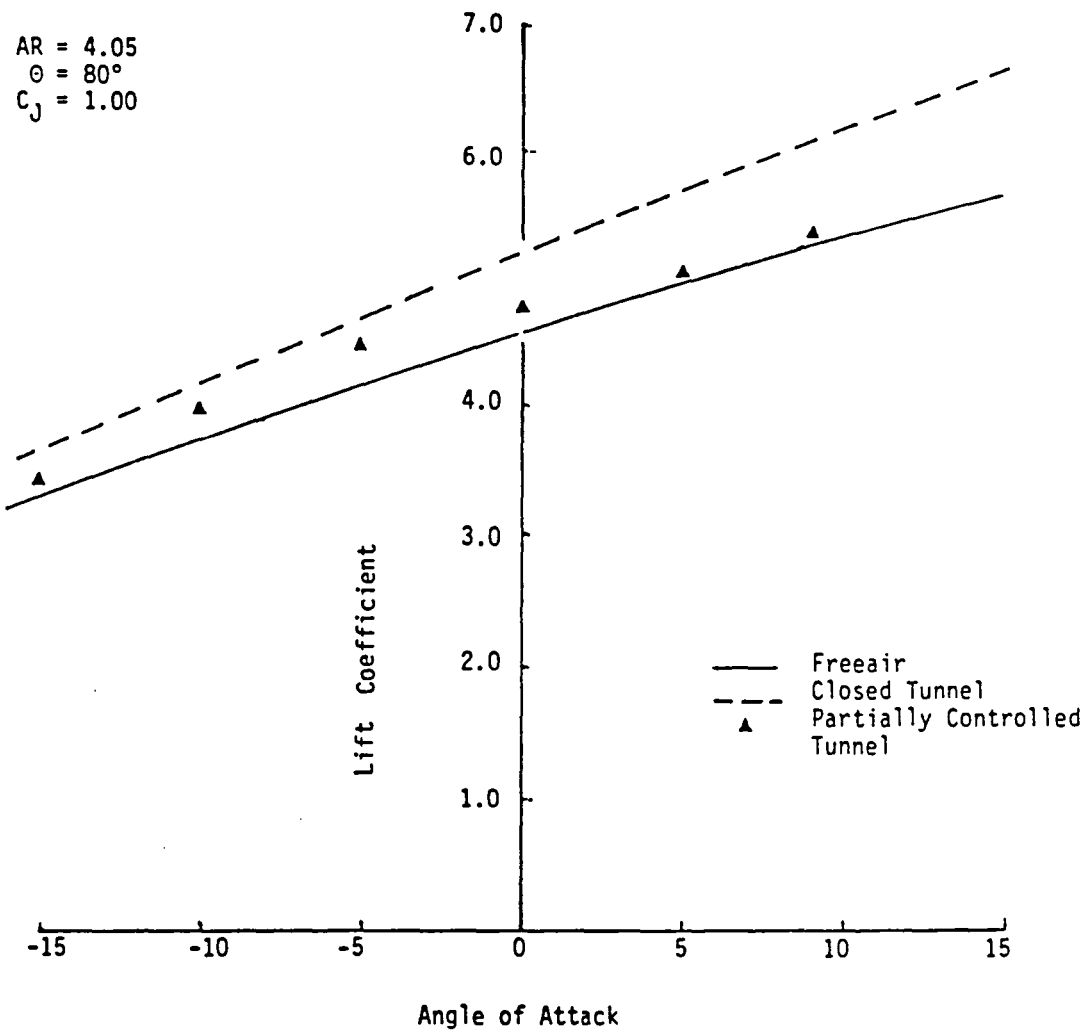

Figure 26: Comparison of Computed Results Showing Effectiveness of Partial Control.

case, the uncontrolled portions do not effect the model much and hence the free air results are almost repeated. For other angles of attack, those in the range -10 degrees to 0 degrees, the wake is away from both the walls so controlling these have only limited effect on the model.

Results of figure 26 clearly indicate the need for a better controlled arrangement. One such arrangement was obtained by transferring the decision making process of whether to control a particular control point or not, to the computer program. Accordingly, the program automatically controlled a point on the tunnel if the normal velocity induced by model at that point was greater than 3% of the freestream velocity. The results so obtained reproduced the free air results almost identically over the entire range of the angles of attack. Between 51-57% of the control points needed to be controlled in the present case as opposed to 26% when controlled using Atkinson's recommendations. Though some more work needs to be done to define the optimum control arrangement, the present results nonetheless show the potential of the controlled flow tunnel.

5.4 Practical Considerations:

The numerical analysis above shows the usefulness of a controlled flow test section for low interference results on high lift systems. Some operational and other problems which may be encountered during testing in an actual controlled flow tunnel are next descibed in

brief.

One of the first problems to be dealt with would be the development of a potential flow representation for each V/STOL model to be tested. With the introduction of new concepts combining jets, rotors and flow deflecting devices, development of computer simulation models will have to keep pace. Fortunately since only an estimate of the gross and the far field effects is demanded by the scheme, advanced vortex lattice computer simulation models (e.g. Margason [30], Maskew [26]) could be used. If sufficient expertise is achieved in the development of simulation models for various components of a high lift system, then most V/STOL systems could be modelled by combining such individual representations. Nonlinear interaction of various components can still be accounted in an iterative manner.

For an ideal controlled flow tunnel injection and extraction of the flow through the walls would be continuously distributed. Both mass flow and momentum across the control surface will then be matched with free air conditions to obtain a perfect control. Such a continuous control is obviously impossible to achieve, forcing the designer of such a facility to use discrete control. For an appreciation of problems associated with such a discrete contol, an example controlled flow test section is shown in figure 27, which is taken from Bernstein's study [ref. 4] on a two dimensional plane wing. The test section in this study was made of segmented plenum chambers each covered by movable porous plates so that the porosity could be adjusted. The flow into or from the plenum chambers was

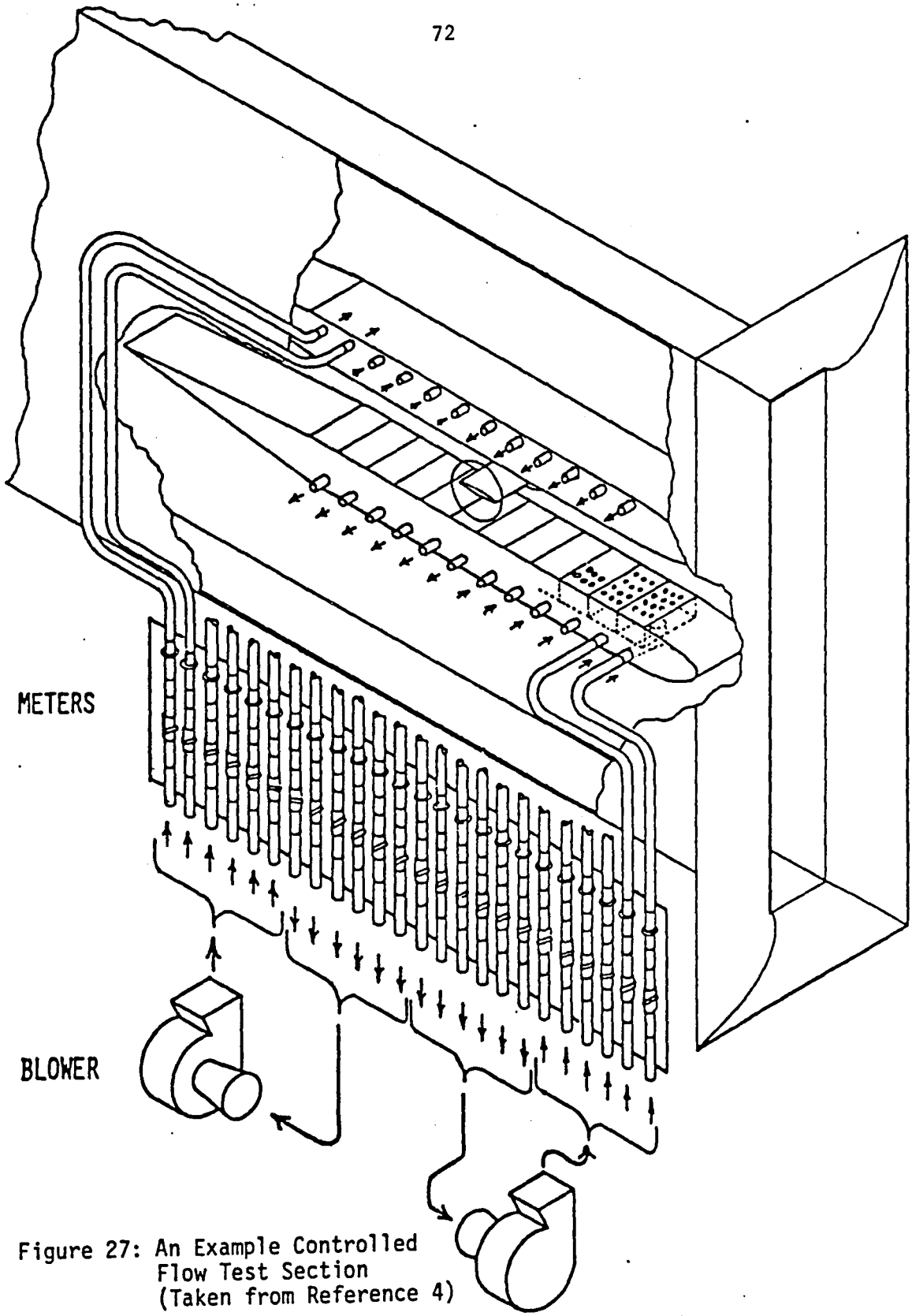

Figure 27: An Example Controlled Flow Test Section (Taken from Reference 4)

generated by blowers, controlled by manual valves and monitored by flow meters. Now if the mass flow through the porous holes over an area is matched to the ideal required then its momentum is found to be greater than the ideal. On the other hand, if momentum of the controlled flow is matched to the ideal one then a mass mismatch results. Bernstein's study showed that with increase in porosity of the plemum chamber this mismatch could be partially restored. This problem of mass or momentum deficit has to be studied carefully with a high lift model in the test section because of large velocities and mass flow rates involved with such a model.

CHAPTER 6

CONCLUSIONS AND RECOMMENDATIONS

The concept of a controlled flow tunnel has been studied by numerical means for the special case of a high lift system. The results of this study demonstrate the utility of this concept for low interference results even in the highly interactive regime. The application of an already proven concept of the controlled flow tunnel to a high lift model is an unique feature of this study.

The potential flow representation developed in chapter 3 for a three dimensional jet flapped wing and its excellent agreement with available results show the adequacy of such representation even for a high lift model. As shown, a special treatment for the characteristic highly curved wake is needed. Other more complex V/STOL models can be confidently represented using similar methods.

The vortex lattice representation of the closed tunnel used in chapter 4 has already been used for simple wings. This study extends it to the case of high energy wake and shows its suitability for a complete numerical study of the interference problem.

Finally, in chapter 5, a scheme has been devised by suitable modifications of the boundary conditions, to study the concept of the controlled flow tunnel. The results show that the ability of such a tunnel to yield interference-free results is dependent upon the extent of the controlled areas. Some difficulties forseen in the operation of such tunnel are mentioned. It is believed that the mass or the momentum mismatch due to the discretised nature of control will have

to be carefully studied.

Despite these difficulties the attractiveness of the concept lies in its ability to provide an interference-free test environment for a variety of V/STOL model without resort to complex analytical treatment. Such controlled flow test sections would be useful to the test engineers when flow around intricate details of a new V/STOL concept is to be studied.

Recommendations for further study are made on several topics. The first and of prime importance is the computational time needed for the potential flow solution of the V/STOL model under consideration. The present being a preliminary study, no attention was given to computing efficiencies. Thus in some cases, e.g. model-in-closed-tunnel solution, time for a converged solution was excessive. If this method is to be applied with success to more complex configuration then further refinements of the programs involved will be necessary.

Though an excellent agreement with the experiments was found for the lift data, that with the downwash data was not so good. A reason for this discrepancy may be the simple representation used here for trailing vortices. It is believed that a nonuniform load distribution on the wing resulting in many trailing vortices may improve the agreement and needs to be looked into.

The analysis should be extended to include part span, multiple jet flaps and their mutual interactions. This will take the analysis a step closer to more complex V/STOL systems, e.g. blown flaps,

augmentor wings, etc., which have multiple jet sheets.

One severe handicap of the present study was the limited availability of experimental data. The available data was for a high jet exit angle, thus restricting comparisons to lower jet momentum coefficients because of the potential flow representation needed here. Since more realistic high lift vehicles are likely to operate at moderate values of these parameters, data is needed for a lower jet exit angle of the order of 45 degrees.

REFERENCES

1. Prandtl, L., Tragflugeltheorie , Vol. II, C, Gottingen, Nachrichten, 1919.
2. Glauert, H., "The Interference of Wind Channel Walls on the Aerodynamic Characteristics of an Aerofoil," British A.R.C. R. & M. No. 867, 1923.
3. Heyson, Harry H., "Linearized Theory of Wind Tunnel Jet Boundary Corrections and Ground Effect for VTOL/STOL Models," NASA TR R-124, 1962.
4. Bernstein S., "The Minimum Interference Wind Tunnel," Ph.D. Dissertation, Department of Aeronautics and Astronautics, University of Washington, Seattle, March 1975.
5. Atkinson, Alan J., "Three Dimensional Low Speed Minimum Interference Wind Tunnel Simulation Based on Potential Modeling," M. S. Thesis, Department of Aeronautics and Astronautics, University of Washington, Seattle, 1978.
6. Rae, W. H. Jr., "Limits on Minimum-Speed V/STOL Wind Tunnel Tests," Journal of Aircraft, Vol. 4, No. 3, May-June 1967, pp. 249-254.
7. Shindo, Shojiro and Rae, W. H., Jr., "Recent Research on V/STOL Test Limits at the University of Washington Aeronautical Laboratory," NASA CR-3237, 1980.
8. Heyson, Harry H. and Grunwald, Kalman J., "Wind Tunnel Boundary Interference for V/STOL Testing," Conference on V/STOL and STOL Aircraft, NASA SP-116, 1966, pp. 409-434.

9. Staff of Powered-Lift Aerodynamics Section, NASA Langley Research Center, "Wall Effects and Scale Effects in V/STOL Model Testing," AIAA Aerodynamic Testing Conference, March 1964, pp. 8-16.

10. Joppa, R. G., "Wind Tunnel Interference Factors for High-Lift Wings in Closed Wind Tunnels," NASA CR-2191, February 1973.

11. Kroeger, R. A. and Martin, W. A., "The Streamline Matching Technique for V/STOL Wind Tunnel Wall Corrections," AIAA Paper 67-183, 1967.

12. Sears, W. R., "Self Correcting Wind Tunnels," Aeronautical Journal, February/March 1974, pp. 80-89.

13. Sears, W. R., Vidal, R. J., Erickson, J. C. Jr., and Ritter, A., "Interference-Free Wind Tunnel Flows by Adaptive Wall Technology", Journal of Aircraft, Vol. 14, No. 11, November 1977, pp. 1042-1050.

14. Sears, W. R., "Adaptable Wind Tunnel for Testing of V/STOL Configurations at High Lift" , Journal of Aircraft, Vol.20, No. 11, November 1983, pp. 968-974.

15. Shindo, S. and Joppa, R. G., "An Experimental Investigation of Three Dimensional Low Speed Minimum Interference Wind Tunnel for High Lift Wings," NASA CR-164439, 1980.

16. Herold, A. C., "A Two Dimensional, Iterative Solution for the Jet Flap," NASA CR 2190, February 1973.

17. Spence, D. A., "The Lift Coefficient of a Thin, Jet-Flapped Wing," Proceedings of the Royal Society, Vol. A 238, 1956, pp. 46-68.

18. Maskell, E. C. and Spence, D. A., "A Theory of the Jet Flap in Three Dimensions," Proceedings of the Royal Society, Vol. A 251, 1959, pp. 407-435.

19. Kerney, K. P., "An Asymptolic Theory of the High-Aspect-Ratio Jet Flap," Ph.D. Thesis, School of Aeronautical Engineering, Cornell University, 1967.

20. Tokuda, N., "An Asymptotic Theory of the Jet Flap in Three Dimensions, " Journal of Fluid Mechanics, Vol. 46, Part 4, 1971, pp. 705-726.

21. Lissaman, P. B. S., "Analysis of High-Aspect-Ratio Jet-Flapped Wings of Arbitrary Geometry," NASA CR-2179, 1973.

22. Halsay, N. D., "Methods of the Design and Analysis of Jet-Flapped Airfoils," Journal of Aircraft, Vol. 11, No. 9, September 1974, pp. 540-546.

23. Addessio, F. L. and Skifstad, J. G., "Theory of an Airfoil Equipped with a Jet Flap under Low-Speed Flight Conditions," NASA CR-2571, July 1975.

24. Pope, Alan, Basic Wing and Airfoil Theory, McGraw - Hill Inc., 1951, p. 229.

25. Belotserkovskii, S. M., "Calculation of the Flow Around Wings of Arbitrary Planform over a Wide Range of Angles of Attack," NASA TTF-12,291, May 1971.

26. Maskew, B., "A Quadrilateral Vortex Method Applied to Configurations with High Circulation," NASA SP-405, Vortex Lattice Utilization, May 1976, pp. 163-186.

27. Tulinius, F., "Unified Subsonic, Transonic, and Supersonic NAR Vortex Lattice," North American Rockwell Report No. TFD-72-523, 1972.

28. Williams, J. and Alexander, A. J., "Three-Dimensional Wind-Tunnel Tests of a 30 Degree Jet Flap Model," A.R.C. CP No. 304, Nov. 1955, pp. 1-49.

29. Silverstein, A. and White, J. A., "Wind Tunnel Interference with Particular Reference to Off-Center Positions of the Wing and to the Downwash at the Tail", NACA T.R. No. 547, 1935.

30. Margason, Richard J. and Lamar, John E., "Vortex Lattice FORTRAN Program for Estimating Subsonic Aerodynamic Characteristics of Complex Planforms" NASA TM D-6142, 1971.

APPENDIX-A

```
      PROGRAM JET(INPUT,OUTPUT,TAPE5=INPUT,TAPE6=OUTPUT)
C ****************************************************
C   PROGRAM TO COMPUTE AERODYNAMIC CHARACTERISTICS OF A
C   RECTANGULAR JET FLAPPED WING WITH FULL SPAN JET FLAP
C ****************************************************
      DIMENSION WA(60),AW(60),BW(60),E(60,60),FS(60),C(60),D(60)
      DIMENSION UU(60),V(60),G(60),WAH(60),WAD(60)
      DIMENSION ANGW(60),ANGB(60)
      DIMENSION SIG(60),GAMA(60),XS(60),YS(60),ZS(60)
      DIMENSION DSM(60),VTRN(60),VTRT(60),TANG(60)
      REAL LIFT
      INTEGER CC
      COMMON /JETIN2/ SPEED,CHORD,GMSPN
 3    FORMAT (3F15.8)
 4    FORMAT (13X,F10.6)
 13   FORMAT (/,29H TOTAL 2D-3D ITERATIONS DONE=,I4)
 110  FORMAT (4F10.4)
 111  FORMAT (/,50H--------------------------------------------------)
 120  FORMAT (9F10.4)
 130  FORMAT (3F10.5)
 605  FORMAT (37H 2D-3D ITERATION LIMIT REACHED. ITER=,I4)
 701  FORMAT (/,41H THE NUMBER OF SEGMENTS IN THE AIRFOIL IS,I5)
 702  FORMAT (/,37H THE NUMBER OF SEGMENTS IN THE JET IS,I5)
 703  FORMAT (/,43H THE INITIAL GUESSES FOR THE JET ANGLES ARE)
 704  FORMAT (/,24H THE VALUE OF EPSILON IS,F7.4, 8H DEGREES)
 705  FORMAT (/,37H THE VALUE OF MOMENTUM COEFFICIENT IS,F7.4)
 706  FORMAT (/,17H ANGLE OF ATTACK=,F6.2)
 708  FORMAT (/,5X,25H AERODYNAMIC COEFFICIENTS)
 709  FORMAT (5X,2F10.5)
 900  FORMAT(1H1,1X,* ONE LINE TITLE FOR OUTPUT *,1X)
      PAI=4.0*ATAN(1.0)
      DEGRA=180.0/PAI
      IT=1
      ISKP=0
C
C          **  INPUT  **
C
C  NC       = NO. OF BOUND VORTICES REPRESENTING THE WING
C  NW       = NO. OF BOUND VORTICES REPRESENTING THE JET
C  EPS      = CONVERGENCE COEFFICIENT FOR 2-D SOLUTION
C  EALP     = CONVERGENCE COEFFICIENT FOR 3-D SOLUTION
C  WA(I)    = INITIAL GUESS FOR JET ANGLES (TRAJECTORY)
C  ALPHA    = GEOMETRICAL ANGLE OF ATTACK OF THE MODEL
C  CJ       = JET MOMENTUM COEFFICIENT
C  COEF1    = FACTOR BY WHICH JET TRAJECTORY IS CORRECTED
C             BETWEEN ITERATIONS
```

```
C  CHORD    = WING CHORD
C  SPEED    = FREE STREAM VELOCITY
C  GMSPN    = WING SPAN
C  CTHR     = 1.0 + WING THICKNESS/CHORD RATIO
C  XT,YT,ZT = COORDINATES OF THE TAIL
C
       READ (5,*) NC,NW
       WRITE(6,900)
       WRITE(6,701) NC
       WRITE (6,702) NW
       KK=NW+1
       READ (5,*) EPS,EALP
       WRITE (6,704) EPS
       WRITE(6,*)EALP
       EPS=EPS/DEGRA
       EALP=EALP/DEGRA
       WRITE (6,703)
       READ(5,*) (WA(I),I=1,KK)
       DO 51 I=1,KK
       WRITE (6,4) WA(I)
       WA(I)=WA(I)/DEGRA
 51    CONTINUE
       READ(5,*)ALPHA
       WRITE(6,706) ALPHA
       ALPHA=ALPHA/DEGRA
       READ (5,*) CJ,COEF1
       WRITE (6,705) CJ
       WRITE (6,*)COEF1
       READ (5,*) CHORD,SPEED,GMSPN,CTHR
       WRITE(6,3) CHORD,SPEED,GMSPN,CTHR
       READ(5,*) XT,YT,ZT
       DO 382 I=1,60
       ZS(I)=PAI*GMSPN/8.0
       VTRN(I)=0.0
       VTRT(I)=0.0
 382   CONTINUE
       BVBY2=ZS(1)
       A3DP=0.0
 38    CONTINUE
       NCC=NC+1
       NC2=NC+2
C
C  COMPUTE COORDINATES OF VORTICES
C
       SEG=CHORD/FLOAT(NC)
       DO 31 I=1,NCC
       AA=(I-1)*SEG-(CHORD/4.)
       AW(I)=AA*COS(ALPHA)
       BW(I)=-AA*SIN(ALPHA)
 31    CONTINUE
```

```
      SEG1=CHORD/7.0
      DO 15 I=1,NW
      NN=NC+I+1
      AW(NN)=AW(NN-1)+SEG1*COS(WA(I)+ALPHA)
 15   BW(NN)=BW(NN-1)-SEG1*SIN(WA(I)+ALPHA)
      CC=NW+NC+1
      NWC=NW+NC
C
C  COMPUTE COORDINATES OF NORMALS
C
      SEG2=0.00001
      DO 25 I=1,NWC
      C(I)=0.5*(AW(I)+AW(I+1))
 25   D(I)=0.5*(BW(I)+BW(I+1))
      C(CC)=AW(CC)+SEG2*COS(WA(KK)+ALPHA)
      D(CC)=BW(CC)-SEG2*SIN(WA(KK)+ALPHA)
C
C  COMPUTE MATRIX OF COEFFICIENTS
C
      DO 30 I=1,NC
      DO 30 J=1,CC
      R=((BW(J)-D(I))**2.+(AW(J)-C(I))**2.)**0.5
      ARG=ABS((BW(J)-D(I))/(AW(J)-C(I)))
      IF(J.EQ.I.OR.J.EQ.I+1) GO TO 29
      GO TO 291
 29   PHI=0.0
      GO TO 292
 291  PHI=ATAN(ARG)-ALPHA
 292  CONTINUE
      DIST=SQRT(R*R+BVBY2*BVBY2)
      COSB=BVBY2/DIST
      E(I,J)=COS(PHI)*COSB/(2.*PAI*R)
      IF (AW(J).GT.C(I)) GO TO 35
      E(I,J)=-E(I,J)
 35   CONTINUE
 30   CONTINUE
      DO 40 I=NCC,CC
      DO 40 J=1,CC
      R=((BW(J)-D(I))**2.+(AW(J)-C(I))**2.)**0.5
      ARG=ABS((BW(J)-D(I))/(AW(J)-C(I)))
      K=I-NC
      IF(J.EQ.I.OR.J.EQ.I+1) GO TO 39
      GO TO 391
 39   PHI=0.0
      GO TO 392
 391  PHI=ALPHA+WA(K)-ATAN(ARG)
 392  CONTINUE
      DIST=SQRT(R*R+BVBY2*BVBY2)
      COSB=BVBY2/DIST
      E(I,J)=COS(PHI)*COSB/(2.*PAI*R)
```

```
      IF (AW(J).GT.C(I)) GO TO 351
      E(I,J)=-E(I,J)
 351  CONTINUE
 40   CONTINUE
C
C  ADD CONTRIBUTION OF TRAILING VORTICES
C
      IF(IT.EQ.1) GO TO 285
      DO 280 I=1,CC
      XC=C(I)
      YC=D(I)
      ZC=0.0
      CALL VTRAIL(CC,XS,YS,ZS,GAMA,XC,YC,ZC,VXTR,VYTR,VZTR,ISKP)
      IF(I.LE.NC)GO TO 281
      DAL=ALPHA+WA(I-NC)
      GO TO 282
 281  DAL=ALPHA
 282  VTRN(I)=VYTR*COS(DAL)+VXTR*SIN(DAL)
 280  CONTINUE
C
C  COMPUTE FREE STREAM COMPONENTS ALONG NORMALS
C
 285  DO  59 I=1,NC
      FS(I)=-SPEED*SIN(ALPHA)-VTRN(I)
 59   CONTINUE
      DO 60 I=1,KK
      III=I+NC
      FS(III)=-SPEED*SIN(WA(I)+ALPHA)-VTRN(III)
 60   CONTINUE
C
C  SOLVE MATRIX EQUATION FOR VORTEX STRENGTHS
C
      CALL SOLVE (E,FS,CC,SIG)
C
C  COMPUTE TANGENTIAL VELOCITIES
C
      IF(IT.EQ.1)GO TO 381
      DO 380 I=NC2,CC
      XC=AW(I)
      YC=BW(I)
      ZC=0.0
      CALL VTRAIL(CC,XS,YS,ZS,GAMA,XC,YC,ZC,VXTR,VYTR,VZTR,ISKP)
      VTRT(I)=VXTR*COS(TANG(I))-VYTR*SIN(TANG(I))
 380  CONTINUE
 381  CALL TV (NW,NC,UU,WA,AW,BW,SIG,ALPHA,TANG,BVBY2)
C
C  CHANGE INDEXING FOR USE IN FOLLOWING SUBROUTINE
C
      DO 45 I=1,NW
      NE=NC+I+1
```

```
      G(I)=SIG(NE)
      UU(NE)=UU(NE)+VTRT(NE)
 45   V(I)=UU(NE)
C
C  STORE JET ANGLES FOR COMPARISON WITH VALUES OF NEXT ITERATION
C
      DO 14 I=1,KK
 14   WAH(I)=WA(I)
C
C  CORRECT JET ANGLES USING VORTICITY AND TANGENTIAL VELOCITIES
C
      CALL WANG (CJ,V,G,WA,NW)
C
C  CHECK FOR 2-D CONVERGENCE
C
      DO 70 I=1,KK
      ERR=ABS(WAH(I)-WA(I))
      IF (ERR.GE.EPS) GO TO 500
 70   CONTINUE
      GO TO 800
 500  CONTINUE
C
C  IF NOT CONVERGED,COMPUTE NEW GUESS FOR JET ANGLES
C
      DO 600 I=1,KK
 600  WA(I)=WAH(I)+COEF1*(WA(I)-WAH(I))
      GO TO 38
 800  CONTINUE
C
C  CALCULATE TRAILING WAKE TRAJECTORY (FIRST GUESS)
C
      DO 82 I=1,NCC
      XS(I)=AW(I)
      YS(I)=BW(I)
 82   CONTINUE
      DO 83 I=NC2,CC
      J=I-1
      YS(I)=0.25*(BW(I)-BW(NCC))+BW(NCC)
      SEGSQ=(AW(I)-AW(J))**2.+(BW(I)-BW(J))**2.
      XS(I)=XS(J)+SQRT(SEGSQ-(YS(I)-YS(J))**2.-(ZS(I)-ZS(J))**2.)
 83   CONTINUE
      GAMA(1)=SIG(1)
      DO 84 I=2,CC
      GAMA(I)=GAMA(I-1)+SIG(I)
 84   CONTINUE
C
C  LONG LAST SEGMENT
C
      L=CC+1
      SPAN=PAI*GMSPN/4.0
```

```
      VI=GAMA(CC)/(2.0*PAI*SPAN)
      A1=ATAN(-VI/SPEED)
      XS(L)=XS(CC)+1000.0*COS(A1)
      YS(L)=YS(CC)+1000.0*SIN(A1)
      ZS(L)=ZS(CC)
C
C  CHECK FOR 3-D CONVERGENCE
C
      DO 79 I=1,CC
      J=I+1
      DSM(I)=SQRT((XS(J)-XS(I))**2.+(YS(J)-YS(I))**2.+
     # (ZS(J)-ZS(I))**2.)
 79   CONTINUE
      CALL WKIT(NC,CC,AW,BW,SIG,XS,YS,ZS,GAMA,DSM)
      XC=0.00 $ YC=0.0 $ ZC=0.0
      CALL VTRAIL(CC,XS,YS,ZS,GAMA,XC,YC,ZC,VXTR,VYTR,VZTR,ISKP)
      V3DX=SPEED-VXTR
      V3DY=-VYTR
      ALPHAI=ATAN(V3DY/V3DX)
      A3D=ALPHA+ALPHAI
      ERRR=ABS(A3D-A3DP)
      IF(ERRR.LE.EALP)GO TO 334
      A3DP=A3D
      IT=IT+1
      IF(IT.GT.40) GO TO 604
      GO TO 38
 604  WRITE(6,605) IT
      GO TO 606
 334  MCC=CC-1
      DO 20 K=1,MCC
      ANGWB=ATAN((BW(K)-BW(K+1))/(AW(K+1)-AW(K)))
      ANGWB=ANGWB-ALPHA
 20   ANGB(K)=DEGRA*ANGWB
      DO 19 K=1,CC
      ANGWT=ATAN((YS(K+1)-YS(K))/(XS(K+1)-XS(K)))
      ANGW(K)=DEGRA*ANGWT
 19   CONTINUE
      WRITE(6,111)
      WRITE(6,110) (AW(I),BW(I),SIG(I),ANGB(I),I=1,CC)
      WRITE(6,111)
      WRITE(6,110) (XS(I),YS(I),ZS(I),ANGW(I),I=1,L)
C
C  COMPUTE AERODYNAMIC QUANTITIES.
C
      SW=CHORD*GMSPN
      Q=SPAN/(SW*SPEED*SPEED)
      SUML=0.0  $ SUMD=0.0
      DO 80 I=1,NCC
      XC=AW(I)
      YC=BW(I)
```

```
      ZC=0.
      CALL VTRAIL(CC,XS,YS,ZS,GAMA,XC,YC,ZC,VXTR,VYTR,VZTR,ISKP)
      CALL VBOUND(CC,AW,BW,SIG,XS,YS,ZS,XT,YT,ZT,VXB,VYB,VZB,ISKP)
      VELX=SPEED+VXTR+VXB
      VELY=-(VYTR+VYB)
      SUML=SUML+2.*SIG(I)*VELX
      SUMD=SUMD+2.*SIG(I)*VELY
 80   CONTINUE
      CLP=SUML*Q
      CDP=SUMD*Q
      WAE=WA(1)+ALPHA
      CLJ=CJ*SIN(WAE)
      CDJ=-CJ*COS(WAE)
      CLT=(CLP*CTHR)+CLJ
      CDT=CDP+CDJ
      WRITE(6,708)
      WRITE(6,709) CLP,CDP
      WRITE(6,709) CLJ,CDJ
      WRITE(6,709) CLT,CDT
C
C  COMPUTE DOWNWASH AT TAIL
C
      CALL VTRAIL(CC,XS,YS,ZS,GAMA,XT,YT,ZT,VXTR,VYTR,VZTR,ISKP)
      CALL VBOUND(CC,AW,BW,SIG,XS,YS,ZS,XT,YT,ZT,VXB,VYB,VZB,ISKP)
      UXT=SPEED+VXTR+VXB
      UYT=VYTR+VYB
      UZT=VZTR+VZB
      WRITE(6,120)VXB,VYB,VZB
      WRITE(6,120)VXTR,VYTR,VZTR
      WRITE(6,120)XT,YT,ZT,UXT,UYT,UZT
      EPSI=ATAN(UYT/UXT)
      EPSI=EPSI*DEGRA
      WRITE(6,130) EPSI
606   STOP
      END

      SUBROUTINE TV (NW,NC,UU,WA,AW,BW,G,ALPHA,TANG,BVBY2)
C
C  SUBROUTINE TO COMPUTE TANGENTIAL COMPONENTS OF VELOCITY
C
      DIMENSION UU(60),WA(60),AW(60)
      DIMENSION BW(60),TANG(60),G(60)
      INTEGER CC
      COMMON /JETIN2/ SPEED,CHORD,GMSPN
      PAI2=2.0*ATAN(1.0)
      DO 30 I=1,NW
      I2=I+1
      II=I+NC+1
30    TANG(II)=0.5*(WA(I)+WA(I2))+ALPHA
      NC2=NC+2
```

```
      CC=NW+NC+1
      DO 100 I=NC2,CC
      EE=0.0
      NO=I-1
      DO 10 J=1,NO
      R=((AW(J)-AW(I))**2.+(BW(J)-BW(I))**2.)**0.5
      ARG=ABS((BW(J)-BW(I))/(AW(J)-AW(I)))
      THETA=ATAN(ARG)
      ANG=(PAI2+THETA-TANG(I))
      DIST=SQRT(R*R+BVBY2*BVBY2)
      COSB=BVBY2/DIST
      ANN=COS(ANG)*COSB
      EE=(G(J)*ANN/(4.0*PAI2*R))+EE
10    CONTINUE
      NP=I+1
      FF=0.0
      IF (I.EQ.CC) GO TO 99
      DO 20 J=NP,CC
      R=((AW(J)-AW(I))**2.+(BW(J)-BW(I))**2.)**0.5
      ARG=ABS((BW(J)-BW(I))/(AW(J)-AW(I)))
      THETA=ATAN(ARG)
      ANG=(PAI2-THETA+TANG(I))
      DIST=SQRT(R*R+BVBY2*BVBY2)
      COSB=BVBY2/DIST
      ANN=COS(ANG)*COSB
      FF=(G(J)*ANN/(4.0*PAI2*R))+FF
20    CONTINUE
99    CONTINUE
      UU(I)=FF+EE+(SPEED*COS(TANG(I)))
100   CONTINUE
      RETURN
      END

      SUBROUTINE WANG (CJ,U,G,WA,NW)
C
C  SUBROUTINE TO CORRECT JET ANGLES
C
      DIMENSION G(60),WA(60),U(60)
      COMMON /JETIN2/ SPEED,CHORD,GMSPN
      DO 5 I=1,NW
      I2=I+1
      FG=G(I)*U(I)/(CJ*CHORD*(SPEED**2.0))
      IF(ABS(FG).GT.1.0) FG=0.0
      WA(I2)=WA(I)-2.0*ASIN(FG)
 5    CONTINUE
      RETURN
      END

      SUBROUTINE VTRAIL(CC,XS,YS,ZS,GAMA,XC,YC,ZC,VXTR,VYTR,VZTR,M1)
C
```

```
C  SUBROUTINE TO CALCULATE VELOCITY INDUCED BY
C  TRAILING VORTEX PAIR
C
      DIMENSION XS(60),YS(60),ZS(60),GAMA(60)
      DIMENSION XD(60),YD(60),ZD(60),XP1(60),YP1(60),ZP1(60),
     * GAMAD(60),GAMAP(60)
      INTEGER CC
      L=CC+1
      M=-1
      PAI=4.0*ATAN(1.0)
      DO 6020 I=1,L
      XD(I)=XS(I)
      YD(I)=YS(I)
      ZD(I)=ZS(I)
 6020 GAMAD(I)=GAMA(I)
      DO 6000 I=1,L
 6000 ZS(I)=-ZS(I)
      ITER=1
      VXTR=0.0
      VYTR=0.0
      VZTR=0.0
 6001 DO 6002 I=1,CC
      IF(I.EQ.M.OR.I.EQ.M+1) GO TO 6002
      RIX=XS(I)-XC
      RIY=YS(I)-YC
      RIZ=ZS(I)-ZC
      RONE=((RIX)**2+(RIY)**2+(RIZ)**2)**0.5
      J=I+1
      RTX=XS(J)-XC
      RTY=YS(J)-YC
      RTZ=ZS(J)-ZC
      RTWO=((RTX)**2+(RTY)**2+(RTZ)**2)**0.5
      SX=XS(J)-XS(I)
      SY=YS(J)-YS(I)
      SZ=ZS(J)-ZS(I)
      SEGM=((SX)**2+(SY)**2+(SZ)**2)**0.5
      CROSS=(SEGM**2-RONE**2+RTWO**2)/(2.0*SEGM*RTWO)
      IF (ABS(CROSS).GT.1.0) CROSS=1.0
      BETA=ACOS(CROSS)
      PERP=RTWO*SIN(BETA)
      IF(PERP.LT.1.0E-06)GO TO 6002
      CONST=(RONE+RTWO)*(SEGM**2-(RONE-RTWO)**2)
      CONST=CONST/(8.0*PAI*RONE*RTWO*(SEGM**2)*(PERP**2))
      VELX= (RIY*SZ-RIZ*SY)*GAMA(I)*CONST
      VELY= (RIZ*SX-RIX*SZ)*GAMA(I)*CONST
      VELZ= (RIX*SY-RIY*SX)*GAMA(I)*CONST
      VXTR=VXTR+VELX
      VYTR=VYTR+VELY
      VZTR=VZTR+VELZ
 6002 CONTINUE
```

```
      IF (ITER.EQ.1) GO TO 6003
      GO TO 6007
 6003 ITER=ITER+1
      DO 6004 I=1,L
      XP1(I)=XS(I)
      YP1(I)=YS(I)
 6004 ZP1(I)=ZS(I)
      DO 6005 I=1,L
      K=L-I+1
      XS(I)=XP1(K)
      YS(I)=YP1(K)
 6005 ZS(I)=-ZP1(K)
      DO 6006 I=1,CC
 6006 GAMAP(I)=GAMA(I)
      M=L-M1
      DO 6008 I=1,CC
      K=CC-I+1
 6008 GAMA(I)=GAMAP(K)
      GO TO 6001
 6007 DO 6021 I=1,L
      XS(I)=XD(I)
      YS(I)=YD(I)
      ZS(I)=ZD(I)
 6021 GAMA(I)=GAMAD(I)
      RETURN
      END

      SUBROUTINE VBOUND(CC,AW,BW,SIG,XS,YS,ZS,XC,YC,ZC,VXB,VYB,VZB,M)
C
C  SUBROUTINE TO CALCULATE VELOCITY INDUCED BY
C  BOUND VORTICES (TAKES V-SHAPED VORTICES)
C
      DIMENSION AW(60),BW(60),SIG(60)
      DIMENSION XS(60),YS(60),ZS(60)
      INTEGER CC
      PAI=4.0*ATAN(1.0)
      VXB=0.0 $VYB=0.0 $ VZB=0.0
      DO 6011 J=1,2
      DO 6011 I=1,CC
      IF(I.EQ.M)GO TO 6011
      IF(J.EQ.2) GO TO 6012
      XS1=XS(I)
      YS1=YS(I)
      ZS1=ZS(I)
      GAMAT=SIG(I)
      XS2=AW(I)
      YS2=BW(I)
      ZS2=0.0
      GO TO 6013
 6012 XS1=AW(I)
```

```
      YS1=BW(I)
      ZS1=0.0
      GAMAT=SIG(I)
      XS2=XS(I)
      YS2=YS(I)
      ZS2=-ZS(I)
 6013 RIX=XS1-XC
      RIY=YS1-YC
      RIZ=ZS1-ZC
      RONE=((RIX)**2+(RIY)**2+(RIZ)**2)**0.5
      RTX=XS2-XC
      RTY=YS2-YC
      RTZ=ZS2-ZC
      RTWO=((RTX)**2+(RTY)**2+(RTZ)**2)**0.5
      SX=XS2-XS1
      SY=YS2-YS1
      SZ=ZS2-ZS1
      SEGM=((SX)**2+(SY)**2+(SZ)**2)**0.5
      CROSS=(SEGM**2-RONE**2+RTWO**2)/(2.0*SEGM*RTWO)
      BETA=ACOS(CROSS)
      PERP=RTWO*SIN(BETA)
      IF(PERP.LT.1.0E-06) GO TO 6011
      CONST=(RONE+RTWO)*(SEGM**2-(RONE-RTWO)**2)
      CONST=CONST/(8.0*PAI*RONE*RTWO*(SEGM**2)*(PERP**2))
      VELX= (RIY*SZ-RIZ*SY)*GAMAT*CONST
      VELY= (RIZ*SX-RIX*SZ)*GAMAT*CONST
      VELZ= (RIX*SY-RIY*SX)*GAMAT*CONST
      VXB=VXB+VELX
      VYB=VYB+VELY
      VZB=VZB+VELZ
 6011 CONTINUE
      RETURN
      END

      SUBROUTINE SOLVE (A,V,N,SIG)
C
C  SUBROUTINE TO SOLVE THE MATRIX EQUATION AX = B
C  USING GAUSSIAN ELIMINATION
C
      DIMENSION A(60,60),B(60,60),D(60),V(60),SIG(60)
      DO 55 I=1,N
      DO 56 J=1,N
 56   B(I,J)=0.0
 55   D(I)=0.0
      DO 10 L=1,N
      LM=L-1
      LP=L+1
      DO 20 I=L,N
      SUM=A(I,L)
      IF(L.EQ.1) GO TO 200
```

```
      DO 30 K=1,LM
30    SUM=SUM-B(I,K)*B(K,L)
200   B(I,L)=SUM
20    CONTINUE
      IF(L.EQ.N)GO TO 10
      AD=1.0/B(L,L)
      DO 40 J=LP,N
      SUM=A(L,J)
      IF(L.EQ.1)GO TO 40
      DO 50 K=1,LM
50    SUM=SUM-B(L,K)*B(K,J)
40    B(L,J)=SUM*AD
10    CONTINUE
      DO 60 M=1,N
      MM=M-1
      AD=1.0/B(M,M)
      SUM=V(M)
      IF(M.EQ.1) GO TO 60
      DO 70 J=1,MM
70    SUM=SUM-B(M,J)*D(J)
60    D(M)=SUM*AD
      DO 90 I=1,N
      M=N+1-I
      SUM=D(M)
      IF(I.EQ.1)GO TO 90
      MP=M+1
      DO 100 J=MP,N
100   SUM=SUM-B(M,J)*SIG(J)
90    SIG(M)=SUM
      RETURN
      END

      SUBROUTINE WKIT(NC,CC,AW,BW,SIG,XS,YS,ZS,GAMA,DSM)
C
C  SUBROUTINE TO DO TRAILING WAKE RELAXATION
C
      DIMENSION DSM(60),AW(60),BW(60),SIG(60)
      DIMENSION XS(60),YS(60),ZS(60),GAMA(60)
      INTEGER CC
      COMMON /JETIN2/ SPEED,CHORD,GMSPN
      L=CC+1
      N1=0
       NCC=NC+1
      DO 20 M=NCC,CC
      MM1=M-1
      DX=XS(M)-XS(MM1)
      DY=YS(M)-YS(MM1)
      DXY=SQRT(DX*DX+DY*DY)
      SINA=DY/DXY
      COSA=DX/DXY
```

```
      XC=1.5*DXY*COSA+XS(MM1)
      YC=1.5*DXY*SINA+YS(MM1)
      ZC=ZS(MM1)
      CALL VTRAIL(CC,XS,YS,ZS,GAMA,XC,YC,ZC,VXTR,VYTR,VZTR,M)
      CALL VBOUND(CC,AW,BW,SIG,XS,YS,ZS,XC,YC,ZC,VXB,VYB,VZB,N1)
      VXT=SPEED+VXTR+VXB
      VYT=VYTR+VYB
      VEL=SQRT(VXT*VXT+VYT*VYT)
      J=M+1
      XSHFT=DSM(M)*VXT/VEL+XS(M)-XS(J)
      YSHFT=DSM(M)*VYT/VEL+YS(M)-YS(J)
      DO 48 L1=J,L
      XS(L1)=XS(L1)+XSHFT
      YS(L1)=YS(L1)+YSHFT
48    CONTINUE
20    CONTINUE
      RETURN
      END
```

APPENDIX - B

```
      PROGRAM MAIN(INPUT,OUTPUT,TAPE5=INPUT,TAPE6=OUTPUT)
C ************************************************************
C
C  PROGRAM FOR THE SOLUTION OF MODEL-IN-CLOSED-TUNNEL PROBLEM
C  THE MODEL IS A 3-D FULL SPAN JET FLAP. THE TUNNEL IS
C  REPRESENTED BY A NETWORK OF VORTEX LATTICES.
C
C ************************************************************
C
C               ** PLEASE NOTE  **
C
C  SOME OF THE SUBROUTINES IN THIS PROGRAM ARE SAME AS
C  IN THE JET FLAP FREE AIR PROGRAM OF APPENDIX-A
C  AND ARE NOT REPEATED HERE FOR SPACE SAVING PURPOSE.
C
      DIMENSION SIDE (25)
      COMMON/TVEL1/ X(15),Y(25),Z(25)
      COMMON /TVEL2/ VN(80,80),GEMA(80)
      COMMON /B2/ VNM(80)
      COMMON /JET1/  WA(30),AW(30),BW(30),E(30,30),FS(30),C(30),D(30)
      COMMON /JET2/  UU(30),V(30),G(30)
      COMMON /JET4/  SIG(30),GAMA(30),XS(30),YS(30),ZS(30)
      COMMON /JET5/ DSM(30),VTRN(30),VTRT(30),TANG(30)
      COMMON /JETIN1/ NC,NW,EPS,EALP,COEF1,ALPHA,CJ
      COMMON /JETIN2/ SPEED,CHORD,GMSPN,CTHR
      COMMON /CTRPT/ XCPT(15),YCPT(25),ZCPT(25)
      COMMON /TUNNEL/ MM,NN,SINPHI(25),COSPHI(25)
      COMMON /TAIL/ XT,YT,ZT
      INTEGER CC
 3    FORMAT(3F15.8)
 4    FORMAT(13X,F10.6)
 6    FORMAT(2I3)
 7    FORMAT(6H NRUN=,I3)
 8    FORMAT(4H MM=,I3,4H NN=,I3)
 9    FORMAT(10E10.3)
10    FORMAT(17H ANGLE OF ATTACK=,F7.3)
 701  FORMAT ( 1H1,41H THE NUMBER OF SEGMENTS IN THE AIRFOIL IS,I5)
 702  FORMAT (/,37H THE NUMBER OF SEGMENTS IN THE JET IS,I5)
 703  FORMAT (/,43H THE INITIAL GUESSES FOR THE JET ANGLES ARE)
 704  FORMAT (/,24H THE VALUE OF EPSILON IS,F7.4, 8H DEGREES)
 705  FORMAT (/,37H THE VALUE OF MOMENTUM COEFFICIENT IS,F7.4)
 706  FORMAT(2F10.4)
      PAI=4.0*ATAN(1.0)
      DEGRA=180.0/PAI
C
C  READ IN MODEL INFORMATION.
```

```
C  THE MODEL INPUT PARAMETERS ARE THE SAME AS
C  IN JET FLAP FREE AIR PROGRAM OF APPENDIX-A
C
      READ (5,*) NC,NW
      WRITE(6,701) NC
      WRITE (6,702) NW
      KK=NW+1
      CC=NC+NW+1
      READ (5,*) EPS,EALP
      WRITE (6,704) EPS
      WRITE(6,*)EALP
      EPS=EPS/DEGRA
      EALP=EALP/DEGRA
      WRITE (6,703)
      READ(5,*) (WA(I),I=1,KK)
      DO 51 I=1,KK
      WRITE (6,4) WA(I)
      WA(I)=WA(I)/DEGRA
 51   CONTINUE
      READ(5,*)ALPHA
      WRITE(6,10)ALPHA
      ALPHA=ALPHA/DEGRA
      READ (5,*) CJ,COEF1
      WRITE (6,705) CJ
      WRITE (6,*)COEF1
      READ (5,*) CHORD,SPEED,GMSPN,CTHR
      WRITE(6,3) CHORD,SPEED,GMSPN,CTHR
C
C          ** TUNNEL INPUT **
C
C  NRUN    = NO. OF ITERATIONS TO BE DONE BETWEEN THE MODEL
C            SOLUTION AND THE TUNNEL SOLUTION
C  MM      = NO. OF VORTEX SEGMENTS DEFINING THE COMPLETE
C            CROSS SECTION SHAPE OF THE TUNNEL
C  NN      = NO. OF VORTEX RECTANGLES ALONG THE LENGTH OF
C            THE TUNNEL
C  Y,Z     = COORDINATES OF THE POINTS DEFINING THE CROSS
C            SECTIONAL SHAPE OF THE TUNNEL
C  THE ORIGIN OF THE COORDINATE SYSTEM IS ON THE MODEL QUARTER
C  CHORD AT MID SPAN WITH X POSITIVE DOWNSTREAM, Y POSITIVE
C  UPWARDS AND Z POSITIVE TO THE RIGHT LOOKING DOWNSTREAM.
C  DELTAX  = LENGTH OF THE VORTEX RECTANGLES IN THE
C            STREAMWISE DIRECTION
C  XI      = X COORDINATE OF THE PLANE CONTAINING THE FIRST
C            RING VORTEX DESCRIBING THE TUNNEL
C
      READ(5,6) NRUN
      WRITE(6,7) NRUN
      READ(5,6)  MM,NN
      WRITE(6,8) MM,NN
```

```
      READ(5,*) (Y(I),Z(I),I=1,MM)
      WRITE(6,706) (Y(I),Z(I),I=1,MM)
      READ(5,*) DELTAX,XI
      READ(5,*) XT,YT,ZT
      Y(MM+1)=Y(1)
      Z(MM+1)=Z(1)
      NM=NN*MM
      N1=NN+1
      X(1)=XI
      DO 20 I=2,NN
   20 X(I)=X(I-1)+DELTAX
      X(N1)=X(NN)+DELTAX
      WRITE(6,*) (X(I),I=1,N1)
      DO 23 I=1,MM
      YCPT(I)=(Y(I)+Y(I+1))/2.
      ZCPT(I)=(Z(I)+Z(I+1))/2.
      SIDE(I)=SQRT((Y(I)-Y(I+1))**2.+(Z(I)-Z(I+1))**2.)
      SINPHI(I)=ABS(Y(I+1)-Y(I))/SIDE(I)
      COSPHI(I)=ABS(Z(I+1)-Z(I))/SIDE(I)
   23 CONTINUE
      N2=NN-1
      DO 25 I=1,N2
      XCPT(I)=(X(I)+X(I+1))/2.
   25 CONTINUE
      XCPT(NN)=X(NN)+DELTAX/2.
      DO 26 I1=1,80
      GEMA(I1)=0.0
   26 CONTINUE
      CALL TUNVEL
      DO 28 K=1,NRUN
      CALL JET(K)
      CALL SOLVET(NM)
      WRITE(6,9) (GEMA(I),I=1,NM)
   28 CONTINUE
      STOP
      END

      SUBROUTINE TUNVEL
C
C  SUBROUTINE TO CALCULATE TUNNEL INFLUENCE
C  COEFFICIENT MATRIX B
C
      COMMON /CTRPT/ XCPT(15),YCPT(25),ZCPT(25)
      COMMON /TUNNEL/ MM,NN,SINPHI(25),COSPHI(25)
      COMMON /TVEL1/ X(15),Y(25),Z(25)
      COMMON /TVEL2/ VN(80,80),GEMA(80)
      DIMENSION XV(5),YV(5),ZV(5)
      M=0
      DO 10 I=1,NN
      DO 11 J=1,MM
```

```
      M=M+1
      XV(1)=X(I)
      XV(2)=XV(1)
      XV(3)=X(I+1)
      XV(4)=XV(3)
      XV(5)=XV(1)
      YV(1)=Y(J)
      YV(2)=Y(J+1)
      YV(3)=YV(2)
      YV(4)=YV(1)
      YV(5)=YV(1)
      ZV(1)=Z(J)
      ZV(2)=Z(J+1)
      ZV(3)=ZV(2)
      ZV(4)=ZV(1)
      ZV(5)=ZV(1)
      VX=0.0
      VY=0.0
      VZ=0.0
      N=0
      DO 12 I1=1,NN
      DO 13 I2=1,MM
      N=N+1
      XC=XCPT(I1)
      YC=YCPT(I2)
      ZC=ZCPT(I2)
      G=1.0
      VXT=0.0
      VYT=0.0
      VZT=0.0
      DO 15 K=1,4
      CALL VORTEX(XV(K),YV(K),ZV(K),XV(K+1),YV(K+1),ZV(K+1),
     @XC,YC,ZC,VX,VY,VZ,G)
      VXT=VXT+VX
      VYT=VYT+VY
      VZT=VZT+VZ
   15 CONTINUE
      VN(N,M)=VYT*COSPHI(I2)+VZT*SINPHI(I2)
   13 CONTINUE
   12 CONTINUE
   11 CONTINUE
   10 CONTINUE
      RETURN
      END

      SUBROUTINE VORTEX(X1,Y1,Z1,X2,Y2,Z2,X,Y,Z,VX,VY,VZ,G)
C
C  SUBROUTINE TO CALCULATE VELOCITY COMPONENTS INDUCED BY
C  A VORTEX SEGMENT
C
```

```
      VX=0.0  $VY=0.0  $VZ=0.0
      R1X=X1-X
      R1Y=Y1-Y
      R1Z=Z1-Z
      R2X=X2-X
      R2Y=Y2-Y
      R2Z=Z2-Z
      SX=X2-X1
      SY=Y2-Y1
      SZ=Z2-Z1
      R1=SQRT(R1X*R1X+R1Y*R1Y+R1Z*R1Z)
      R2=SQRT(R2X*R2X+R2Y*R2Y+R2Z*R2Z)
      S=SQRT(SX*SX+SY*SY+SZ*SZ)
      CROSS=(S*S+R2*R2-R1*R1)/(2.*S*R2)
      ALPHA=ACOS(CROSS)
      H=R2*SIN(ALPHA)
      CONST=((R1+R2)*G*(S*S-(R1-R2)**2.))/(25.13274*R1*R2*S*S*H*H)
      VX=(R1Y*SZ-R1Z*SY)*CONST
      VY=(R1Z*SX-R1X*SZ)*CONST
      VZ=(R1X*SY-R1Y*SX)*CONST
      RETURN
      END

      SUBROUTINE JET(NIT)
C
C  SUBROUTINE TO CALCULATE THE MODEL SOLUTION TAKING
C  ACCOUNT OF THE PRESENCE OF THE TUNNEL
C
      COMMON /JET1/  WA(30),AW(30),BW(30),E(30,30),FS(30),C(30),D(30)
      COMMON /JET2/  UU(30),V(30),G(30)
      COMMON /JET4/  SIG(30),GAMA(30),XS(30),YS(30),ZS(30)
      COMMON /JET5/ DSM(30),VTRN(30),VTRT(30),TANG(30)
      COMMON /JETIN1/ NC,NW,EPS,EALP,COEF1,ALPHA,CJ
      COMMON /JETIN2/ SPEED,CHORD,GMSPN,CTHR
      DIMENSION WAH(30),WAD(30)
      INTEGER CC
      PAI=4.0*ATAN(1.0)
      DEGRA=180.0/PAI
      IT=1
      ISKP=0
      KK=NW+1
 13   FORMAT(/,29H TOTAL 2D-3D ITERATIONS DONE=,I4)
      DO 382 I=1,30
      ZS(I)=PAI*GMSPN/8.0
      VTRN(I)=0.0
      VTRT(I)=0.0
 382  CONTINUE
      BVBY2=ZS(1)
      A3DP=0.0
 38   CONTINUE
```

```
      NCC=NC+1
      NC2=NC+2
C
C  COMPUTE COORDINATES OF VORTICES
C
       SEG=CHORD/FLOAT(NC)
       DO 31 I=1,NCC
       AA=(I-1)*SEG-(CHORD/4.)
       AW(I)=AA*COS(ALPHA)
       BW(I)=-AA*SIN(ALPHA)
 31    CONTINUE
       SEG1=CHORD/7.0
       DO 15 I=1,NW
       NN=NC+I+1
       AW(NN)=AW(NN-1)+SEG1*COS(WA(I)+ALPHA)
 15    BW(NN)=BW(NN-1)-SEG1*SIN(WA(I)+ALPHA)
       CC=NW+NC+1
       NWC=NW+NC
C
C  COMPUTE COORDINATES OF NORMALS
C
       SEG2=0.00001
       DO 25 I=1,NWC
       C(I)=0.5*(AW(I)+AW(I+1))
 25    D(I)=0.5*(BW(I)+BW(I+1))
       C(CC)=AW(CC)+SEG2*COS(WA(KK)+ALPHA)
       D(CC)=BW(CC)-SEG2*SIN(WA(KK)+ALPHA)
C
C  COMPUTE MATRIX OF COEFFICIENTS
C
       DO 30 I=1,NC
       DO 30 J=1,CC
       R=((BW(J)-D(I))**2.+(AW(J)-C(I))**2.)**0.5
       ARG=ABS((BW(J)-D(I))/(AW(J)-C(I)))
       IF(J.EQ.I.OR.J.EQ.I+1) GO TO 29
       GO TO 291
 29    PHI=0.0
       GO TO 292
 291   PHI=ATAN(ARG)-ALPHA
 292   CONTINUE
       DIST=SQRT(R*R+BVBY2*BVBY2)
       COSB=BVBY2/DIST
       E(I,J)=COS(PHI)*COSB/(2.*PAI*R)
       IF (AW(J).GT.C(I)) GO TO 35
       E(I,J)=-E(I,J)
 35    CONTINUE
 30    CONTINUE
       DO 40 I=NCC,CC
       DO 40 J=1,CC
       R=((BW(J)-D(I))**2.+(AW(J)-C(I))**2.)**0.5
```

```
      ARG=ABS((BW(J)-D(I))/(AW(J)-C(I)))
      K=I-NC
      IF(J.EQ.I.OR.J.EQ.I+1) GO TO 39
      GO TO 391
 39   PHI=0.0
      GO TO 392
 391  PHI=ALPHA+WA(K)-ATAN(ARG)
 392  CONTINUE
      DIST=SQRT(R*R+BVBY2*BVBY2)
      COSB=BVBY2/DIST
      E(I,J)=COS(PHI)*COSB/(2.*PAI*R)
      IF (AW(J).GT.C(I)) GO TO 351
      E(I,J)=-E(I,J)
 351  CONTINUE
 40   CONTINUE
C
C  ADD CONTRIBUTION OF TUNNEL AND TRAILING VORTICES
C
      IF(IT.EQ.1) GO TO 285
      VTUX=0.0
      VTUY=0.0
      VTUZ=0.0
      DO 280 I=1,CC
      XC=C(I)
      YC=D(I)
      ZC=0.0
      CALL VTRAIL(CC,XS,YS,ZS,GAMA,XC,YC,ZC,VXTR,VYTR,VZTR,ISKP)
      IF(NIT.EQ.1)GO TO 283
      CALL TUNCON(XC,YC,ZC,VTUX,VTUY,VTUZ)
      VXTR=VXTR+VTUX
      VYTR=VYTR+VTUY
 283  IF(I.LE.NC)GO TO 281
      DAL=ALPHA+WA(I-NC)
      GO TO 282
 281  DAL=ALPHA
 282  VTRN(I)=VYTR*COS(DAL)+VXTR*SIN(DAL)
 280  CONTINUE
C
C  COMPUTE FREE STREAM COMPONENTS ALONG NORMALS
C
 285  DO  59 I=1,NC
      FS(I)=-SPEED*SIN(ALPHA)-VTRN(I)
 59   CONTINUE
      DO 60 I=1,KK
      III=I+NC
      FS(III)=-SPEED*SIN(WA(I)+ALPHA)-VTRN(III)
 60   CONTINUE
C
C  SOLVE MATRIX EQUATION FOR VORTEX STRENGTHS
C
```

```
      CALL SOLVE (E,FS,CC,SIG)
C
C  COMPUTE TANGENTIAL VELOCITIES
C
      IF(IT.EQ.1)GO TO 381
      VTUX=0.0
      VTUY=0.0
      VTUZ=0.0
      DO 380 I=NC2,CC
      XC=AW(I)
      YC=BW(I)
      ZC=0.0
      CALL VTRAIL(CC,XS,YS,ZS,GAMA,XC,YC,ZC,VXTR,VYTR,VZTR,ISKP)
      IF(NIT.EQ.1) GO TO 383
      CALL TUNCON (XC,YC,ZC,VTUX,VTUY,VTUZ)
      VXTR=VXTR+VTUX
      VYTR=VYTR+VTUY
 383  VTRT(I)=VXTR*COS(TANG(I))-VYTR*SIN(TANG(I))
 380  CONTINUE
 381  CALL TV (NW,NC,UU,WA,AW,BW,SIG,ALPHA,TANG,BVBY2)
C
C  CHANGE INDEXING FOR USE IN FOLLOWING SUBROUTINE
C
      DO 45 I=1,NW
      NE=NC+I+1
      G(I)=SIG(NE)
      UU(NE)=UU(NE)+VTRT(NE)
 45   V(I)=UU(NE)
C
C  STORE JET ANGLES FOR COMPARISON WITH VALUES OF NEXT ITERATION
C
      DO 14 I=1,KK
 14   WAH(I)=WA(I)
C
C  CORRECT JET ANGLES USING VORTICITY AND TANGENTIAL VELOCITIES
C
      CALL WANG (CJ,V,G,WA,NW)
C
C  CHECK FOR 2-D CONVERGENCE
C
      DO 70 I=1,KK
      ERR=ABS(WAH(I)-WA(I))
      IF (ERR.GE.EPS) GO TO 500
 70   CONTINUE
      GO TO 800
 500  CONTINUE
C
C  IF NOT CONVERGED,COMPUTE NEW GUESS FOR JET ANGLES
C
      DO 600 I=1,KK
```

```
 600    WA(I)=WAH(I)+COEF1*(WA(I)-WAH(I))
        GO TO 38
 800    CONTINUE
C
C  CALCULATE TRAILING WAKE TRAJECTORY
C
        DO 82 I=1,NCC
        XS(I)=AW(I)
        YS(I)=BW(I)
 82     CONTINUE
        DO 83 I=NC2,CC
        J=I-1
        YS(I)=0.25*(BW(I)-BW(NCC))+BW(NCC)
        SEGSQ=(AW(I)-AW(J))**2.+(BW(I)-BW(J))**2.
        XS(I)=XS(J)+SQRT(SEGSQ-(YS(I)-YS(J))**2.-(ZS(I)-ZS(J))**2.)
 83     CONTINUE
        GAMA(1)=SIG(1)
        DO 84 I=2,CC
        GAMA(I)=GAMA(I-1)+SIG(I)
 84     CONTINUE
C
C  COMPUTE LONG LAST SEGMENT
C
        L=CC+1
        SPAN=PAI*GMSPN/4.0
        VI=GAMA(CC)/(2.0*PAI*SPAN)
        A1=ATAN(-VI/SPEED)
        XS(L)=XS(CC)+1000.0*COS(A1)
        YS(L)=YS(CC)+1000.0*SIN(A1)
        ZS(L)=ZS(CC)
C
C  CHECK FOR 3-D CONVERGENCE
C
      DO 79 I=1,CC
      J=I+1
      DSM(I)=SQRT((XS(J)-XS(I))**2.+(YS(J)-YS(I))**2.+
     #(ZS(J)-ZS(I))**2.)
 79   CONTINUE
 977  CALL WKIT(NC,CC,AW,BW,SIG,XS,YS,ZS,GAMA,DSM,NIT)
      XC=0.00 $ YC=0.0 $ ZC=0.0
      CALL VTRAIL(CC,XS,YS,ZS,GAMA,XC,YC,ZC,VXTR,VYTR,VZTR,ISKP)
      V3DX=SPEED-VXTR
      V3DY=-VYTR
      ALPHAI=ATAN(V3DY/V3DX)
      A3D=ALPHA+ALPHAI
      ERRR=ABS(A3D-A3DP)
      IF(ERRR.LE.EALP)GO TO 334
      A3DP=A3D
      IT=IT+1
      GO TO 38
```

```
 334  WRITE(6,13) IT
      CALL AEROC(NC,CC,ALPHA,CJ,NIT)
      RETURN
      END

       SUBROUTINE AEROC(NC,CC,ALPHA,CJ,NIT)
C
C  SUBROUTINE TO CALCULATE AERODYNAMIC COEFFICIENTS, VELOCITY
C  INDUCED AT THE TUNNEL CONTROL POINTS BY THE MODEL AND THE
C  ANGLE OF DOWNWASH AT TAIL
C
       DIMENSION ANGW(30),ANGB(30)
       COMMON /B2/ VNM(80)
       COMMON /JET1/  WA(30),AW(30),BW(30),E(30,30),FS(30),C(30),D(30)
       COMMON /JET4/  SIG(30),GAMA(30),XS(30),YS(30),ZS(30)
       COMMON /JETIN2/ SPEED,CHORD,GMSPN,CTHR
       COMMON /TAIL/ XT,YT,ZT
       COMMON /CTRPT/ XCPT(15),YCPT(25),ZCPT(25)
       COMMON /TUNNEL/ MM,NN,SINPHI(25),COSPHI(25)
       INTEGER CC
 709   FORMAT(5X,2F10.5)
 708   FORMAT(/,5X,25H AERODYNAMIC COEFFICIENTS)
 130   FORMAT(/1X,*DOWNWASH AT TAIL=*,F10.5)
 120   FORMAT(6F10.4)
 110   FORMAT(4F10.4)
 30    FORMAT(10E10.3)
 3     FORMAT(3F15.6)
       PI=4.0*ATAN(1.0)
       DEGRA=180.0/PI
       SPAN=PI*GMSPN/4.0
       ISKP=0
       NCC=NC+1
       L=CC+1
       SW=CHORD*GMSPN
       Q=SPAN/(SW*SPEED*SPEED)
       SUML=0.0  $ SUMD=0.0
       DO 80 I=1,NCC
       XC=AW(I)
       YC=BW(I)
       ZC=0.0
       VTUX=0.0
       VTUY=0.0
       CALL VTRAIL(CC,XS,YS,ZS,GAMA,XC,YC,ZC,VXTR,VYTR,VZTR,ISKP)
       CALL VBOUND(CC,AW,BW,SIG,XS,YS,ZS,XT,YT,ZT,VXB,VYB,VZB,ISKP)
       VELX=SPEED+VXTR+VXB+VTUX
       VELY=-(VYTR+VYB+VTUY)
       SUML=SUML+2.*SIG(I)*VELX
       SUMD=SUMD+2.*SIG(I)*VELY
  80   CONTINUE
       CLP=SUML*Q
```

```
      CDP=SUMD*Q
      WAE=WA(1)+ALPHA
      CLJ=CJ*SIN(WAE)
      CDJ=-CJ*COS(WAE)
      CLT=(CLP*CTHR)+CLJ
      CDT=CDP+CDJ
      WRITE(6,708)
      WRITE(6,709)CLP,CDP
      WRITE(6,709) CLJ,CDJ
      WRITE(6,709) CLT,CDT
      MCC=CC-1
      DO 20 K=1,MCC
      ANGWB=ATAN((BW(K)-BW(K+1))/(AW(K+1)-AW(K)))
      ANGWB=ANGWB-ALPHA
 20   ANGB(K)=DEGRA*ANGWB
      DO 19 K=1,CC
      ANGWT=ATAN((YS(K+1)-YS(K))/(XS(K+1)-XS(K)))
 19   ANGW(K)=DEGRA*ANGWT
      WRITE(6,110) (AW(I),BW(I),SIG(I),ANGB(I),I=1,CC)
      WRITE(6,110) (XS(I),YS(I),ZS(I),ANGW(I),I=1,L)
C
C VELOCITY INDUCED AT TUNNEL CONTROL POINTS
C
      DO 21 I2=1,NN
      DO 21 J2=1,MM
      I=(I2-1)*MM+J2
      XC=XCPT(I2)
      YC=YCPT(J2)
      ZC=ZCPT(J2)
      CALL VTRAIL(CC,XS,YS,ZS,GAMA,XC,YC,ZC,VXTR,VYTR,VZTR,ISKP)
      CALL VBOUND(CC,AW,BW,SIG,XS,YS,ZS,XC,YC,ZC,VXB,VYB,VZB,ISKP)
      VYM=VYTR+VYB
      VZM=VZTR+VZB
      VNM(I)=-(VYM*COSPHI(J2)+VZM*SINPHI(J2))
 21   CONTINUE
      NM=NN*MM
      WRITE(6,30) (VNM(I),I=1,NM)
C
C  COMPUTE DOWNWASH AT TAIL
C
      VTUX=0.0  $VTUY=0.0  $VTUZ=0.0
      CALL VTRAIL(CC,XS,YS,ZS,GAMA,XT,YT,ZT,VXTR,VYTR,VZTR,ISKP)
      CALL VBOUND(CC,AW,BW,SIG,XS,YS,ZS,XT,YT,ZT,VXB,VYB,VZB,ISKP)
      IF(NIT.EQ.1)GO TO 300
      CALL TUNCON(XT,YT,ZT,VTUX,VTUY,VTUZ)
 300  UXT=SPEED+VXTR+VXB+VTUX
      UYT=VYTR+VYB+VTUY
      UZT=VZTR+VZB+VTUZ
      WRITE(6,120) VXTR,VYTR,VZTR
      WRITE(6,120) VXB,VYB,VZB
```

```
      WRITE(6,120) VTUX,VTUY,VTUZ
      WRITE(6,120) XT,YT,ZT,UXT,UYT,UZT
      EPSI=ATAN(UYT/UXT)
      EPSI=EPSI*DEGRA
      WRITE(6,130) EPSI
      RETURN
      END

       SUBROUTINE SOLVET(NM)
C
C  SUBROUTINE TO SOLVE FOR THE TUNNEL VORTEX
C  LATTICE STRENGTH
C
       COMMON /TVEL2/ VN(80,80),GEMA(80)
       COMMON /B2/ VNM(80)
       DIMENSION  B(80,80),D(80)
       DO 55 I=1,NM
       DO 56 J=1,NM
 56    B(I,J)=0.0
 55    D(I)=0.0
       DO 10 L=1,NM
       LM=L-1
       LP=L+1
       DO 20 I=L,NM
       SUM=VN(I,L)
       IF(L.EQ.1) GO TO 200
       DO 30 K=1,LM
 30    SUM=SUM-B(I,K)*B(K,L)
 200   B(I,L)=SUM
 20    CONTINUE
       IF(L.EQ.NM)GO TO 10
       AD=1.0/B(L,L)
       DO 40 J=LP,NM
       SUM=VN(L,J)
       IF(L.EQ.1)GO TO 40
       DO 50 K=1,LM
 50    SUM=SUM-B(L,K)*B(K,J)
 40    B(L,J)=SUM*AD
 10    CONTINUE
       DO 60 M=1,NM
       MM=M-1
       AD=1.0/B(M,M)
       SUM=VNM(M)
       IF(M.EQ.1) GO TO 60
       DO 70 J=1,MM
 70    SUM=SUM-B(M,J)*D(J)
 60    D(M)=SUM*AD
       DO 90 I=1,NM
       M=NM+1-I
       SUM=D(M)
```

```
      IF(I.EQ.1)GO TO 90
      MP=M+1
      DO 100 J=MP,NM
100   SUM=SUM-B(M,J)*GEMA(J)
90    GEMA(M)=SUM
      RETURN
      END

      SUBROUTINE WKIT(NC,CC,AW,BW,SIG,XS,YS,ZS,GAMA,DSM,NIT)
C
C  SUBROUTINE TO DO WAKE RELOCATION TAKING TUNNEL EFFECTS
C
      DIMENSION AW(30),BW(30),DSM(30),SIG(30)
      DIMENSION XS(30),YS(30),ZS(30),GAMA(30)
      INTEGER CC
      COMMON /JETIN2/ SPEED,CHORD,GMSPN,CTHR
      VTUX=0.0   $  VTUY=0.0   $  VTUZ=0.0
      L=CC+1
      N1=0
      NCC=NC+1
      DO 20 M=NCC,CC
      MM1=M-1
      DX=XS(M)-XS(MM1)
      DY=YS(M)-YS(MM1)
      DXY=SQRT(DX*DX+DY*DY)
      SINA=DY/DXY
      COSA=DX/DXY
      XC=1.5*DXY*COSA+XS(MM1)
      YC=1.5*DXY*SINA+YS(MM1)
      ZC=ZS(MM1)
      CALL VTRAIL(CC,XS,YS,ZS,GAMA,XC,YC,ZC,VXTR,VYTR,VZTR,M)
      CALL VBOUND(CC,AW,BW,SIG,XS,YS,ZS,XC,YC,ZC,VXB,VYB,VZB,N1)
      IF(NIT.EQ.1) GO TO 30
      CALL TUNCON(XC,YC,ZC,VTUX,VTUY,VTUZ)
 30   VXT=SPEED+VXTR+VXB+VTUX
      VYT=VYTR+VYB+VTUY
      VEL=SQRT(VXT*VXT+VYT*VYT)
      J=M+1
      XSHFT=DSM(M)*VXT/VEL+XS(M)-XS(J)
      YSHFT=DSM(M)*VYT/VEL+YS(M)-YS(J)
      DO 48 L1=J,L
      XS(L1)=XS(L1)+XSHFT
      YS(L1)=YS(L1)+YSHFT
48    CONTINUE
20    CONTINUE
      RETURN
      END

     SUBROUTINE TUNCON(XC,YC,ZC,VTUX,VTUY,VTUZ)
C
```

```
C  SUBROUTINE TO CALCULATE VELOCITY COMPONENTS
C  INDUCED BY THE TUNNEL
C
      COMMON /TUNNEL/ MM,NN,SINPHI(25),COSPHI(25)
      COMMON /TVEL1/ X(15),Y(25),Z(25)
      COMMON /TVEL2/ VN(80,80),GEMA(80)
      DIMENSION XV(5),YV(5),ZV(5)
      VTUX=0.0 $VTUY=0.0  $VTUZ=0.0
      M=0
      DO 10 I=1,NN
      DO 11 J=1,MM
      M=M+1
      XV(1)=X(I)
      XV(2)=XV(1)
      XV(3)=X(I+1)
      XV(4)=XV(3)
      XV(5)=XV(1)
      YV(1)=Y(J)
      YV(2)=Y(J+1)
      YV(3)=YV(2)
      YV(4)=YV(1)
      YV(5)=YV(1)
      ZV(1)=Z(J)
      ZV(2)=Z(J+1)
      ZV(3)=ZV(2)
      ZV(4)=ZV(1)
      ZV(5)=ZV(1)
      G=GEMA(M)
      DO 15 K=1,4
      CALL VORTEX(XV(K),YV(K),ZV(K),XV(K+1),YV(K+1),ZV(K+1),
     @XC,YC,ZC,VX,VY,VZ,G)
      VTUX=VTUX+VX
      VTUY=VTUY+VY
      VTUZ=VTUZ+VZ
  15  CONTINUE
  11  CONTINUE
  10  CONTINUE
      RETURN
      END
```

APPENDIX - C

```
      PROGRAM CNTRLED(INPUT,OUTPUT,TAPE5=INPUT,TAPE6=OUTPUT)
C *********************************************************
C
C  PROGRAM FOR THE SOLUTION OF MODEL IN THE CONTROLLED
C  FLOW TUNNEL PROBLEM.  THE MODEL IS A 3-D FULL SPAN
C  JET FLAP.  IN THIS VERSION OF THE PROGRAM FLOW
C  THROUGH A POINT ON THE TUNNEL IS CONTROLLED IF THE
C  NORMAL VELOCITY THROUGH THAT POINT IS GREATER THAN
C  'PERTG' PERCENT OF THE FREE STREAM VELOCITY.
C
C *********************************************************
      COMMON /AERO/ VNFA(80),PERTG
C
C             **  PLEASE NOTE  **
C
C  AS MENTIONED IN THE TEXT, THE MODEL IN THE CONTROLLED
C  FLOW TUNNEL SOLUTION IS OBTAINED BY APPROPRIATE
C  MODIFICATIONS TO THE TUNNEL CONTROL POINT BOUNDARY
C  CONDITION OF THE MODEL IN THE CLOSED TUNNEL PROGRAM.
C  THIS NEEDS MODIFICATION OF THE SUBROUTINE AEROC.
C  SINCE OTHER PARTS OF THE PROGRAM ARE SAME AS IN
C  APPENDIX - B, ONLY THE MODIFIED SUBROUTINE AEROC
C  IS GIVEN HERE.
C
      SUBROUTINE AEROC(NC,CC,ALPHA,CJ,NIT)
C
C  SUBROUTINE TO CALCULATE AERODYNAMIC COEFFICIENTS, VELOCITY
C  INDUCED AT THE TUNNEL CONTROL POINTS BY THE MODEL AND THE
C  ANGLE OF DOWNWASH AT TAIL
C
      DIMENSION ANGW(30),ANGB(30)
      COMMON /B2/ VNM(80)
      COMMON /AERO/ VNFA (80),PERTG
      COMMON /JET1/  WA(30),AW(30),BW(30),E(30,30),FS(30),C(30),D(30)
      COMMON /JET4/  SIG(30),GAMA(30),XS(30),YS(30),ZS(30)
      COMMON /JETIN2/ SPEED,CHORD,GMSPN,CTHR
      COMMON /TAIL/ XT,YT,ZT
      COMMON /CTRPT/ XCPT(15),YCPT(25),ZCPT(25)
      COMMON /TUNNEL/ MM,NN,SINPHI(25),COSPHI(25)
      INTEGER CC
 709  FORMAT(5X,2F10.5)
 708  FORMAT(/,5X,25H AERODYNAMIC COEFFICIENTS)
 130  FORMAT(/1X,*DOWNWASH AT TAIL=*,F10.5)
 120  FORMAT(6F10.4)
 110  FORMAT(4F10.4)
 31   FORMAT(//)
```

```
30    FORMAT(10E10.3)
3     FORMAT(3F15.6)
      PI=4.0*ATAN(1.0)
      DEGRA=180.0/PI
      SPAN=PI*GMSPN/4.0
      ISKP=0
      NCC=NC+1
      L=CC+1
      SW=CHORD*GMSPN
      Q=SPAN/(SW*SPEED*SPEED)
      SUML=0.0  $ SUMD=0.0
      DO 80 I=1,NCC
      XC=AW(I)
      YC=BW(I)
      ZC=0.0
      VTUX=0.0
      VTUY=0.0
      CALL VTRAIL(CC,XS,YS,ZS,GAMA,XC,YC,ZC,VXTR,VYTR,VZTR,ISKP)
      CALL VBOUND(CC,AW,BW,SIG,XS,YS,ZS,XT,YT,ZT,VXB,VYB,VZB,ISKP)
      VELX=SPEED+VXTR+VXB+VTUX
      VELY=-(VYTR+VYB+VTUY)
      SUML=SUML+2.*SIG(I)*VELX
      SUMD=SUMD+2.*SIG(I)*VELY
 80   CONTINUE
      CLP=SUML*Q
      CDP=SUMD*Q
      WAE=WA(1)+ALPHA
      CLJ=CJ*SIN(WAE)
      CDJ=-CJ*COS(WAE)
      CLT=(CLP*CTHR)+CLJ
      CDT=CDP+CDJ
      WRITE(6,708)
      WRITE(6,709)CLP,CDP
      WRITE(6,709) CLJ,CDJ
      WRITE(6,709) CLT,CDT
      MCC=CC-1
      DO 20 K=1,MCC
      ANGWB=ATAN((BW(K)-BW(K+1))/(AW(K+1)-AW(K)))
      ANGWB=ANGWB-ALPHA
20    ANGB(K)=DEGRA*ANGWB
      DO 19 K=1,CC
      ANGWT=ATAN((YS(K+1)-YS(K))/(XS(K+1)-XS(K)))
19    ANGW(K)=DEGRA*ANGWT
      WRITE(6,110) (AW(I),BW(I),SIG(I),ANGB(I),I=1,CC)
      WRITE(6,110) (XS(I),YS(I),ZS(I),ANGW(I),I=1,L)
C
C VELOCITY INDUCED AT TUNNEL CONTROL POINTS
C
      DO 21 I2=1,NN
      DO 21 J2=1,MM
```

```
      I=(I2-1)*MM+J2
      XC=XCPT(I2)
      YC=YCPT(J2)
      ZC=ZCPT(J2)
      CALL VTRAIL(CC,XS,YS,ZS,GAMA,XC,YC,ZC,VXTR,VYTR,VZTR,ISKP)
      CALL VBOUND(CC,AW,BW,SIG,XS,YS,ZS,XC,YC,ZC,VXB,VYB,VZB,ISKP)
      VYM=VYTR+VYB
      VZM=VZTR+VZB
      VNM(I)=-(VYM*COSPHI(J2)+VZM*SINPHI(J2))
      IF(NIT.EQ.1) GO TO 25
      IF(VNFA(I).NE.0.0) VNM(I)=VNFA(I)+VNM(I)
      GO TO 26
C
C  DECIDE WHICH POINTS TO CONTROL
C
 25   IF(ABS(VNM(I)).LT.PERTG) GO TO 22
      VNFA(I)=-VNM(I)
      GO TO 23
 22   VNFA(I)=0.0
 23   VNM(I)=VNM(I)+VNFA(I)
 26   CONTINUE
 21   CONTINUE
      NM=NN*MM
      WRITE(6,30) (VNM(I),I=1,NM)
      WRITE(6,31)
      WRITE(6,30) (VNFA(I),I=1,NM)
C
C  COMPUTE DOWNWASH AT TAIL
C
      VTUX=0.0  $VTUY=0.0  $VTUZ=0.0
      CALL VTRAIL(CC,XS,YS,ZS,GAMA,XT,YT,ZT,VXTR,VYTR,VZTR,ISKP)
      CALL VBOUND(CC,AW,BW,SIG,XS,YS,ZS,XT,YT,ZT,VXB,VYB,VZB,ISKP)
      IF(NIT.EQ.1)GO TO 300
      CALL TUNCON(XT,YT,ZT,VTUX,VTUY,VTUZ)
 300  UXT=SPEED+VXTR+VXB+VTUX
      UYT=VYTR+VYB+VTUY
      UZT=VZTR+VZB+VTUZ
      WRITE(6,120) VXTR,VYTR,VZTR
      WRITE(6,120) VXB,VYB,VZB
      WRITE(6,120) VTUX,VTUY,VTUZ
      WRITE(6,120) XT,YT,ZT,UXT,UYT,UZT
      EPSI=ATAN(UYT/UXT)
      EPSI=EPSI*DEGRA
      WRITE(6,130) EPSI
      RETURN
      END
```

1. Report No.	2. Government Accession No.	3. Recipient's Catalog No.
NASA CR 166572		

4. Title and Subtitle	5. Report Date
A NUMERICAL STUDY OF THE CONTROLLED FLOW TUNNEL FOR A HIGH LIFT MODEL	1984
	6. Performing Organization Code
7. Author(s)	8. Performing Organization Report No.
Pareshkumar C. Parikh	
	10. Work Unit No. J.O. T-4947YA
9. Performing Organization Name and Address	11. Contract or Grant No.
University of Washington 1 Administration Bldg. AD-24 Seattle, Washington 98195	NSG 2260
	13. Type of Report and Period Covered
12. Sponsoring Agency Name and Address	Contractor Report
National Aeronautics and Space Administration Washington, D.C. 20546	14. Sponsoring Agency Code 505-42-11

15. Supplementary Notes

Point of Contact: Technical Monitor, Victor R. Corsiglia, MS 247-1
Ames Research Center, Moffett Field, CA 94035
(415) 965-6677 or FTS 448-6677

16. Abstract

A controlled flow tunnel employs active control of flow through the walls of the wind tunnel so that the model is in approximately free air conditions during the test. This improves the wind tunnel test environment, enhancing the validity of the experimentally obtained test data.

In the present study this concept is applied to a three dimensional jet flapped wing with full span jet flap. It is shown that a special treatment is required for the high energy wake associated with this and other V/STOL models. An iterative numerical scheme is developed to describe working of an actual controlled flow tunnel and comparisons are shown with other available results. It is shown that control need be exerted over only part of the tunnel walls to closely approximate free air flow conditions. It is concluded that such a tunnel is able to produce a nearly interference free test environment even with a high lift model in the tunnel.

17. Key Words (Suggested by Author(s))	18. Distribution Statement
Wind Tunnel Design Wind Tunnel Wall Interference	Unclassified - Unlimited Subject category 02

19. Security Classif. (of this report)	20. Security Classif. (of this page)	21. No. of Pages	22. Price*
Unclassified	Unclassified		

*For sale by the National Technical Information Service, Springfield, Virginia 22161

End of Document